UNIVERSITY OF COPENHAGEN
FACULTY OF SCIENCE

Master's Thesis

Georgios Georgogiannis

Field Theoretical Modeling of Parafermion Devices for Quantum Transport

September 30^{th} 2022

Supervisor: Michele Burrello

Abstract

Since the realization of zero-energy modes localized at the ends of a 1D topological p-wave superconductor, these zero-modes (Majorana modes) have been vigorously pursued, and many heterostructures to engineer them have been proposed. These theoretical proposals have motivated the development of hybrid systems which include topological insulators, spin-orbit coupled semiconductors, and integer quantum Hall edges all in combination with a superconductor. But Majorana modes are not the only exotic particles that can appear with topological properties at such heterostructures. As preliminary works have predicted, Fractional Quantum Hall/superconductor hybrids devices can host parafermions. Parafermions, unlike Majoranas, require electron-electron interactions to form, which result in richer non-Abelian braiding statistics.

This thesis aims to construct a field theoretical model based on Bosonization and other analytical techniques to describe such Fractional Quantum Hall/superconductor hybrid devices. In particular, it aims to model the Crossed Andreev pairing between counter-propagating quantum Hall edge modes induced by the proximity with a superconductor with strong spin-orbit coupling (NbN), motivated by recent (by the time of writing) experimental results [1]. At First, it is studied the Integer Quantum Hall (non-Interacting) case by means of Perturbation Theory and the Feynman Path Integral where an estimation of the induced gap is given and next, by bosonizing the system it is studied the Interacting FQH system, and an estimation about the induced gap using the Renormalization Group analysis is provided.

Acknowledgements

First and foremost, I would like to thank my supervisor Michele Burrello for suggesting this challenging but rather very interesting project to work on my thesis. Michele was always there to provide me with guidance and help me progress. Through our discussions, he helped me overcome all the challenges encountered during this thesis and made me realize how important it is to discuss with colleagues when you have questions, especially in a research environment. For me, he acted not only as a supervisor but also as a mentor and for that he has my utmost gratitude. I would also like to thank the CMT group for providing such great vibes and made the working place more inspiring. Finally, I would like to thank my family and friends for supporting me through my studies.

Contents

Introduction

Theoretical proposals to synthesize a topological superconductor from a topological insulator and a conventional (s-wave) superconductor have motivated hybrid approaches to realize Majorana modes. Besides topological insulators, these approaches now include spin-orbit coupled semiconductors, magnetic atom chains, and integer quantum Hall edges all in combination with a superconductor offering either a testbed for or a route towards topological qubits. Common to all of these is the non-interacting description of charge carriers and Ising topological order which is insufficient for universal quantum computation. These approaches, however, can be extended to the computationally universal Fibonacci order predicted to emerge in a coupled parafermion array.

Parafermions, unlike Majoranas, require electron-electron interactions to form, which result in richer non-Abelian braiding statistics. A standard condensed matter system that forms with interactions is the Fractional Quantum Hall (FQH) state, which is the basis of different approaches for synthesizing parafermions. The primary approach combining FQH, appearing in semiconductor heterostructures, with superconductivity has so far presented a major experimental challenge. That is because FQH thrives in high magnetic fields, whilst the superconductor loses his superconductivity. The solution to this problem was given from a recent experiment performed by Philip Kim and his group [1]. They used graphene-based Van der Waals (VdW) heterostructures coupled to superconducting niobium nitride (NbN). The high device quality decreases the magnetic fields required for robust FQH to the regime where NbN remains superconducting owing to its large critical field. The superconductor edge-contact to graphene provides an interface transparent enough to allow Crossed Andreev Reflection (CAR)[1] in quantum Hall edges. The most important thing used in this setup is choice of the superconductor. Even in high magnetic fields, as high as 14T, the NbN does not lose its superconductivity. Another equally important property is the large spin-orbit coupling in NbN superconductor, which provides a necessary ingredient for a spin-flip process allowing for a pairing between electrons with the same spin polarization. The experimental results they found were encouraging, because a negative resistance ($R_{CAR} < 0$) indicates that the electron-like carriers drained from the superconductor produce hole-like carriers with opposite charge, a direct result of Crossed Andreev

[1]Crossed Andreev Reflection (CAR) is a non-local process that converts an incoming electron (hole) from one normal electrode to an out-going hole (electron) in another normal electrode through a superconductor (SC). Such a non-local process occurs only when the separation between two normal metals (N1 and N2), who are in contact with a SC, is comparable to or less than the superconducting coherence length ξ_s.

Reflection, which reverses the sign of the edge potential.

The goal of this thesis is to construct a field theoretical model based on Bosonization that describes Crossed Andreev Reflection of particles with the same spin between the counter propagating (Integer and Fractional) Quantum Hall edges and a conventional Superconductor. This describes an electron entering the SC from one side and a hole leaving from other side. For this purpose, we choose our Superconductor to be the NbN, because of its uniqueness, as mentioned before. These CAR pairings of the same spin will induce a proximity superconducting gap to our system, which we are called to estimate. The outline of this thesis is as follows: In $\boldsymbol{Chapter\ 1}$ we give a theoretical Background to the physics that is important to us in order to understand better how such heterostructures work. In $\boldsymbol{Chapter\ 2}$ we introduce our model and focus on deriving a field theoretical description that describes CAR for the non-Interacting (Integer Quantum Hall) case only. This is achieved by using 3 methods (2 analytical and 1 computational). The first one is by using 2nd order Perturbation theory. For the second, we use the Feynman Path Integral approach and for the third we plot our system and show the induced gap. In $\boldsymbol{Chapter\ 3}$ we focus on estimating the gap by using the Bosonization technique, which is based on an effective low-energy theory, and the Renormalization Group which is a transformation that maps a system with a set of coupling constants and a scale (representing the short-distance or high-energy cutoff) to another equivalent system with a different set of (renormalized) coupling constants and a different scale. Finally, in $\boldsymbol{Chapter\ 4}$ we present the Conclusions and Outlook.

Chapter 1

Background

In this Chapter, we present a background introduction of the theory for the physics that is hidden in the model that we are describing in this project. For that purpose, we will use a lot of material that can be found in the book of Fradkin [2] and in [3], [4], [5].

1.1 Majorana modes

In order to characterize fermions that are their own antiparticle, Ettore Majorana found real solutions to Dirac equation in 1937. This solution is commonly referred to as the Majorana equation. Even though this was a "ancient" notion, it continues to influence many areas of contemporary physics. Majorana's original hypothesis that neutrinos could actually be Majorana fermions is still taken seriously in the context of high energy. Furthermore, according to supersymmetric theories, bosonic particles like photons have a Majorana "super partner" that corresponds to them. This "super partner" might hold the solution to the mystery of dark matter. In a wide range of solid state systems, condensed matter physicists are also ardently pursuing Majorana's vision due to their interest in both novel basic physics and quantum computing applications.

The Majorana fermions pursued in solid state systems are not basic particles, in contrast to the Majorana fermions sought by high-energy physicists. The likelihood of success in this quest is greatly constrained by the fact that regular electrons and ions are unavoidably the components of condensed matter. For instance, electron and hole excitations in ordinary metals can annihilate, but since they carry the opposite charge, they are unquestionably not Majorana fermions. Such excitations are naturally being seeked out in superconductors (and other systems where fermions couple and condense). Indeed, quasiparticles in a superconductor require superpositions of electrons and holes because spontaneous Cooper pair condensation defies charge conservation in its mean field theory description. Unfortunately, this does not meet the requirements for Majorana fermions to appear. Majorana fermions are best supported by "spinless" superconductors, which are paired systems with just one ac-

tive fermionic species as opposed to two. Spinless superconductors, i.e. paired systems with only one active fermionic species rather than two, provide ideal platforms for Majorana fermions. Cooper pairing, which produces p-wave superconductivity in one dimension (1D) and $p_x \pm ip_y$ superconductivity in two dimensions, must take place with odd parity in a "spinless" metal according to Pauli exclusion (2D). Because they achieve topological phases that enable exotic excitations at their borders and at topological defects, these superconductors are highly unique. Most crucially, in the 2D $p_x \pm ip_y$ăsituation, zero-energy modes bond to superconducting vortices and localize at the ends of a 1D topological p-wave superconductor. These zero-modes are precisely the Majorana fermions in condensed matter that are the subject of current active research. Topological superconductivity is therefore a fascinating state of matter, in part because it is linked to Majorana fermion-based quasiparticle excitations (MFs). As a result, the presence of (spatially separated) MFs is an invariant of topology (hence the name topological superconductors). As a result, they will be present in all systems that have p-wave or $p_x \pm ip_y$-wave superconductors' topological features.

Let γ be the operator that corresponds to one of these modes. Being its own anti-particle implies that $\gamma = \gamma^\dagger$ (hermitian) and $\gamma^2 = 1$. Also, γ should be seen as a fractionalized zero-mode consisting of 'half' of a normal fermion. Any fermion may be expressed as a combination of two MFs, which essentially means separating the fermion into a real and an imaginary part, each of which is an MF. To be more specific, to generate a fermionic state with a well-defined occupation number, a pair of Majorana zero modes, say γ_1 and γ_2, must be combined through $f = \frac{\gamma_1 + i\gamma_2}{2}$. This new operator clearly represents a standard fermionic operator that satisfies $f \neq f^\dagger$ and obeys the standard fermionic anticommutation relations.With this definition, there are two essential features that support by far the most intriguing Majorana fermion consequence. The first is that γ_1 and γ_2 can locate arbitrarily far away; as a result, f encodes strongly non-local entanglement. Similarly, when we discuss MFs here, we imply that a fermionic state may be expressed as a superposition of two spatially separated MFs (or prevented from overlapping in some other manner). "Such a highly delocalized fermionic state is protected from most types of decoherence, since it cannot be changed by local perturbations affecting only one of its Majorana constituents. And second, one can empty or fill the non-local state described by f with no energy cost, resulting in a ground-state degeneracy. These two properties signals the emergence of non-Abelian statistics" [5].

One of the pillars of quantum theory is exchange statistics, which describes how many-particle wavefunctions change when interchanges of identical particles take place. Metals, superfluids, superconductors, and many other quantum phases are in fact accessible by a rather direct route from particle statistics. It has long been understood that 2D systems can contain particles whose statistics are neither fermionic nor bosonic due to topological considerations. Such anyons are available in both Abelian and non-Abelian varieties. A statistical phase $e^{i\theta}$ that is halfway between -1 and 1 is acquired by the wavefunction as a result of the exchange of Abelian anyons, which are present in the majority of fractional quantum Hall states.

From the perspective of basic physics, the observation of Majorana fermions in condensed matter is a significant accomplishment since it confirms Ettore Majorana's theoretical finding and, more significantly, because they include non-Abelian statistics. The synthesis of a scalable quantum computer is one of the field's greatest difficulties, and conquering it may eventually depend on the results of this quest. The core notion is that "topological qubits" may be encoded using the occupation numbers $n_j = 0, 1$, which indicate the degenerate ground states of $|n_1, n_2, \ldots, n_N\rangle$. Due to the arbitrary spatial separation between pairs of Majorana modes corresponding to a given n_j, this quantum information is stored strongly non-locally. The system effectively stays contained to the ground-state manifold if we assume that the temperature is low relative to the bulk gap and that the manipulations are done adiabatically. Due to the availability of non-Abelian statistics, the user is able to controllably alter the qubit's state by adiabatically swapping the locations of Majorana modes. In theory, the environment may potentially cause (unwanted) exchanges, damaging the qubit, however because such processes are non-local, the likelihood of this happening is quite low. This serves as the foundation for fault-tolerant topological quantum computing systems that gracefully defeat hardware-level decoherence. However, the extra unprotected operations required for universal quantum computation have exceptionally large error thresholds. While braiding of Majorana fermions alone allows for some limited topological quantum information processing. Thus, future revolutionary technology applications are also a driving force behind the quest for Majorana fermions.

1.1.1 Properties of Majorana fermions

The information for this subsection have been taken from an excellent paper of Martin Leijnse and Karsten Flensberg [4]. Assume now, that we have a system with 2N spatially well-separated MFs, $\gamma_1, \ldots, \gamma_{2N}$. Since one MF has half the degrees of freedom of a typical fermion, the number of MFs must be even. The Majorana operators are created by dividing a normal fermion f_i into its real and imaginary components, just like in the case of Kitaev's chain:

$$f_i = \frac{\gamma_{2i-1} + i\gamma_{2i}}{2} \tag{1.1}$$

The inverse relation is

$$\gamma_{2i-1} = f^\dagger + f, \tag{1.2}$$

$$\gamma_{2i} = i(f^\dagger - f) \tag{1.3}$$

One can easily see that the Majorana operators are hermitian, $\gamma_j = \gamma_j^\dagger$. The Majorana operators compliance with the anti-commutation relation may be easily checked using the fermionic anti-commutation relations for the f_i fermions:

$$\{\gamma_i, \gamma_j\} = 2\delta_{ij} \tag{1.4}$$

which resembles conventional fermions in certain ways. However, there are some considerable differences. There is no Pauli principle ($c^2 = (c^\dagger)^2 = 0$ for regular fermion operators c) for MFs since, according to eq. (1.4), $\gamma^2 = 1$. In fact, we are unable to even discuss Majorana mode occupancy. By creating a "Majorana number operator," $n_i^{MF} = \gamma_i \gamma_i^\dagger$, we may attempt to count the occupancy. However, when we take into consideration the aforementioned characteristics, we can observe that $n_i^{MF} = \gamma_i \gamma_i^\dagger = 1$. Therefore, counting is useless since the Majorana mode is paradoxically both always empty and always filled.

The f_i fermionic operators in this case supply the number of states, $n_i = f_i f_i^\dagger$, and the Pauli exclusion principle causes its eigenvalues to be $n_i = 0, 1$. It is only natural to select to merge two MFs into a fermion if they are close enough to overlap. The sole term that can be added to the Hamiltonian to explain an overlap, t, between γ_{2i-1} and γ_{2i} is

$$\frac{i}{2} t \gamma_{2i-1} \gamma_{2i} = t(n_i - \frac{1}{2}) \tag{1.5}$$

which indicates that holding the appropriate fermionic state has a finite energy cost ($t > 0$). The groundstate is 2N-fold degenerate if the MFs do not overlap, which corresponds to each n_i being equal to zero or one. The total number of electrons in the superconductor is now determined by whether the sum of all occupancy numbers, $\sum_{i=1}^{N} n_i$, is even or odd (even or odd parity). Electrons must be physically introduced to or withdrawn from the superconductor in order to adjust the parity. Noting that a single MF includes just "half a degree of freedom," it is clear that discussing the "state of an MF" is meaningless. The fermionic occupancy numbers are the only physically observables.

1.2 Hall Effect

1.2.1 Classical Quantum Hall

This section aims to show on how from the Classical Hall effect one can end up to the Quantum Hall effect (Integer and Fractional). The information provided here are based on the work of David Tong [3] who gathered and presented the information for this consolidated theory.

We will continue here by providing a small introduction first to the classical picture of the Hall effect.

Our basics ingredients to describe this theory will be a magnetic field $\overrightarrow{B}$ that causes charged particles to move in circles with a cyclotron frequency of $\omega_B = \frac{eB}{m_e}$, where e is the charge of the particle and m_e its mass, an electric field $\overrightarrow{E}$ which will accelerate the charges and, in the absence of a magnetic field, would result in a current in the direction of E and finally, last ingredient is a linear friction term, which is supposed to capture the effect of the electron bouncing off whatever impedes its progress, whether impurities, the underlying lattice or other electrons. This system will correspond

to an equation of motion, of the form:

$$m_e \frac{d\overrightarrow{v}}{dt} = -e\overrightarrow{E} - e\overrightarrow{v} \times \overrightarrow{B} - \frac{m_e \overrightarrow{v}}{\tau} \tag{1.6}$$

where τ in the friction term is called the scattering time and can be thought of as the average time between collisions. Eq. (1.6) is the simplest model of charge transport and it is called the Drude model.

The current density is associated with the velocity and has the form:

$$\overrightarrow{J} = -ne\overrightarrow{v} \tag{1.7}$$

where n is the density of charge carriers. We are interested in solving eq. (1.6) in the equilibrium, where $\frac{d\overrightarrow{v}}{dt} = 0$. This means that we have:

$$\overrightarrow{v} + \frac{e\tau}{m_e}\overrightarrow{v} \times \overrightarrow{B} = -\frac{e\tau}{m_e}\overrightarrow{E} \Rightarrow \begin{pmatrix} 1 & \omega_B\tau \\ -\omega_B\tau & 1 \end{pmatrix} \overrightarrow{J} = \frac{ne^2\tau}{m_e}\overrightarrow{E} \tag{1.8}$$

and by inverting it we get the equation of Ohm's law, which tells us how the how the current flows in response to an electric field:

$$\overrightarrow{J} = \sigma\overrightarrow{E} \tag{1.9}$$

Here, σ is the conductivity and has the matrix form:

$$\sigma = \frac{\sigma_0}{1 + (\omega_B\tau)^2} \begin{pmatrix} 1 & -\omega_B\tau \\ \omega_B\tau & 1 \end{pmatrix} \tag{1.10}$$

with $\sigma_0 = \frac{ne^2\tau}{m_e}$ being the conductivity in the absence of a magnetic field and the off-diagonal terms in the matrix are responsible for the Hall effect.

An important parameter now is the (Hall) resistivity which is defined as:

$$\rho = \sigma^{-1} = \frac{1}{\sigma_0} \begin{pmatrix} 1 & \omega_B\tau \\ -\omega_B\tau & 1 \end{pmatrix} = \begin{pmatrix} \rho_{xx} & \rho_{xy} \\ -\rho_{xy} & \rho_{yy} \end{pmatrix} \tag{1.11}$$

and shows that the off-diagonal terms are independent of the scattering time τ. Another reason why this parameter is important, is because it is related to the Resistance which is a parameter we can measure in experiments. In particular, the Hall coefficient is defined as:

$$R_H = \frac{\rho_{xy}}{|B|} \tag{1.12}$$

which in the Drude theory is given by:

$$R_H = -\frac{1}{ne} \tag{1.13}$$

and allows us to measure the density of electrons in a metal [6].

1.2.2 Integer Quantum Hall Effect

In one of the earliest experiments, the integer quantum Hall effect (IQHE) was observed when a very clean (mobility about $10^5 cm^2/Vs$) two-dimensional electron gas was cooled below 2 K and subjected to a perpendicular magnetic field of the order of 20 T. Von Klitzing conducted this experiment in 1980 [7]. The intriguing outcome of this experiment is that the Hall resistivity ρ_{xy} plateaus for a range of magnetic fields before abruptly moving to the next plateau (see Fig.(1.1)).

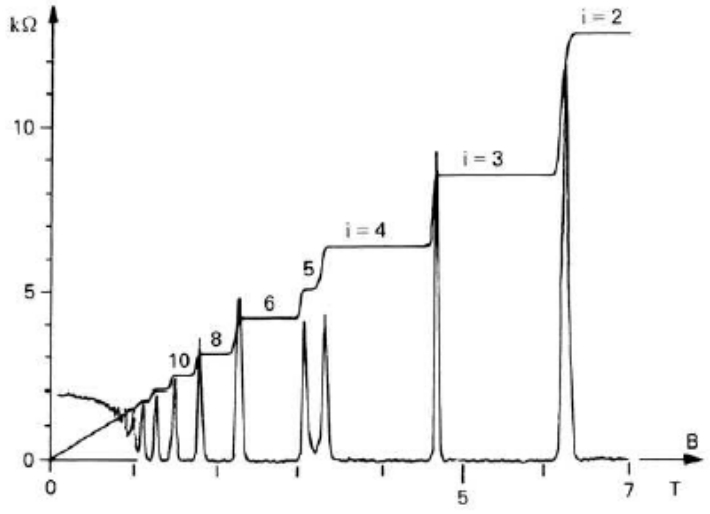

Figure 1.1: "Experimental curves for the Hall resistance $R_H = \rho_{xy}$ and the resistivity $\rho_{xx} \approx R_x$ of a heterostructure as a function the magnetic field at a fixed carrier density corresponding to a gate voltage $V_g = 0V$. The temperature is about 8 mK" [7].

On these plateau, the resistivity takes the value:

$$\rho_{xy} = \frac{2\pi\hbar}{e^2}\frac{1}{\nu}, \qquad \nu \in \mathbb{Z} \tag{1.14}$$

The value of ν is measured to be an integer to an extraordinary accuracy and the quantity $\frac{2\pi\hbar}{e^2}$ is called the quantum of resistivity. The centre of each of these plateaus occurs when the magnetic field takes the value:

$$B = \frac{2\pi\hbar n_e}{e\nu} = \frac{n_e}{\nu}\Phi_0 \tag{1.15}$$

where n_e is the electron density and $\Phi_0 = \frac{2\pi\hbar}{e}$ is the flux quantum.

Another important finding that is shown in Fig.(1.1) is the surprising behaviour of the longitudinal

resistivity ρ_{xx}. In particular, when ρ_{xy} sits on a plateau, the longitudinal resistivity vanishes: $\rho_{xx} = 0$. It spikes only when ρ_{xy} jumps to the next plateau. This surprising fact has nothing to do with quantum mechanics , but instead is a classical of the Drude model in the limit where $\tau \to \infty$ where there is no scattering. In this case, the current is flowing perpendicular to the applied electric field, so $\overrightarrow{E} \cdot \overrightarrow{J} = 0$. This means that we have a steady current flowing without doing any work and, correspondingly, without any dissipation. The fact that $\sigma_{xx} = 0$ is telling us that no current is flowing in the longitudinal direction (like an insulator) while the fact that $\rho_{xx} = 0$ is telling us that there is no dissipation of energy (like in a perfect conductor).

The experimental findings include a hint on the genesis of the plateaus. Typically, experimental systems are impure and unclean. This is known as disorder in technical terms. Normally, one wishes to clear away this debris in order to expose the underlying physics. However, the plateaus in the quantum Hall effect grow more noticeable, not less, when the level of disorder is increased (within reason). In fact, it is anticipated that the plateaus will totally disappear in the absence of disorder. How could something as precise and pure as an integer arise from the presence of dirt? To find the solution to this, it is necessary to observe how these ailments would affect the system. The degenerate eigenstates that make up a Landau level are first predicted to separate. This comes generally from the quantum perturbation theory, which states that degeneracies will be broken by any broad disturbance that does not retain a symmetry. In relation to the separation of the Landau levels, the strength of the disorder must be minimal:

$$V \ll \hbar\omega_B \tag{1.16}$$

This implies that the samples that display the quantum Hall effect must really be quite clean in practice. Alternatively, we require some chaos, but not too much!

Another kind of disorder causes many quantum states to become localized instead of extended. In this case, an extended state extends throughout the entire system. A localized state, in contrast, is constrained to occupy a certain area of space. In a semi-classical model that is valid if the potential, in addition to abiding by (1.16), fluctuates noticeably on scales far larger than the magnetic length l_B, we can plainly discern the presence of these localized states:

$$|\nabla V| \ll \frac{\hbar\omega_B}{l_B} \tag{1.17}$$

According to this assumption, an electron's cyclotron orbit occurs in a region of virtually constant potential. In this instance, there is a division of scales: when the electron motion is viewed classically, it may be divided into two phases: a rapid cyclotron orbit revolving around an instantaneous guiding center, and a long drift of this guiding center. The drift is parallel to the local electric field and follows equipotentials as a result. The energy of the equipotential along which an electron moves displaces the electron's energy within each Landau level created by the quantization of the fast cyclotron motion.

The contrast between localized and extended states in conductivity is significant. The only states

that may move charge from one side of the sample to the other are the extended states. So, the conductivity can only come from these states. Let's assume that all of the extended states in a certain Landau level have been filled. Each Landau level may hold fewer electrons when B is reduced while keeping neăunchanged, hence the Fermi energy will rise. he localised states begin to fill, however, rather than advance to the next Landau level. The conductivity remains unchanged since these states cannot add to the current. This results in exactly the same kind of plateaus as those that are seen, with constant conductivities throughout a range of magnetic field.

If we accept this explanation for how disorder affects electron eigenstates, we can understand the existence of Hall plateaus, but the precise quantization of Hall conductance is immediately unexpected. After all, one might have anticipated that a decrease in the number of extended states would be accompanied by a decrease in the Hall conductance. In order to precisely make up for their decreased number, it is obvious that the remaining extended states must carry an additional current.

To understand this, consider a quantum Hall sample in the form of an annulus as shown in Fig.(1.2) In addition to the magnetic field responsible for the quantum Hall effect, which pierces the surface

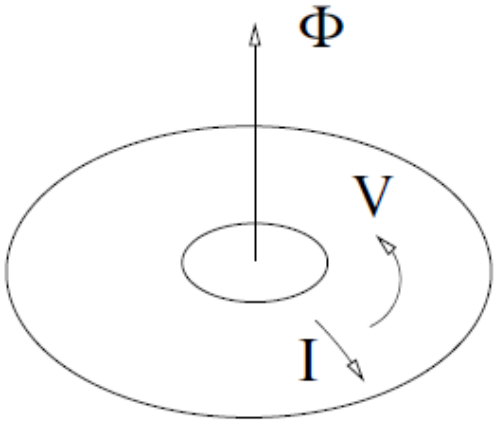

Figure 1.2: Geometry considered in Laughlin argument for exactness of quantisation of Hall conductance

of the annulus, we introduce a second magnetic flux Φ, threading through the hole at the centre of the annulus. Allowing this flux to vary as a function of time, we generate a voltage V around the circumference of the quantum Hall sample. From Faradays law, we have:

$$V = -\frac{d\Phi}{dt} \tag{1.18}$$

Within a Hall plateau, this produces a current flow:

$$I = \sigma_{xy} V \tag{1.19}$$

in the perpendicular direction, which is radial. Integrating the rates of flux change and current flow

over time, a given flux difference $\Delta\Phi$ corresponds to the transport of a certain charge Q between the inner and outer edges of the annulus. Now, we expect that a change in Φ of one flux quantum (h/e) will return the interior of the quantum Hall system to its initial state, implying that an integer number of electrons have then been transported across the annulus. We have:

$$\nu \times e = Q = \sigma_{xy} \cdot \Delta\Phi = \sigma_{xy}\frac{h}{e} \Rightarrow \sigma_{xy} = \nu\frac{e^2}{h} \tag{1.20}$$

where ν is integer number.

1.2.3 Fractional Quantum Hall Effect

In addition to the integer plateaus we have examined, quantum Hall plateaus with specific straightforward fractional values of the Hall conductance are seen in sufficiently high mobility samples. In particular, one gets $\sigma_{xy} = \frac{p}{q}\frac{e^2}{h}$, where p and q are integers and q is almost always odd. The fact that this is seen in samples with little disorder suggests that interactions are what lift the partially filled Landau level's degeneracy and create unique associated ground states at particular filling factors. Additionally, the fact that $\sigma_{xx} \rightarrow 0$ at low temperatures (with an activated temperature dependency) denotes the possibility of an excitation gap from these connected ground states. Furthermore, since we claimed that the charge transferred across an annular system when one flux quantum is introduced should be equal to $\sigma_{xy} \times \frac{h}{e}$, Laughlin's argument for the quantisation of Hall conductance shows that excitations contain fractional charge. We obtain $(p/q)e = \nu \times e^*$ when we assume that this charge is made up of an integer number of quasiparticles, each with a charge of e^*.

As mentioned in [3], "the integer quantum Hall effect was originally discovered in a Si MOSFET (this stands for metal-oxide-semiconductor field-effect transistor). This is a metal-insulator semiconductor sandwich, with electrons trapped in the inversion band of width ~ 30 Å between the insulator and semi-conductor. Meanwhile the fractional quantum Hall effect was discovered in a GaAs-GaAlAs heterostructure. and a lot of the subsequent work was done on this system, and it usually goes by the name GaAs (Gallium Arsenide). In both these systems, the density of electrons is around $n_e \sim 10^{11} - 10^{12}\, cm^{-2}$"[3].

"More recently, both Integer and Fractional Quantum Hall Effects have been discovered in graphene, which is a two dimensional material with relativistic electrons. The physics here is similar in spirit, but differs in details"[3]. These differences will be analyzed in section (1.2.4).

1.2.4 Landau Levels

Let us try to analyze the physics behind the Quantum Hall Effect by reviewing the quantum mechanics of free particles moving in a background magnetic field and the resulting phenomenon of Landau

levels. In the following we will consider two cases. The first one will be the non-relativistic and the second will be the relativistic.

Non-relativistic case

We begin with the non-relativistic case. In the presence of a magnetic there is a Zeeman splitting between the energies of spin up and down $\Delta_B = 2\mu_B B$ where $\mu_B = e\hbar/2m_e$ is the Bohr magneton. In strong magnetic fields, large energies are needed to flip the spin. This means that, if we restrict to low energies, the electrons act as if they are effectively spinless. Furthermore, the magnetic field is applied perpendicular to the plane of motion of the particle (the z-axis is taken perpendicular to the plane) and may be written in the following vector form:

$$\overrightarrow{B} = (0, 0, B_z) \tag{1.21}$$

In the presence of a magnetic field, the free particle Hamiltonian can be described as:

$$H = \frac{1}{2m}\big(\overrightarrow{p} + e\overrightarrow{A}\big)^2 \tag{1.22}$$

where $\overrightarrow{A}$ is the magnetic vector potential and is connected with the magnetic field via the relation $\overrightarrow{B} = \nabla \times \overrightarrow{A}$. We will work in symmetric gauge potential which has the form:

$$\overrightarrow{A}(\overrightarrow{r}) = \frac{1}{2}\overrightarrow{B} \times \overrightarrow{r} = \frac{B_z}{2}(-y, x, 0) \tag{1.23}$$

where $\overrightarrow{r} = (x, y, 0)$ and $B_z = B > 0$. This choice of gauge breaks translational symmetry in both the x and the y directions. However, it does preserve rotational symmetry about the origin. This means that angular momentum is a good quantum number.

We define the mechanical momentum operators:

$$\pi = \overrightarrow{p} + e\overrightarrow{A} \tag{1.24}$$

which is gauge invariant, but non-canonical and satisfies the commutation relation $[\pi_x, \pi_y] = -ie\hbar B_z$. We will use this to construct the raising and lowering operators:

$$\alpha = \frac{1}{\sqrt{2e\hbar B_z}}(\pi_x - i\pi_y), \qquad \alpha^\dagger = \frac{1}{\sqrt{2e\hbar B_z}}(\pi_x + i\pi_y) \tag{1.25}$$

which obey $\left[\alpha, \alpha^\dagger\right] = 1$. In terms of these creation operators, the Hamiltonian takes the harmonic oscillator form:

$$H = \frac{1}{2m}\pi \cdot \pi = \hbar\omega_B(\alpha^\dagger\alpha + \frac{1}{2}) \tag{1.26}$$

We can construct the Hilbert space in the same by introducing a ground state $|0\rangle$ obeying $\alpha\,|0\rangle = 0$ and build the rest of the Hilbert space by acting with $\alpha^\dagger$:

$$\alpha^\dagger\,|n\rangle = \sqrt{n+1}\,|n+1\rangle\,, \qquad \alpha\,|n\rangle = \sqrt{n}\,|n-1\rangle \tag{1.27}$$

The state $|n\rangle$ has energy:

$$E_n = \hbar\omega_B\Big(n+\frac{1}{2}\Big), \qquad n \in \mathbb{N} \tag{1.28}$$

This shows that in the presence of a magnetic field, the energy levels of a particle become equally spaced, with the gap between each level proportional to the magnetic field B. These energy levels are called Landau Levels.

By starting with a particle moving in a plane, which has two degrees of freedom, we ended up writing this in terms of the harmonic oscillator which has just a single degree of freedom. What we lost along the way is the fact that eq. (1.28) does not have a unique state associated to it. Instead there is a degeneracy of states.

In order to see the degeneracy in this language, we need to introduce another kind of mechanical momentum:

$$\tilde{\pi} = \overrightarrow{p} - e\overrightarrow{A} \tag{1.29}$$

In contrast to eq. (1.24) this differs by the minus sign which makes this new mechanical momentum not gauge invariant. Their commutators differ also by a minus sign $[\tilde{\pi}_x, \tilde{\pi}_y] = ie\hbar B_z$. By taking the commutation relations of these 2 mechanical momentum operators, we find that $[\pi_i, \tilde{\pi_j}] \neq 0$ and they cannot be diagonalized simultaneously. This shows the lack of gauge invariance.

The reason we choose the symmetric gauge of eq. (1.23) is because it solves this problem. Namely, we get:

$$[\pi_i, \tilde{\pi_j}] = 0 \tag{1.30}$$

We can now define a second pair of raising and lowering operators:

$$b = \frac{1}{\sqrt{2e\hbar B_z}}(\tilde{\pi}_x + i\tilde{\pi}_y), \qquad b^\dagger = \frac{1}{\sqrt{2e\hbar B_z}}(\tilde{\pi}_x - i\tilde{\pi}_y) \tag{1.31}$$

which also obey now the commutation relation $\left[b, b^\dagger\right] = 1$. It is this second pair of creation operators that provide the degeneracy of the Landau levels. We define the ground state $|0,0\rangle$ to be annihilated by both lowering operators, so that $\alpha\,|0,0\rangle = b\,|0,0\rangle = 0$. Then the general state in the Hilbert space is $|n,m\rangle$ defined by:

$$|n,m\rangle = \frac{\alpha^\dagger b^\dagger}{\sqrt{n!m!}}\,|0,0\rangle \tag{1.32}$$

where the energy of this state is given by the usual Landau Level expression of eq. (1.28) and it depends on n but not on m.

What we want next, is to derive the wavefunctions of the symmetric gauge. We will focus on the Lowest Landau Level ($n = 0$) for simplicity. It help to rewrite the annihilation operator α as:

$$\alpha = \frac{1}{\sqrt{2e\hbar B_z}}(\pi_x - i\pi_y) = \frac{1}{\sqrt{2e\hbar B_z}}\big(p_x - ip_y + e(A_x - iA_y)\big) = \frac{1}{\sqrt{2e\hbar B_z}}\Big(- i\hbar\Big(\frac{\partial}{\partial_x} - i\frac{\partial}{\partial_y}\Big) + \frac{eB}{2}(-y - ix)\Big) \tag{1.33}$$

We introduce the complex coordinates:

$$z = x - iy, \qquad \bar{z} = x + iy \tag{1.34}$$

which will make our wavefunctions holomorphic[1]. The corresponding holomorphic derivatives are:

$$\partial_z = \frac{1}{2}\Big(\frac{\partial}{\partial_x} + i\frac{\partial}{\partial_y}\Big) \qquad \bar{\partial_z} = \frac{1}{2}\Big(\frac{\partial}{\partial_x} - i\frac{\partial}{\partial_y}\Big) \tag{1.35}$$

which obey $\partial_z z = \bar{\partial}_{\bar{z}}\bar{z} = 1$ and $\partial_{\bar{z}} z = \bar{\partial_z}\bar{z} = 0$. In terms of these holomorphic coordinates, α b operators takes the form:

$$\alpha = -i\sqrt{2}\Big(l_B\bar{\partial_z} + \frac{z}{4l_B}\Big) \qquad \alpha^\dagger = -i\sqrt{2}\Big(l_B\partial_z - \frac{\bar{z}}{4l_B}\Big) \tag{1.36}$$

$$b = -i\sqrt{2}\Big(l_B\partial_z + \frac{\bar{z}}{4l_B}\Big) \qquad b^\dagger = -i\sqrt{2}\Big(l_B\bar{\partial_z} - \frac{z}{4l_B}\Big) \tag{1.37}$$

with $l_B = \sqrt{\hbar/eB}$ the magnetic length. The lowest Landau level wavefunctions $\psi_{LLL}(z, \bar{z})$ are then those which are annihilated by this differential operator and can be found to be equal with:

$$\psi_{LLL}(z, \bar{z}) = f(z)e^{-|z|^2/4l_B^2} \tag{1.38}$$

for any holomorphic wavefunction $f(z)$. We can now construct the higher states by acting with $b^\dagger$. This results to:

$$\psi_{LLL,m}(z, \bar{z}) = f(z)\big(\frac{z}{l_B}\big)^m e^{-|z|^2/4l_B^2} \tag{1.39}$$

This particular basis of states has another advantage, these are eigenstates of angular momentum. This means also that m labels the angular momentum. For a system with N_Φ flux quanta there are N_Φ linearly independent states. Thus, an arbitrary state in the lowest Landau level is a polynomial in z of degree N_Φ times the exponential factor. For a more detailed solution, one can refer to [2] or [8].

Let us consider now the case of a system with exactly $N = N_\Phi$ electrons in a magnetic field B with N_Φ flux quanta. The ground-state wave function (for a non-interacting Hamiltonian) ψ_N for the

[1] A holomorphic function is a complex-valued function of one or more complex variables that is complex differentiable in a neighbourhood of each point in a domain in complex coordinate space $\mathbb{C}^n$.

N-particle system is the Slater determinant:

$$\psi_N(z_1,\ldots,z_N) = \begin{vmatrix} z_1^0 & \ldots & z_N^0 \\ z_1^1 & \ldots & z_N^1 \\ \vdots & \vdots & \vdots \\ z_1^N & \ldots & z_N^N \end{vmatrix} e^{-\frac{1}{4l_B^2}\sum_{j=1}^{N}|z_j|^2} \tag{1.40}$$

This determinant has the form of a Vandermonde determinant. By application of a standard algebraic identity, the wave function ψ_N can be written in the form:

$$\psi_N(z_1,\ldots,z_N) = \prod_{1\le j<k\le N}(z_j - z_k)\left(e^{-\frac{1}{4l_B^2}\sum_{j=1}^{N}|z_j|^2}\right) \tag{1.41}$$

Thus, we derived the many-body wave function of a filled Lowest Landau Level.

The Laughlin wave function

We have so far thought about the issue of how electrons move on a 2D surface when a perpendicular magnetic field is present. We made the assumption that an integer number of Landau Levels (or bands) would be fully filled due to the electron density. The interactions are not particularly significant since there is an energy gap in the system. The IQHE matches the description here.

Let's assume that one Landau Level (or band) has some remaining space. As a result, perturbation theory will break down. The filling fraction $\nu = \frac{N}{N_\Phi}$ in the straightforward scenario of N particles in a magnetic field B with N_Φ flux quanta penetrating the surface is not an integer. We will focus on the more straightforward (and well-known) scenario of $\nu = 1/m$, where m is an odd number and there are m flux quanta for each electron. Furthermore, we assume that the magnetic field is sufficiently enough to provide all of the Zeeman energy necessary for full spin polarization of the system. The majority of the experimentally available systems are represented by this instance, although not all of them.

Now, a non-interacting fractionally filled state would still exhibit a fractional Hall conductance σ_{xy} since, at least for a Galilean-invariant system, the conductance is determined by the amount of charge present. But such a state would not support the very precise plateaus which are seen in experiments, since additional particles can be added at almost no energy cost. The fact that the FQHE is seen only in the purest samples indicates that the effect is the result of electron correlations due to the Coulomb interactions. Moreover, the quenching of the single-particle kinetic energies by the magnetic field is telling us that the interactions play a dominant role. The FQHE is the result of the competition between degeneracy and interactions. In this sense, the FQHE is an example of strongly correlated electron systems.

The model which naturally describes the essential features of the physical system consists of an assembly of N electrons that occupy a fraction of the N_Φ states of the lowest Landau Level and interact with each other via Coulomb interactions. The ground state of the system should not support any gapless excitations (otherwise the plateaux of σ_{xy} could not be so sharp), with an exemption the edges, and it should be essentially insensitive to the presence of impurities. Furthermore, the wave function should be a complex function of the electron coordinates, because in the presence of a magnetic field time-reversal invariance is broken explicitly. Finally, Fermi statistics demands that the wave function $\psi_N(z_1, \ldots, z_N)$ should be anti-symmetric under the permutation of the positions of any pair of particles. Thus, ψ_N vanishes as the positions of two particles approach each other.

Laughlin was the first to realize that the liquid state is fundamentally different from other known condensed states, such as magnetism or superconductivity. Drawing on intuition he gained by studying systems with small numbers of particles, Laughlin proposed the following class of wave functions [9]:

$$\psi_N(z_1, \ldots, z_N) = \prod_{1 \le j < k \le N} f(z_j - z_k) \left(e^{-\frac{1}{4l_B^2} \sum_{j=1}^{N} |z_j|^2} \right) \tag{1.42}$$

Fermi statistics demands that $f(z_j - z_k)$ be an odd function of $z_j - z_k$ that vanishes as $z_j \to z_k$. These requirements, together with the demand that ψ_N should be an eigenstate of the total L_z orbital angular momentum, can be met by the simple choice of $f(z) \sim z^m$, where m is an odd integer. We thus arrive at the Laughlin wave function ψ_m:

$$\psi_m(z_1, \ldots, z_N) = \prod_{1 \le j < k \le N} (z_j - z_k)^m \left(e^{-\frac{1}{4l_B^2} \sum_{j=1}^{N} |z_j|^2} \right) \tag{1.43}$$

The ground state is determined by just finding the values of m that minimize the energy. But m is in fact determined by the total angular momentum.

Relativistic case

As we mentioned earlier, both Integer and Fractional Quantum Hall Effects have been discovered in graphene. Electrons in graphene behave as if they were relativistic massless particles. This means, that their quantum-mechanical behaviour is no longer described in terms of a (non-relativistic) Schrödinger equation, but rather by a relativistic 2D Dirac equation. As a consequence, Landau quantisation of the electrons kinetic energy turns out to be different in graphene than in conventional (non-relativistic) 2D electron systems.

Here we will focus on the relativistic Hamiltonian:

$$H_D = v\big(\overrightarrow{p} + e\overrightarrow{A}\big)\overrightarrow{\sigma} \tag{1.44}$$

For more details on how to arrive from the Honeycomb lattice in the tight binding model Hamiltonian to the Dirac Hamiltonian, one can look at [10].

The relativistic case (1.44) for electrons in graphene may be treated exactly in the same manner as the non-relativistic one. In terms of the ladder operators, the Hamiltonian reads:

$$H_D = v \begin{pmatrix} 0 & \pi_{\mathbf{x}} - i\pi_{\mathbf{y}} \\ \pi_{\mathbf{x}} + i\pi_{\mathbf{y}} & 0 \end{pmatrix} = \sqrt{2}\frac{\hbar v}{l_B} \begin{pmatrix} 0 & \alpha \\ \alpha^\dagger & 0 \end{pmatrix} \tag{1.45}$$

One remarks the occurrence of a characteristic frequency $\omega' = \frac{\sqrt{2}v}{l_B}$, which plays the role of the cyclotron frequency in the relativistic case. Note, however, that this frequency cannot be written in the form eB/m_b because the band mass is strictly zero in graphene, so that the frequency would diverge.

In order to obtain the eigenvalues and the eigenstates of the Hamiltonian (1.45), one needs to solve the eigenvalue equation $H_D\psi_n = E_n\psi_n$. where the eigenstates are 2-spinors:

$$\psi_n = \begin{pmatrix} u_n \\ v_n \end{pmatrix} \tag{1.46}$$

Thus, we need to solve the system of equations:

$$\hbar\omega'\alpha v_n = E_n u_n \quad \textit{and} \quad \hbar\omega'\alpha^\dagger u_n = E_n v_n \tag{1.47}$$

which results to the equation:

$$\alpha^\dagger\alpha v_n = \left(\frac{E_n}{\hbar\omega'}v_n\right)^2 \tag{1.48}$$

for the second spinor component. One may therefore identify, up to a numerical factor, the second spinor component v_n with the eigenstate $|n\rangle$ of the usual number operator $\alpha^\dagger\alpha = n$, with $\alpha^\dagger\alpha\,|n\rangle = n\,|n\rangle$ in terms of the integer $n \geq 0$. Furthermore, one observes that the square of the energy is proportional to this quantum number, $E_n = (\hbar\omega')^2 n$. This equation has two solutions, a positive and a negative one, and one needs to introduce another quantum number $\lambda = \pm$, which labels the states of positive and negative energy, respectively. We thus obtains the spectrum:

$$E_{\lambda,n} = \lambda\frac{\hbar\omega'}{l_B}\sqrt{2n} \tag{1.49}$$

of relativistic Landau Levels that disperse as $\lambda\sqrt{Bn}$ as a function of the magnetic field.

Once we know the second spinor component, the first spinor component is obtained from eq. (1.47), which reads $u_n \propto \alpha v_n \sim \alpha\,|n\rangle \sim |n-1\rangle$. One then needs to distinguish the zero-energy LL ($n = 0$) from all other levels. Indeed, for $n = 0$, the first component is zero. In this case one obtains

the spinor:

$$\psi_{n=0} = \begin{pmatrix} 0 \\ |n=0\rangle \end{pmatrix} \tag{1.50}$$

In all other cases ($n \neq 0$), one has positive and negative energy solutions, which differ among each other by a relative sign in one of the components. A convenient representation of the associated spinors is given by:

$$\psi_{\lambda,n\neq 0} = \frac{1}{\sqrt{2}} \begin{pmatrix} |n-1\rangle \\ \lambda\,|n\rangle \end{pmatrix} \tag{1.51}$$

It is worth noting, that in the massive Dirac Hamiltonian:

$$H_D^m = \begin{pmatrix} M & v(\pi_{\mathbf{x}} - i\pi_{\mathbf{y}}) \\ v(\pi_{\mathbf{x}} + i\pi_{\mathbf{y}}) & -M \end{pmatrix} = \begin{pmatrix} M & \sqrt{2}\frac{\hbar v}{l_B}\alpha \\ \sqrt{2}\frac{\hbar v}{l_B}\alpha^\dagger & -M \end{pmatrix} \tag{1.52}$$

one can obtain the eigenvalues in the same manner as in the $M = 0$ case, and finds:

$$E_{\lambda,n}^m = \lambda\sqrt{M^2 + 2\frac{\hbar^2 v^2}{l_B^2}n} \tag{1.53}$$

for the massive relativistic LLs with $n \neq 0$. The case of $n = 0$ needs special care.For more details one can look at [10].

1.3 The Luttinger Liquid

In this section we will present why the description of the Luttinger liquid is important to us. We will however not go into much of the technical details of the theory, which is a very rich one, but instead we discuss the most important parts which will be useful for our final steps of the project. Again, if one wants to take a more in-depth look into Luttinger liquid theory, we recommend to take a look into the book of Fradkin [2] from where we take a lot of the material for this Chapter.

We will look at the situation where the Landau theory fails in one-dimensional (1-D) Fermi systems. How about 1-D systems, though? Our environment is three dimensional, hence it is only approximate to describe a system in terms of just one space dimension. This approximation is based on the fact that we may consider the degrees of freedom in the transverse directions $\hat{y}$ and $\hat{z}$ frozen in their ground state at low enough temperatures and low enough energy scales for motion along the direction $\hat{x}$.

A wide range of physical systems, including nanowires, chains or ladders of ultracold atoms, optical waveguides, the edge states of 2D topological materials, and many more, may be described using this type of 1D approximation.

Now, by starting from the 1D system of non-interacting spinless fermions with fermions hopping along a chain:

$$H_0 = -t \sum_r \left[c^\dagger_{r+\alpha} c_r \; + \; H.c. \right] + \mu \sum_r c^\dagger_r c_r \tag{1.54}$$

where t is the hopping coefficient and α the lattice spacing, we can manipulate it by considering the physics at low temperature and energies and linearize the dispersion close to the Fermi surface to end up to the Hamiltonian of the form:

$$H_0 = \int i v_F \psi^\dagger_L \partial_x \psi_L - i v_F \psi^\dagger_R \partial_x \psi_R \tag{1.55}$$

where we introduced two fermionic chiral fields ψ_L and ψ_R and $v_F = \partial E(k)/\partial_k$ the Fermi velocity. By introducing the the spinor $\psi = (\psi_L, \psi_R)^T$ we finally obtain:

$$H_0 = \int i v_F \psi^\dagger \sigma_z \partial_x \psi \tag{1.56}$$

which is the 1-D Dirac Hamiltonian with σ_z the Pauli matrix.

This Dirac Hamiltonian can be expressed in terms of non-interacting boson fields as:

$$\mathcal{H}_{FQH} = \frac{v_F}{2\pi} \int dx \Big(\mathcal{K} (\partial_x \phi(x))^2 + \frac{1}{\mathcal{K}} (\partial_x \theta(x))^2 \Big) \tag{1.57}$$

where the fields $\phi(x)$ and $\theta(x)$ obey the duality relation:

$$\partial_\tau \theta = i v_F \mathcal{K} \partial_x \phi, \quad \partial_x \theta = i \frac{\mathcal{K}}{v_F} \partial_t \phi \tag{1.58}$$

Here $\mathcal{K}$ is called the Luttinger parameter and encodes many information for the system.

A process known as bosonization is used to describe interacting models of fermions (or bosons) on the basis of the (Tomonaga and) Luttinger model, a model of interacting and linearly dispersing fermions that can be precisely solved. The Luttinger liquid Hamiltonian will be described by the following , for instance, if we take into account a density-density interaction:

$$H = H_0 + H_{int} = H_0 + U \sum_r c^\dagger_{r+1} c_{r+1} c^\dagger_r c_r \tag{1.59}$$

where H_0 is the free Hamiltonian of eq. (1.54). This interacting model of spinless 1D fermions can be recast into a non-interacting model of bosons of the form of eq. (1.57). In this case however, the Fermi velocity will be a new renormalized velocity and the Luttinger parameter $\mathcal{K}$ will encode all the informations for interacting term whereas in the non-interacting case it has value $\mathcal{K} = 1$.

The above results can be extended also to the case of spin $1/2$ fermions, where the results will be

a bit more complicated. This will be the case similar to ours in this project.

This is just an introduction for the reader to have an idea of what is about to follow. More details about bosonization will come at Chapter (3).

1.4 Physics at the edge

The oscillations in the bulk result in fluctuations at the border in an incompressible quantum fluid, such as the Laughlin state. Local fluctuations in the bulk are linked to local changes in density, whereas local fluctuations in the states at the border are linked to variations in the appearance of the electron fluid's "droplet." The only gapless excitations of the system are these "edge waves." Although it may seem strange that even incompressible fluids have gapless excitations, typical fluids like water frequently exhibit gapless modes near the surface. The gaplessness in the FQHE is caused by the fact that the geometric edge of the fluid corresponds with the locus of sites where the Fermi energy crosses the external potential that limits the fluid. As a result, the fluid's border behaves like a "Fermi surface," and as we proceed from the edge into the bulk, we get deeper and deeper into the Fermi sea of occupied states. Edge waves are chiral excitations that travel at the drift velocity of the particles at that place due to the presence of a magnetic field. As a result, edge states may only travel in one direction, which is determined by the magnetic field.

The Fractional Quantum Hall Effect may alternatively be thought of as an IQHE of an analogous system of fermions within a mean (or average)-field approximation. As a result, we will discuss the FQHE edge states.

1.4.1 Hydrodynamic theory of the edge states

Consider a 2-Dimension Electron Gas (2DEG) confined by a confining potential to a limited (but huge) area of a sample. A quantum Hall state (integer or fractional), of such a system is an incompressible fluid because all states in the bulk contain a gap that may be made arbitrarily big by increasing the external magnetic field (while keeping the filling fraction of the Landau level fixed). A weak external electromagnetic disturbance acting on this charge fluid can only have a net influence on its border, resulting in slow and long-wavelength changes in its form. Because of the fluid's incompressibility, adiabatically adding or removing some charge from the bulk of the fluid is equal to adding or removing the same amount of charge from the edge. To put it another way, the entire fluid (bulk plus edge) must preserve charge. A fluid with local charge conservation obeys a continuity equation, which implies that its electromagnetic response must be gauge-invariant. This indicates that the charge cannot be preserved independently in the bulk or at the edge, but only in the system as a whole. This leads to the key discovery that breaches of gauge invariance in the bulk and at the edge must cancel out perfectly. This local conservation of charge leads to a simple and elegant

hydrodynamic theory.

We will not get into more details about the construction of this hydrodynamic theory since it is explained in Chapter 15 of [2]. We will however note here an important result of the calculation that can be found there.

After the construction of the hydrodynamic theory for the edge states, the Hamiltonian that describes one chiral edge state is:

$$H = \int dx \frac{v}{4\pi\nu} (\partial_x \phi)^2 \tag{1.60}$$

where $\nu = 1/m$ is the filling factor. Hence, the edge states of a fractional quantum Hall fluid constitute a chiral Luttinger liquid.

In this hydrodynamic theory it is assumed all along that the incompressible fluid has a unique edge with natural properties. The results of this quantized theory are telling that, without assuming any additional structure, a fractional quantum Hall state with a single edge can exist only for the Laughlin states at $\nu = 1/m$. As a result, for the Laughlin states, the electron operator at the edge is provided by (up to a normalization):

$$\psi_e(x) = e^{im\phi(x)} \tag{1.61}$$

These are some of the basic results of this Hydrodynamic theory for the edge states that we are going to use to our analysis for the bosonized description of our model.

1.5 Motivation

A theoretical proposal to synthesize a topological superconductor from a topological insulator and a conventional (s-wave) superconductor has motivated hybrid approaches to realize Majorana modes. Besides topological insulators, these approaches now include spin-orbit coupled semiconductors, magnetic atom chains, and integer quantum Hall edges all in combination with a superconductor offering either a testbed for or a route towards topological qubits. Common to all of these is the non-interacting description of charge carriers and Ising topological order which is insufficient for universal quantum computation. These approaches, however, can be extended to the computationally universal Fibonacci order predicted to emerge in a coupled parafermion array. Thus, in this subsection we are going to answer 3 important questions that may arise to the reader:

1. Why parafermions?
2. How exactly can one engineer parafermions?
3. How can they be detected experimentally?

Let's answer the first question, Why parafermions? Parafermions, unlike Majoranas, require electron-electron interactions to form, which result in richer non-Abelian braiding statistics. A standard condensed matter system that forms with interactions is the Fractional Quantum Hall (FQH) state, which is the basis of different approaches for synthesizing parafermions. The primary approach combining FQH, appearing in semiconductor heterostructures, with superconductivity has so far presented two major experimental challenges. First, the strong magnetic fields required for FQH suppress superconductivity. Second, coupling a superconductor to a semiconductor heterostructure can be difficult, often leading to a nontransparent interface.

In order to answer the second question , How exactly can one engineer parafermions?, we take a look at the theory. Theory predicts that Fractional Quantum Hall/superconductor hybrids devices can host parafermions, (since parafermions are Fractional Majorana modes it is only natural to search for them in the Fractional Quantum Hall systems). But FQH thrives in high magnetic fields, whilst the superconductor loses his superconductivity. The solution to this problem was given from a recent experiment performed by $\ddot{O}nder\ G\ddot{u}l$ who belongs in Philip Kim's group [1]. They used graphene-based Van der Waals (VdW) heterostructures coupled to superconducting niobium nitride (NbN), basically they cut the graphene and place the superconductor as shown in Figure (1.3). The high device quality decreases the magnetic fields required for robust FQH to the regime where NbN remains superconducting owing to its large critical field. The superconductor edge-contact to graphene provides an interface transparent enough to allow Crossed Andreev Reflection (CAR) in quantum Hall edges. The most important thing used in this setup is choice of the superconductor. Even in high magnetic fields, as high as 14T, the NbN does not loses its superconductivity. Another equally important property

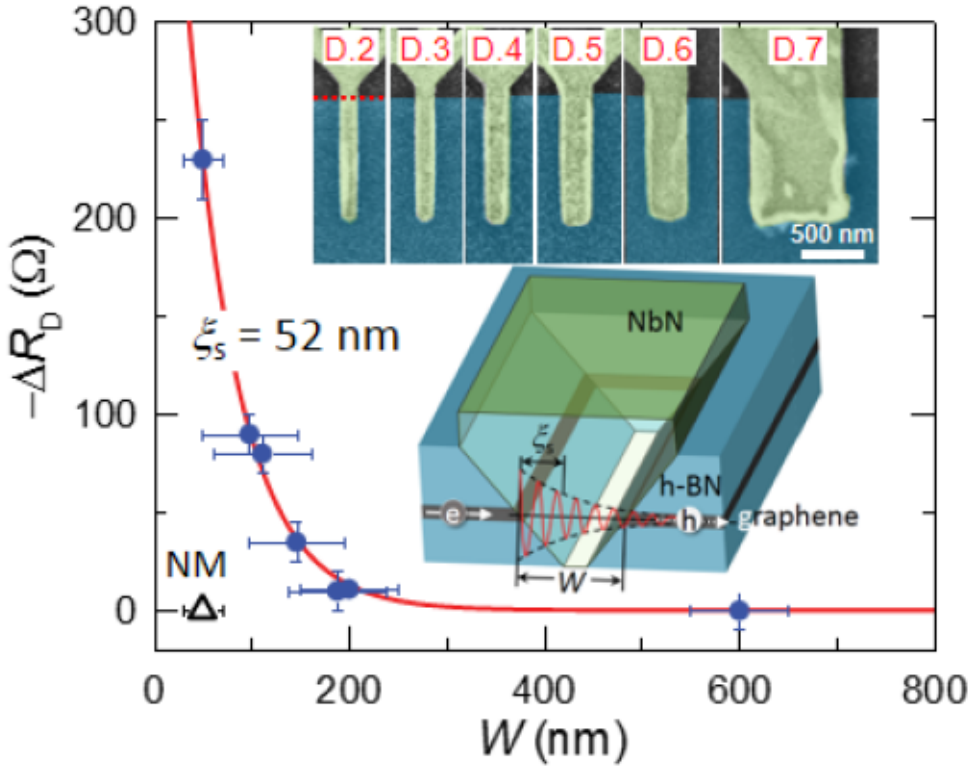

Figure 1.3: **Image taken from [11]**.The downstream resistance change (Δ_{RD}) exponentially decreases as W increases, due to the suppression of the CAC in a wide SC electrode. The data is fitted to the exponential function of $\Delta_{RD} = \Delta_{RD,0} exp(-W/\xi_s)$, with the superconducting coherence length (ξ_s) of NbN and the zero-width-limit value ($\Delta_{RD,0}$) as fitting parameters. Upper inset, False-coloured scanning electron microscope images of the devices of $W = 98, 111, 146, 188, 200, 600$nm, from the left to the right, respectively. Lower inset, A detailed schematic of the cross-section along the dotted red line in upper inset. Owing to the finite slope of the etching profile of the top h-BN, the effective width (W) between two graphene/NbN contacts is smaller than the apparent width of the superconducting electrode measured by the scanning electron microscope on the order of top h-BN thickness.

is the large spin-orbit coupling in NbN superconductor, which provides a necessary ingredient for a spin-flip process allowing for a pairing between electrons with the same spin polarization. The experimental results they found (shown in Figure (1.4)) are very important, because an $R_{CAR} < 0$ indicates that the electron-like carriers drained from the superconductor produce hole-like carriers with opposite charge, a direct result of Crossed Andreev Reflection, which reverses the sign of the edge potential. R_{CAR} acquires positive values either when R_{XY} is non-quantized and the bulk of the device conducts, or when superconductivity is suppressed with increasing T, both destroying CAR as expected. These results answer our third question of How can they be detected experimentally?

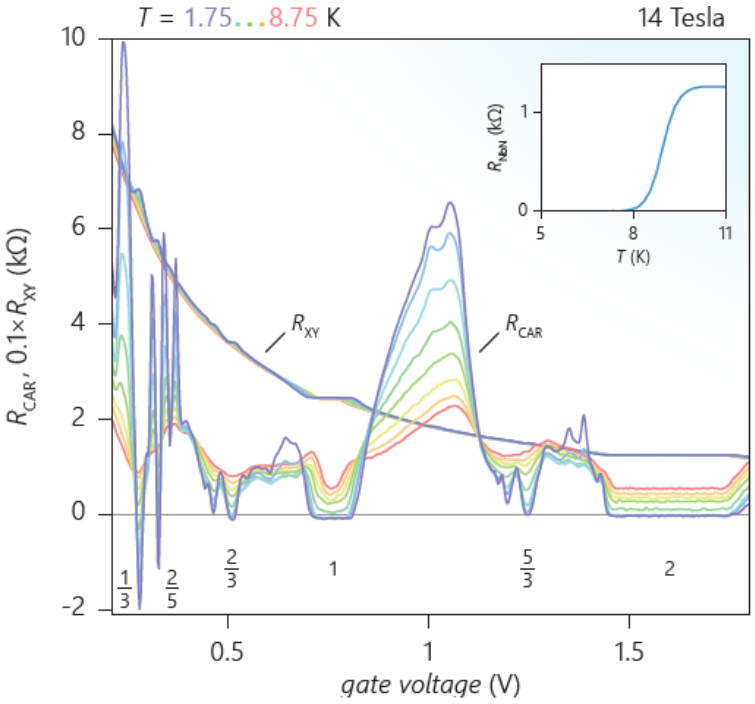

Figure 1.4: **Image taken from [1].** Indication of CAR in FQH. $R_{CAR} = V_{CAR}/I_{exc}$ and $R_{XY} = V_{XY}/I_{exc}$ as a function of gate voltage measured at B=14 T for different temperatures T. An R_{CAR} at Fractional Quantum Hall plateaus indicates hole conductance (CAR).

1.5.1 Parafermion properties

Having introduce the motivation behind this project it is time to introduce some of the algebraic properties of these exotic particles, the parafermions. For this purpose, we present here the parafermion properties as they are derived in [12].

According to [12], by implementing a non-local transformation on the generalized N-state quantum clock model, one can access some exotic zero modes. The clock model Hamiltonian is:

$$H = -J\sum_{j=1}^{L-1}\left(\sigma_j^{\dagger}\sigma_{j+1} + H.c\right) - h\sum_{j}^{L}\left(\tau_j^{\dagger} + \tau_j\right) \tag{1.62}$$

where $J \geq 0$ couples neighboring spins ferromagnetically, $h \geq 0$ is the transverse field, j labels sites of an L-site chain, and σ_j, τ_j are operators defined on an N-state Hilbert space that satisfy $\sigma_j^N = 1$, $\sigma_j^{\dagger} = \sigma_j^{N-1}$ and similarly for τ_j. The only non-trivial commutation relation among these operators reads $\sigma_j\tau_j = \sigma_j\tau_j e^{2\pi i/N}$. When $N = 2$ eq. (1.62) reduces to the familiar transverse field Ising model, though the phases realized in this special case appear also for general N. For example, with $J = 0$, $h > 0$ there exists a unique paramagnetic ground state with $\tau_j = +1$, while in the $J > 0$, $h = 0$ regime an N-fold degenerate ferromagnetic ground state with $\sigma_j e^{2\pi i q/N}$ emerges ($q = 1, \ldots N$).

By considering the non-local transformation:

$$\alpha_{2j-1} = \sigma_j \prod_{i<j} \tau_i, \quad \alpha_{2j} = -e^{i\pi/N} \tau_j \sigma_j \prod_{i<j} \tau_i \tag{1.63}$$

The properties of σ_j, τ_j dictate that these new operators satisfy

$$\alpha_j^N = 1, \tag{1.64}$$

$$\alpha_j^\dagger = \alpha_j^{N-1} \tag{1.65}$$

and

$$\alpha_j \alpha_{j'} = \alpha_{j'} \alpha_j e^{i\frac{2\pi}{N} sgn(j'-j)} \tag{1.66}$$

these operators are unitary and exhibit eigenvalues of the form $e^{2\pi iq/N}$ for integral q. Eq. (1.65) and (1.66) imply that:

$$\alpha_j^\dagger \alpha_{j'} = \alpha_{j'} \alpha_j^\dagger e^{-i\frac{2\pi}{N} sgn(j'-j)} \tag{1.67}$$

Moving $\alpha_{j'}$ past α_j therefore produces the opposite phase factor compared to moving $\alpha_{j'}$ past $\alpha_j^\dagger$. Consequently we obtain the following commutation relations:

$$\left[\alpha_i^\dagger \alpha_j, \alpha_k\right] = \left[\alpha_i^\dagger \alpha_j, \alpha_k^\dagger\right] = 0, \quad (k < i, j \ \ or \ \ k > i, j) \tag{1.68}$$

which further imply that:

$$\left[\alpha_i^\dagger \alpha_j, \alpha_k^\dagger \alpha_l\right] = 0 \tag{1.69}$$

so long as neither k nor l lie between i and j.

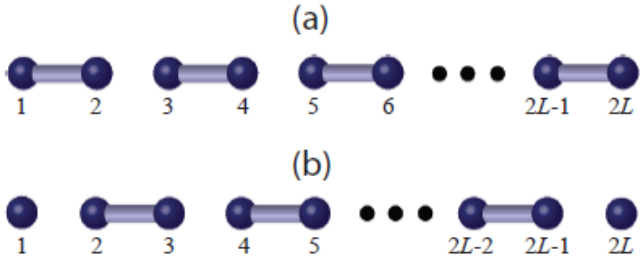

Figure 1.5: **Image taken from [12]**. Schematic illustration of the parafermion chain Hamiltonian in Eq. (1.62) when (a) $J = 0$ and (b) $h = 0$. In the latter case the ends of the chain support unpaired parafermion zero-modes that give rise to an N-fold ground-state degeneracy.

From eq. (1.68) and (1.69) one can simultaneously diagonalize each of the "dimers" sketched

in Figure 1.5 (a) and (b), as well as the combination of zero-mode operators $\alpha_{2L}^{\dagger}\alpha_1$ in case (b). To deduce the allowed eigenvalues, one can show from the above properties that:

$$\left(\alpha_i^{\dagger}\alpha_j\right)^N = (-1)^{N+1}, \tag{1.70}$$

which constrains the eigenvalues of $\alpha_i^{\dagger}\alpha_j$ to the form $-e^{i\frac{2\pi}{N}sgn(q-1/2)}$ where q is an integer. In the quantum clock model context, the eigenvalues of the relevant "dimer" operators can alternatively be found using the relations: gather*

$$\begin{aligned} \alpha_{2j-1}^{\dagger}\alpha_{2j} &= -e^{i\pi/N}\tau_j \\ \alpha_{2j}^{\dagger}\alpha_{2j+1} &= -e^{i\pi/N}\sigma_j^{\dagger}\sigma_{j+1} \\ \alpha_{2L}^{\dagger}\alpha_1 &= -e^{i\pi/N}\Big(\prod_i^L \tau_i^{\dagger}\Big)\sigma_L^{\dagger}\sigma_1 \end{aligned} \tag{1.71}$$

that arise from the non-local transformation specified in eq. 1.63. Equations (1.71) yield the same eigenvalue spectrum for the operators on the left-hand side as noted above since τ_j and σ_j both exhibit non-degenerate eigenvalues $e^{2\pi iq/N}$ for $q = 1, \ldots, N$.

Consider now the case where α_1 and α_{2L} represent zero-modes and deduce the action of these operators on the ground state manifold. If $|q\rangle$ is a ground state satisfying $\alpha_1^{\dagger}\alpha_{2L}\,|q\rangle$, then by using the parafermion commutation relations one can show that:

$$(\alpha_1^{\dagger}\alpha_{2L})\alpha_j = e^{-i\frac{2\pi}{N}}\alpha_j(\alpha_1^{\dagger}\alpha_{2L}) \tag{1.72}$$

for either $j = 1$ or $j = 2L$. "This equation implies that $\alpha_{1,2L}^{\dagger}\,|q\rangle \propto |q+1\rangle$ where the proportionality constants have unit magnitude. One can always fix the relative phases of the ground states such that" [12]:

$$\alpha_1^{\dagger}\,|q\rangle = |q+1\rangle\,, \quad \alpha_1\,|q\rangle = |q-1\rangle \tag{1.73}$$

By using this convention, α_{2L} acts as:

$$\alpha_{2L}^{\dagger}\,|q\rangle = -e^{-i\frac{2\pi}{N}(q-1/2)}\,|q+1\rangle\,, \quad \alpha_{2L}\,|q\rangle = -e^{i\frac{2\pi}{N}(q-1/2)}\,|q-1\rangle \tag{1.74}$$

Having introduce the properties of these parafermion operators one can write the Hamiltonian in eq. (1.62) as:

$$H = J\sum_{j=1}^{L-1}\left(e^{-i\frac{\pi}{N}}\alpha_{2j}^{\dagger}\alpha_{2j+1} \;+\; H.c\right) + h\sum_{j}^{L}\left(e^{i\frac{\pi}{N}}\alpha_{2j-1}^{\dagger}\alpha_{2j} \;+\; H.c\right) \tag{1.75}$$

"In the paramagnetic limit with $J = 0$ the operators "pair up" as sketched in Figuge 1.5(a).

Simultaneously diagonalization of this collection of "dimers", gives the eigenvalues $\alpha^\dagger_{2j-1}\alpha_{2j} = -e^{i\frac{2\pi}{N}(n_j-1/2)}$ for integer n_j. Here there exists a unique ground state with $n_j = 0$ that is fully gapped since exciting any of these dimers costs finite energy. More interestingly, the ferromagnetic case $h = 0$ produces the shifted dimerization shown in Fig. 1.5(b). A bulk gap arises here for the same reason, though the ends of the chain now support "unpaired" zero-modes α_1 and α_{2L} that encode the N-fold degeneracy of the clock models ferromagnetic phase ($\alpha^\dagger_{2L}\alpha_1$ admits N distinct eigenvalues that do not affect the energy). At N = 2 the zero-mode operators $\alpha_{1,2L}$ form the unpaired Majoranas, while for N > 2 they correspond to parafermion zero-modes" [12].

1.6 Single Particle of 1D Quantum Wires

Previously, we noted the importance of a strong spin orbit coupling (SOC) and a strong magnetic field. What we want now, is to define a Hamiltonian that describes a 1D Quantum Wire with a SOC and a high magnetic field. This Hamiltonian will have the form:

$$H_{wire} = \sum_{ss'} \int dk \big[\psi^\dagger_{s,k}(\xi_k + \alpha k\sigma_y + \tilde{B}\sigma_z)\psi_{s',k}\big] \tag{1.76}$$

where s, s' denotes the spin components, $\xi_k = \frac{k^2}{2m} - \mu$ the kinetic term with μ the chemical potential, α the strength of spin-orbit Rashba interaction and $\tilde{B} = g\mu_B B$ the Zeeman field with μ_B the Bohr magneton, g is the Landé g-factor, B the magnetic field and $\overrightarrow{\sigma} = (\sigma_x, \sigma_y, \sigma_z)$ the Pauli matrices.(The precise spin-orbit and magnetic field axes are unimportant so long as they are perpendicular cause this help to induce topological superconductivity). By taking the magnetic field in $\hat{z}$-direction the spin orbit coupling will be in $\hat{y}$-direction. To see why, let's consider that the chemical pontential is $\mu(z) = \mu_0\hat{z}$ (in 3D systems it is not entirely correct, but it is a good approximation considering the average chemical potential contribution for systems like in Figure 1.3). The Rashba effect is a direct result of inversion symmetry breaking in the direction perpendicular to the 2-dimensional plane. Thus, it enters the Hamiltonian as a term that breaks this symmetry in the form of an electric field. The direction of the electric field is found by solving the Poisson equation:

$$\overrightarrow{E} = -\overrightarrow{\nabla}\mu(z) = E_0\hat{z}$$

Assuming that we have a 1D quantum wire (or 2D, still the same) we will have the momemtunm along $\hat{x}$-direction. i.e $\overrightarrow{p_x} = p_x\hat{x}$, with v_x velocity. Due to relativistic corrections, an electron moving with velocity $\overrightarrow{v}$ in the electric field, will experience an effective magnetic field $\overrightarrow{B}$. The Magnetic field experienced due to Electric field is:

$$\overrightarrow{B} = -(\overrightarrow{v} \times \overrightarrow{E})/c^2$$

where $\overrightarrow{v} = (v_x, 0, 0)$ the velocity, $\overrightarrow{E} = (0, 0, E_0)$ the Electric field and c is the speed of light. This magnetic field couples to electron spin in a spin orbit term:

$$H_{SO} = \frac{g\mu_B}{2c^2}\overrightarrow{\sigma} \cdot (\overrightarrow{p} \times \overrightarrow{E}) = -\frac{g\mu_B}{2c^2}\overrightarrow{\sigma} \cdot (E_0\hat{z} \times p_x\hat{x})$$
$$\Rightarrow H_{SO} = -\frac{g\mu_B}{2c^2}E_0 p_x \overrightarrow{\sigma} \cdot \hat{y} = \alpha p_x \sigma_y$$

where $\alpha = -\frac{g\mu_B E_0}{2c^2}$ the Rashba coefficient, $\mu_B = \frac{eh}{4\pi m_e}$ the Bohr magneton and $\overrightarrow{\sigma} = (\sigma_x, \sigma_y, \sigma_z)$ the Pauli matrices. Note here, that these coefficients are for a signle particle, i.e that for our later calculations we will not have these values, but in terms of directions are the same.

We proceed by solving the 1D Quantum wire Hamiltonian for a single particle:

$$H_{sp} = \xi_k + \alpha k \sigma_y + \tilde{B}\sigma_z \tag{1.77}$$

which can be written in a matrix form as :

$$H_{sp} = \begin{pmatrix} \xi_k + \tilde{B} & -i\alpha k \\ i\alpha k & \xi_k - \tilde{B} \end{pmatrix} \tag{1.78}$$

To find its eigenvalues, we solve the determinant of the matrix:

$$\begin{vmatrix} \xi_k + \tilde{B} - E & -i\alpha k \\ i\alpha k & \xi_k - \tilde{B} - E \end{vmatrix} = 0 \Rightarrow E_\pm = \xi_k \pm \sqrt{\tilde{B}^2 + (\alpha k)^2} \tag{1.79}$$

Let's analyze its spectrum:

- For $\alpha = \tilde{B} = 0$, we have :

$$E_\pm = \xi_k$$

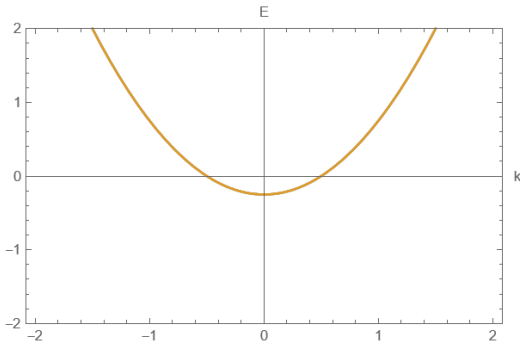

Figure 1.6: Here we see the spectrum of the kinetic term only where we do not include the strong SOC, the magnetic field is turned off ($\tilde{B} = 0$) and the superconducting pairing potential $\Delta = 0$.

- For $\alpha \neq 0, \tilde{B} = 0$, we have :

$$E_{\pm} = \xi_k \pm \alpha k$$

the spectrum is shifted.

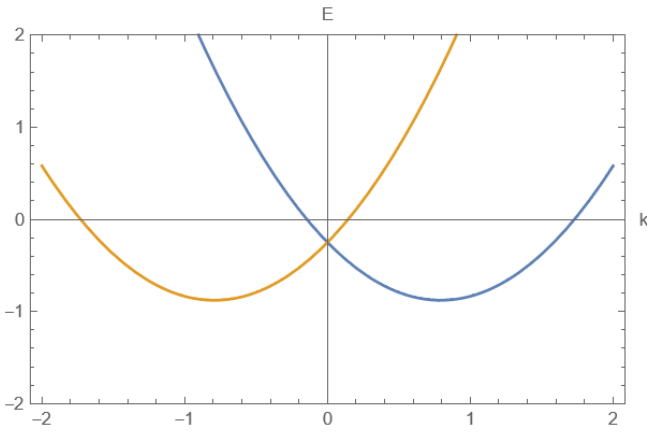

Figure 1.7: Here we see that the spectrum is shifted when we include the strong SOC and we get 2 energy bands, the magnetic field is turned off ($\tilde{B} = 0$) and the superconducting pairing potential $\Delta = 0$.

- For $\alpha \neq 0, \tilde{B} \neq 0$, we have :

$$E_{\pm} = \xi_k \pm \sqrt{\tilde{B}^2 + (\alpha k)^2}$$

A gap opens between the 2 energy bands $E_+(k)$,$E_-(k)$ that depends on $\tilde{B}$ and is equal to $2\tilde{B}$.

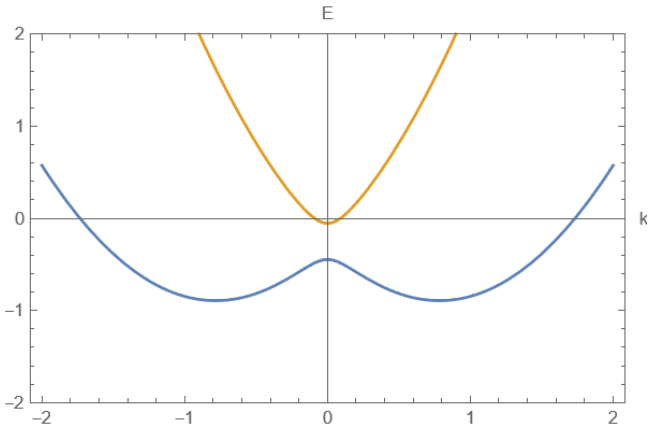

Figure 1.8: Here we see that the spectrum is shifted when we include the strong SOC, the magnetic field is turned on now ($\tilde{B} \neq 0$) which result to the Zeeman splitting between the 2 energy bands and the superconducting pairing potential $\Delta = 0$.

In the previous calculations we assumed $\mu = 0$ for simplicity. Therefore, if μ is placed inside the

gap, spinless superconductivity can be induced by the proximity effect. Note, that larger $\tilde{B}$ makes the effectively spinless regime larger and provides a larger window to place the chemical potential, which is important if disorders causes the chemical potential to vary. However, the larger field also enforces the alignment to the spin within each band and makes it harder to induce superconductivity. This is what meant when we mentioned earlier that high magnetic fields destroy superconductivity and why using the NbN superconductor is very important.

Our next step is to calculate the eigenvectors corresponding to eq. (1.79). We define these eigenvectors as:

$$\psi = \begin{pmatrix} \psi_+ \\ \psi_- \end{pmatrix} = \psi_+ \left|\uparrow\right\rangle + \psi_- \left|\downarrow\right\rangle . \tag{1.80}$$

where $|\uparrow\rangle$ and $|\downarrow\rangle$ are the eigenstates in σ_z-basis. To dermine them, we solve the Schrödinger equation:

$$H_{sp}\psi_\pm = E_\pm\psi_\pm \Rightarrow \begin{pmatrix} \xi_k + \tilde{B} - E_\pm & -i\alpha k \\ i\alpha k & \xi_k - \tilde{B} - E_\pm \end{pmatrix} \begin{pmatrix} \psi_+ \\ \psi_- \end{pmatrix} = 0 \Rightarrow$$
$$\begin{pmatrix} \psi_+ \\ \psi_- \end{pmatrix} = \begin{pmatrix} \left(\frac{\tilde{B}\pm\sqrt{\tilde{B}^2+(\alpha k)^2}}{i\alpha k}\right)\psi_- \\ \psi_- \end{pmatrix} = \left(\frac{\tilde{B} \pm \sqrt{\tilde{B}^2 + (\alpha k)^2}}{i\alpha k}\right)\psi_- \left|\uparrow\right\rangle + \psi_- \left|\downarrow\right\rangle \tag{1.81}$$

We want our state to be normalized, so it needs to obey the relation:

$$|\psi_+|^2 + |\psi_-|^2 = 1 \Rightarrow \psi_- = \pm\frac{ak}{\left(\left(\tilde{B} \pm \sqrt{\tilde{B}^2 + (\alpha k)^2}\right)^2 + (\alpha k)^2\right)^{1/2}} \tag{1.82}$$

Thus, we get also:

$$\psi_+ = \left(\frac{\tilde{B} \pm \sqrt{\tilde{B}^2 + (\alpha k)^2}}{i\alpha k}\right)\psi_- = \frac{\tilde{B} \pm \sqrt{\tilde{B}^2 + (\alpha k)^2}}{i\alpha k}\frac{\pm ak}{\left(\left(\tilde{B} \pm \sqrt{\tilde{B}^2 + (\alpha k)^2}\right)^2 + (\alpha k)^2\right)^{1/2}} \Rightarrow$$
$$\psi_+ = \pm\frac{\left(\tilde{B} \pm \sqrt{\tilde{B}^2 + (\alpha k)^2}\right)}{i\left(\left(\tilde{B} \pm \sqrt{\tilde{B}^2 + (\alpha k)^2}\right)^2 + (\alpha k)^2\right)^{1/2}} \tag{1.83}$$

Thus, we have:

$$\psi = \begin{pmatrix} \psi_+ \\ \psi_- \end{pmatrix} = \begin{pmatrix} \frac{\left(\tilde{B}+\sqrt{\tilde{B}^2+(\alpha k)^2}\right)}{i\left(\left(\tilde{B}+\sqrt{\tilde{B}^2+(\alpha k)^2}\right)^2+(\alpha k)^2\right)^{1/2}} \\ \frac{ak}{\left(\left(\tilde{B}+\sqrt{\tilde{B}^2+(\alpha k)^2}\right)^2+(\alpha k)^2\right)^{1/2}} \end{pmatrix} \tag{1.84}$$

In genetal, a quantum state can be expressed as a projection to the Bloch sphere as:

$$|\psi\rangle = \cos\frac{\vartheta}{2}\,|\uparrow\rangle + e^{i\phi}\sin\frac{\vartheta}{2}\,|\downarrow\rangle \tag{1.85}$$

(keeping the notation of our previous σ_z-basis) where $0 \leq \theta \leq \pi$ and $0 \leq \phi \leq 2\pi$. We can get rid of of the ϕ angle by multiplying our whole state by a so-called global phase. This multiplication does not change the state as two states which differ in global phase are identical. If we want to project the states of eq, (1.84) in the Bloch sphere, we have first (for the state with the $-$ sign in front of αk because this gives us the lowest energy band) to define:

$$\cos\frac{\vartheta(k)}{2} = \frac{\left(\tilde{B} + \sqrt{\tilde{B}^2 + (\alpha k)^2}\right)}{\left(\left(\tilde{B} + \sqrt{\tilde{B}^2 + (\alpha k)^2}\right)^2 + (\alpha k)^2\right)^{1/2}}, \sin\frac{\vartheta(k)}{2} = \frac{-ak}{\left(\left(\tilde{B} \pm \sqrt{\tilde{B}^2 + (\alpha k)^2}\right)^2 + (\alpha k)^2\right)^{1/2}} \tag{1.86}$$

Thus, we get:

$$\left|\psi^+\right\rangle = i\Big(\cos\frac{\vartheta}{2}\,|\uparrow\rangle - i\sin\frac{\vartheta}{2}\,|\downarrow\rangle\Big) = e^{i\phi'}\Big(\cos\frac{\vartheta}{2}\,|\uparrow\rangle + e^{i\phi}\sin\frac{\vartheta}{2}\,|\downarrow\rangle\Big) \tag{1.87}$$

where $\phi' = \frac{1}{2}(4\pi n + \pi)$, $n \in \mathbb{Z}$ a global phase, $\phi = \frac{1}{2}(4\pi n - \pi)$ with $0 \leq \phi \leq 2\pi$ and the dependence over momentum k (for $\psi_\pm(k)$ and $\vartheta(k)$) is implied. Here, the $+$ sign in the state denotes that we are considering the upper energy band. In order to calculate the angle θ, we need to determine first the $\tan\theta$. Thus, we have:

$$\tan\vartheta = \frac{2\tan\frac{\vartheta}{2}}{1-\tan^2\frac{\vartheta}{2}} = 2\frac{\frac{\sin\frac{\vartheta}{2}}{\cos\frac{\vartheta}{2}}}{1-\frac{\sin^2\frac{\vartheta}{2}}{\cos^2\frac{\vartheta}{2}}} = 2\frac{\frac{\sin\frac{\vartheta}{2}}{\cos\frac{\vartheta}{2}}}{\frac{\cos^2\frac{\vartheta}{2}-\sin^2\frac{\vartheta}{2}}{\cos^2\frac{\vartheta}{2}}} = \frac{2\cos\frac{\vartheta}{2}\sin\frac{\vartheta}{2}}{\cos^2\frac{\vartheta}{2}-\sin^2\frac{\vartheta}{2}} \tag{1.88}$$

By replacing the above expressions for $\cos\frac{\vartheta}{2}$ and $\sin\frac{\vartheta}{2}$ we can determine the expression for θ by writting $y = \tan\vartheta$ and calculating:

$$\vartheta = \arctan y \tag{1.89}$$

This is the more general way on how to treat the angles in the Bloch sphere. As we will show in Chapter (3) we use another way to determine the angle ϑ. The state orthogonal to $|\psi^+\rangle$ is:

$$\left|\psi^-\right\rangle = \sin\frac{\vartheta}{2}\,|\uparrow\rangle + i\cos\frac{\vartheta}{2}\,|\downarrow\rangle \tag{1.90}$$

where we can neglect the global phase. We ensured, by writing these states in the Bloch sphere representation, that these are pure states and can be treated as qubits.

In this project we are considering high magnetic fields, which means that our Quantum Hall will be polarized in the σ_z-direction (direction of the magnetic field). But as we will explain later it will be more time consuming, in terms of calculations, to keep our SC eigenstates in this basis. Thus, it would be good to express our eigenstates in the σ_y-basis. To do so, we need to find the relations between the σ_y and σ_z eigenstates.

If we solve the eigenvalue problem for σ_y, it is easy to see that:

$$|+\rangle = \frac{1}{\sqrt{2}} \begin{pmatrix} 1 \\ i \end{pmatrix} = \frac{1}{\sqrt{2}}(|\uparrow\rangle + i\,|\downarrow\rangle) \tag{1.91}$$

and

$$|-\rangle = \frac{1}{\sqrt{2}} \begin{pmatrix} 1 \\ -i \end{pmatrix} = \frac{1}{\sqrt{2}}(|\uparrow\rangle - i\,|\downarrow\rangle) \tag{1.92}$$

Now, we can project our eigenstates from σ_z to σ_y-basis, by inverting the previous relations as follows:

$$\begin{gathered} \big|\psi^+(k)\big\rangle = \cos\frac{\vartheta}{2}\,|\uparrow\rangle - i\sin\frac{\vartheta}{2}\,|\downarrow\rangle \Rightarrow \\ \big|\psi^+(k)\big\rangle = \frac{1}{\sqrt{2}}\big(\cos\frac{\vartheta}{2} - \sin\frac{\vartheta}{2}\big)\,|+\rangle + \frac{1}{\sqrt{2}}\big(\cos\frac{\vartheta}{2} + \sin\frac{\vartheta}{2}\big)\,|-\rangle \end{gathered} \tag{1.93}$$

Similar, we get for $|\psi^-(k)\rangle$:

$$\big|\psi^-(k)\big\rangle = \frac{1}{\sqrt{2}}\big(\sin\frac{\vartheta}{2} + \cos\frac{\vartheta}{2}\big)\,|+\rangle + \frac{1}{\sqrt{2}}\big(\sin\frac{\vartheta}{2} - \cos\frac{\vartheta}{2}\big)\,|-\rangle \tag{1.94}$$

In a matrix form, these states can be written as:

$$\begin{pmatrix} |\psi^+(k)\rangle \\ |\psi^-(k)\rangle \end{pmatrix} = \frac{1}{\sqrt{2}} \begin{pmatrix} \cos\frac{\vartheta}{2} - \sin\frac{\vartheta}{2} & \cos\frac{\vartheta}{2} + \sin\frac{\vartheta}{2} \\ \sin\frac{\vartheta}{2} + \cos\frac{\vartheta}{2} & \sin\frac{\vartheta}{2} - \cos\frac{\vartheta}{2} \end{pmatrix} \begin{pmatrix} |+\rangle \\ |-\rangle \end{pmatrix} \tag{1.95}$$

Since these states were found in momentum space, we can perform a Fourier transformation to go to real space where we will get:

$$\big|\psi^\pm(x)\big\rangle = \int \frac{dk}{\sqrt{2\pi}} e^{ikx}\,\big|\psi^\pm(k)\big\rangle \tag{1.96}$$

We are gonna make use of these definitions again in the beginning of Chapter (3).

Chapter 2

Model

As we mentioned previously, in Chapter 1.6 we defined the 1-D Hamiltonian that describes a quantum wire with a SOC and a high magnetic field. The reason we chose our Hamiltonian to be 1-D is because it is the simplest case to describe the physics that governs our model. At first glimpse, one might wonder how can this 1-D model find applications in a 3-D world? To answer that question we will follow the same procedure as they do in [13].

Their starting point is a BCS Hamiltonian describing an s-wave SC in a magnetic field:

$$H_{BCS} = \sum_{\sigma} \int d^3r \left[c^{\dagger}(\mathbf{r}) \Big(\frac{[-i\nabla + e\mathbf{A}(y)]^2}{2m_s} - \mu_s \Big) c(\mathbf{r}) - \big(\Delta_0 c^{\dagger}_{\uparrow}(\mathbf{r}) c^{\dagger}_{\downarrow}(\mathbf{r}) + H.c. \big) \right] \tag{2.1}$$

where $c(\mathbf{r})$ is the annihilation operator for an electron with spin σ at position $r = (x, y, z)$, m_s is the effective electron mass, μ_s is the chemical potential, Δ_0 is the superconducting order parameter in the form of a complex-valued constant and $\mathbf{A}(y)$ is a suitable gauge potential. By making some approximations they end up to describing the SC surface states by the Hamiltonian:

$$H^{surface}_{BCS} = \sum_{\sigma} \int d^3r \left[c^{\dagger}(\mathbf{r}) \Big(-\frac{1}{2m_s} \nabla^2 - \mu_s \Big) c(\mathbf{r}) - \big(\Delta_0 e^{-2ik_s x} c^{\dagger}_{\uparrow}(\mathbf{r}) c^{\dagger}_{\downarrow}(\mathbf{r}) + H.c. \big) \right] \tag{2.2}$$

where $k_s = |k_s| = eB_0\lambda = \lambda/l^2$ is the constant value of the vector potential at the interface with λ the magnetic penetration depth and l the magnetic length. Then, in order for Andreev reflection to occur between an s-wave SC and a spin-polarized edge state, they want some spin-flip mechanism to be present. Thus, they include a SOC term in their Hamiltonian.

$$H_{SOC} = \alpha \sum_{\mathbf{k}} (k_z + ik_x) c^{\dagger}_{\mathbf{k},\uparrow} c_{\mathbf{k},\downarrow} \;\; + \;\; h.c \tag{2.3}$$

But as they state, the origin of Andreev reflection is the tunneling of single electrons from the QH edge state into the SC near the interface. Weak tunneling across the interface can be described as

single-electron tunneling between electronic states with identical spins states within a limited range in the y and z dimensions. Assuming the tunneling to be local in the fields $\psi(x)$ and $c_\uparrow(r)$ the tunneling Hamiltonian is given by:

$$H_{tunn} = \Gamma \sum_{q,\mathbf{k}} \delta_{q,\mathbf{k_x}} \left(\psi_q^\dagger c_{\uparrow,\mathbf{k}} + H.c.\right) \tag{2.4}$$

where Γ represents an effective tunneling amplitude and the Kronecker delta $\delta_{q,\mathbf{k_x}}$ reflects the fact that local tunneling and translational invariance along the x axis implies conservation of x-momentum. Thus tunneling can only occur between electron states with the same momentum in x direction.

This observation is enough for us to treat our model in one dimension and examine its results for future practical applications.

2.1 Model

In our project we are interested in describing the Crossed Andreev Reflection (CAR) between the Superconductor and the Quantum Hall edge system. This system can be described by the Hamiltonian:

$$\mathcal{H}(k) = H_{SC}(k) + H_{QH}(k) + H_t(k) \tag{2.5}$$

where

$$H_{SC}(k) = \sum_{ss'} \int dk [\psi^\dagger_{SC,s,k}(\xi_k + \alpha k \sigma_y + \tilde{B}\sigma_z)\psi_{SC,s',k} - \Delta \psi^\dagger_{SC,\uparrow,k}\psi^\dagger_{SC,\downarrow,-k} - \Delta^* \psi_{SC,\downarrow,-k}\psi_{SC,\uparrow,k}] \tag{2.6}$$

$$\begin{aligned} H_{QH}(k) = \frac{v}{2\pi} \int dk [(\psi^\dagger_{QH,\uparrow,k,L}(k)\psi_{QH,\uparrow,k,L} - \psi^\dagger_{QH,\uparrow,k,R}(k)\psi_{QH,\uparrow,k,R}) + \\ \mu_{QH}(\psi^\dagger_{QH,\uparrow,k,L}\psi_{QH,\uparrow,k,L} + \psi^\dagger_{QH,\uparrow,k,R}\psi_{QH,\uparrow,k,R}(k))] \end{aligned} \tag{2.7}$$

$$H_t(k) = -t \int dk \sum_{j=L,R} [\psi^\dagger_{QH,\uparrow,k,j}\psi_{SC,\uparrow,k} + \psi^\dagger_{SC,\uparrow,k}\psi_{QH,\uparrow,k,j}] \tag{2.8}$$

where t is the tunneling coefficient and $\mu_{QH} \neq \mu_{SC}$. The $H_{SC}(k)$ will be presented in the Chapter (2.2) analytically. As for the form the Quantum Hall Hamiltonian, it describes the 2 propagating chiral edge modes which we denote as Left- and Right-movers. Furthermore, the due to the strong magnetic field the spin in the quantuma hall is polarized the in the direction of the magnetic field, which in our case is the $\hat{z}$-direction and corresponds to spin $\uparrow$. Finally, the $H_t(k)$ is the classical tunneling Hamiltonian between 2 systems. We will approach the derivation of these CAR with 2 analytical methods. The first will be via perturbation theory (2.3) and the second will be by performing the path integral technique (2.4) for field theory.

2.2 S-wave Superconductor

We start by constructing our conventional 1-D wire. The basic ingredients are a 1D wire with appreciable spin-orbit coupling, a conventional s-wave superconductor, and a modest magnetic field. This is the general way that we construct an a Hamiltonian that describes an s-wave Superconductor. In our case, the superconductor will be the NbN which as we mentioned already it contains the SOC mechanism. Thus, we present the Hamiltonian for s-wave Superconductor with a SOC and in a strong magnetic field to be of the form:

$$H_{SC} = \sum_{ss'} \int dk [\psi^{\dagger}_{s,k}(\xi_k + \alpha k \sigma_y + \tilde{B}\sigma_z)\psi_{s',k} - \Delta \psi^{\dagger}_{\uparrow,k}\psi^{\dagger}_{\downarrow,-k} - \Delta^* \psi_{\downarrow,-k}\psi_{\uparrow,k}] \tag{2.9}$$

where $\xi_k = \frac{k^2}{2m} + \mu$ is the kinetic term and the chemical potential μ, α states the intensity of the Rashba interaction, $\tilde{B}$ is the Zeeman energy arising from a magnetic field applied along z-direction and $\psi_{s,k}$ is the fermionic field. We can write the Bogoliubov de Gennes Hamiltonian in the Nambu space by introducing the the Nambu spinors:

$$\Psi = \begin{pmatrix} \psi_{\uparrow,k} \\ \psi_{\downarrow,k} \\ -\psi^{\dagger}_{\downarrow,-k} \\ \psi^{\dagger}_{\uparrow,-k} \end{pmatrix} \tag{2.10}$$

This Nambu spinor has been written in the σ_z basis. In the matrix form, our Bogoliubov de Gennes Hamiltonian is written as:

$$H_{BdG}(k) = \begin{pmatrix} H_0(k) & -\Delta\mathbb{I} \\ -\Delta\mathbb{I} & -\sigma_y H_0^*(-k)\sigma_y \end{pmatrix} = \begin{pmatrix} \xi_k + \tilde{B} & -i\alpha k & -\Delta & 0 \\ i\alpha k & \xi_k - \tilde{B} & 0 & -\Delta \\ -\Delta & 0 & -\xi_k + \tilde{B} & i\alpha k \\ 0 & -\Delta & -i\alpha k & -\xi_k - \tilde{B} \end{pmatrix} \tag{2.11}$$

where $\mathbb{I}$ labels the 2×2 identity matrix. The term $-\sigma_y H_0^*(-k)\sigma_y$ in eq. (2.11) denotes the time-reversal of $H_0(k)$ and appears since holes are time-reversed electrons. In particular here, the time reversal operator is $\hat{\mathcal{T}} = \mathbb{I}K$, where K is the operator for complex conjugation. The magnetic field breaks this time-reversal symmetry as can easily be seen.

We are writing now the BdG Hamiltonian in the form:

$$H_{BdG} = \xi_k \tau_z + \alpha k \sigma_y \tau_z + \tilde{B}\sigma_z - \Delta\tau_x \tag{2.12}$$

where $\tau(x, y, z)$ are the Pauli matrices in Nambu space and we have assumed Δ is real for simplicity

(σ and τ operate in spin and particle-hole space respectively). In particular, the $\tau(x, y, z)$ matrices have the same form as the Pauli matrices $\sigma(x, y, z)$ but act in different sub-block in the 4×4 matrix of eq. (2.11). In order to construct this 4×4 matrix one has to calculate the tensor product of the $\tau(x, y, z)$ matrices with the identity and with the $\sigma(x, y, z)$ matrices where it is needed. For example:

$$\tau_r = \tau_r \otimes \mathbb{I}, \qquad r = x, y, z \tag{2.13}$$

In this way, we can express our original Superconducting Hamiltonian in the Nambu base as:

$$H_{SC} = \int dk \Psi^\dagger (H_{BdG}) \Psi \tag{2.14}$$

What we manage so far was not to introduce some new physics in the system, but to unveil the hidden physics of our model. This means, that by doubling the dimensions of our Hamiltonian by introducing the holes, we also doubled the number of eigenstates. Therefore, there must be some symmetry relation between the eigenstates such that the number of independent solutions remains the same. This symmetry is called electron-hole symmetry and is expressed through the operator:

$$P = \tau_y \otimes \sigma_y K = \begin{pmatrix} 0 & 0 & 0 & -1 \\ 0 & 0 & 1 & 0 \\ 0 & 1 & 0 & 0 \\ -1 & 0 & 0 & 0 \end{pmatrix} K \tag{2.15}$$

where K is the operator for complex conjugation. One can easily verify by using the anti-commutation relations of the Pauli matrices, that:

$$P H_0(k) P^\dagger = -H_0(k) \tag{2.16}$$

$$P \Delta P^\dagger = -\Delta \tag{2.17}$$

By writing our Hamiltonian in the form of eq. (2.12) we manage to make an eigenstate problem into an eigenvalue problem. We can easily find analytically the eigenvalues of eq. (2.12) as shown in Appendix (A.1). Thus, we found them to be:

$$E^2_{BdG,\pm} = \xi_k^2 + (\alpha k)^2 + \tilde{B}^2 + \Delta^2 \pm 2\sqrt{\xi_k^2\big((\alpha k)^2 + \tilde{B}^2\big) + \tilde{B}^2\Delta^2} \tag{2.18}$$

This trick is general and we can use it whenever our Hamiltonian consists of matrices (or their tensor products) which satisfy Clifford algebra.

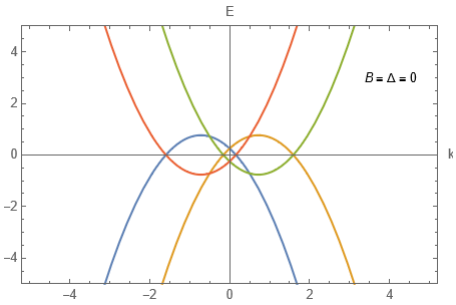

(a) Spin splitting

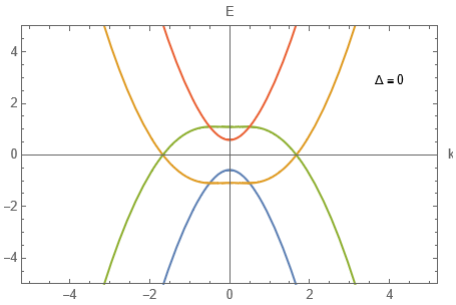

(b) Zeeman splitting

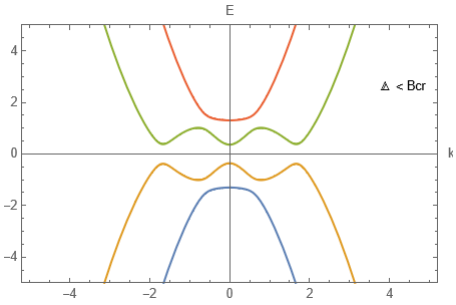

(c) Topological Phase of the SC

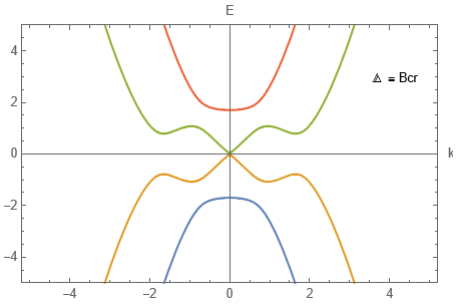

(d) Transition from Normal to Topological phase

Figure 2.1: Here are shown the plots for the eigenvalues of eq. (2.18). In the first image we see the spin splitting of the two bands with $\tilde{B} = 0$. In the second image we turn on the magnetic field and we see the Zeeman splitting of the bands. In the third image we see that as we switch on also the proximity-induced superconducting pairing, for small values of $\Delta > 0$, we are in the topological phase of the Superconductor, provided that the chemical potential is placed within the spinless regime, $|\tilde{B}| > |\mu|$. Finally, the gap at zero momentum decreases with increasing Δ and closes completely when $|\tilde{B}_{cr}| = |\Delta|$ (assuming $\mu = 0$). For larger values of Δ the gap opens again, but now in a non-topological superconducting state. Therefore, in this critical value of $\tilde{B}_{cr}$ a phase transition occurs from the topological to the normal state.

We notice that we have 4 eigenvalues, 2 for particles and 2 for holes. In particular, we have:

$$E_1 = \left(\tilde{B}^2 + \Delta^2 + \xi^2 + \alpha^2 k^2 - 2(\tilde{B}^2\xi^2 + \tilde{B}^2\Delta^2 + \alpha^2 k^2 \xi^2)^{1/2}\right)^{1/2} \tag{2.19}$$

$$E_2 = \left(\tilde{B}^2 + \Delta^2 + \xi^2 + \alpha^2 k^2 + 2(\tilde{B}^2\xi^2 + \tilde{B}^2\Delta^2 + \alpha^2 k^2 \xi^2)^{1/2}\right)^{1/2} \tag{2.20}$$

$$E_3 = -\left(\tilde{B}^2 + \Delta^2 + \xi^2 + \alpha^2 k^2 - 2(\tilde{B}^2\xi^2 + \tilde{B}^2\Delta^2 + \alpha^2 k^2 \xi^2)^{1/2}\right)^{1/2} \tag{2.21}$$

$$E_4 = -\left(\tilde{B}^2 + \Delta^2 + \xi^2 + \alpha^2 k^2 + 2(\tilde{B}^2\xi^2 + \tilde{B}^2\Delta^2 + \alpha^2 k^2 \xi^2)^{1/2}\right)^{1/2} \tag{2.22}$$

where E_1, E_2 correspond to the particle energy, E_3, E_4 correspond to the hole energy, and as expected the relations $E_1 = -E_3$ and $E_2 = -E_4$ are true since the holes are the anti-particles. We set as M_1 the term :

$$M_1 = (\tilde{B}^2\xi^2 + \tilde{B}^2\Delta^2 + \alpha^2 k^2 \xi^2)^{1/2} \tag{2.23}$$

that is inside the eigenvalues for reasons that will be obvious later.

In order to determine the critical value for which the phase transition that we see in Fig.(2.1d) occurs, we need to take the eigenvalues of eq. (2.18) to be equal to zero at zero momentum ($k = 0$). If we do so, we see that the critical value for the Zeeman term is equal to:

$$\tilde{B}_{cr} = \sqrt{\Delta^2 + \mu^2} \tag{2.24}$$

Therefore, the criteria for topological superconductivity, which is associated to Majorana edge states, is:

$$\tilde{B}_{cr} > \sqrt{\Delta^2 + \mu^2} \tag{2.25}$$

2.2.1 Diagonalization

Now that we have the form of our Bogoliubov de Gennes Hamiltonian, eq. (2.12), we will proceed by diagonalize it. In order to so, we need to find a suitable unitary transformation, that is why we introduce the following Bogoliubov operators (following [14] and [15]):

$$\gamma^\dagger_{i,k} = \sum_{i=1,2} \sum_{s=\uparrow,\downarrow} u_{i,s,k}\psi^\dagger_{s,k} + v_{i,s,-k}\psi_{s,-k} \tag{2.26}$$

$$\gamma_{i,k} = \sum_{i=1,2} \sum_{s=\uparrow,\downarrow} u^*_{i,s,k}\psi_{s,k} + v^*_{i,s,-k}\psi^\dagger_{s,-k} \tag{2.27}$$

Note that the spin degree of freedom has now been transferred to the wave functions rather than the quasiparticle operators. By inverting these unitary transformations we obtain:

$$\psi_{s,k} = \sum_{i=1,2} u_{i,s,k}\gamma_{i,k} + v^*_{i,s,k}\gamma^\dagger_{i,-k} \tag{2.28}$$

$$\psi^\dagger_{s,k} = \sum_{i=1,2} u^*_{i,s,k}\gamma^\dagger_{i,k} + v_{i,s,k}\gamma_{i,-k} \tag{2.29}$$

where the eigenvalues of the H_{BdG} correspond to the four Bogoliubov operators $\gamma^\dagger_{1,k}, \gamma_{1,-k}, \gamma^\dagger_{2,k}, \gamma_{2,-k}$. Since the $\psi_{s,k}$ are fermionic operators, then the Bogoliubov quasiparticles must also be fermionic operators. That means that they must satisfy the usual fermionic anti-commutation relations in order to be well defined. Thus, we have the relations:

$$\left\{\psi_{s,k}, \psi^\dagger_{s',k'}\right\} = \delta_{s,s'}\delta_{k,k'}, \quad and \quad \left\{\gamma_{i,k}, \gamma^\dagger_{j,k'}\right\} = \delta_{i,j}\delta_{k,k'} \tag{2.30}$$

Furthermore, we have $\{\psi_{s,k}, \psi_{s,k'}\} = \left\{\psi^\dagger_{s,k}, \psi^\dagger_{s,k'}\right\} = 0$ for $k = k'$ or $k \neq k'$. Similar we have $\{\gamma_{i,k}, \gamma_{i,k'}\} = \left\{\gamma^\dagger_{i,k}, \gamma^\dagger_{i,k'}\right\} = 0$. These anti-commutation relations will put some restrictions to the

elements of our Unitary matrix.

Since the Bogoliubov quasiparticles describe particle-hole one must note that creating a particle with momentum k is like annihilating a hole with momentum $-k$. This comes from the Particle-hole operator (2.15). To make this more clear, let's consider the following:

$$\begin{gathered} H(k)\gamma_{i,k} = E_i(k)\gamma_{i,k} \Rightarrow -P^\dagger H^*(-k)P\gamma_{i,k} = E_i(k)\gamma_{i,k} \Rightarrow \\ H^*(-k)\big(P\gamma_{i,k}\big) = -E_i(k)\big(P\gamma_{i,k}\big) \Rightarrow \big(\gamma^\dagger_{i,k}P^\dagger\big)H(-k) = -\big(\gamma^\dagger_{i,k}P^\dagger\big)E_i(k) \\ or \quad H(k)\big(P\gamma^*_{i,-k}\big) = -E_i(-k)\big(P\gamma^*_{i,-k}\big) \end{gathered} \tag{2.31}$$

This means that state $P\gamma^*_{i,-k}$ is also an eigenstate of $H(k)$ and we know also from eq. (2.18) that $E(k) = E(-k)$.

$$P^\dagger\gamma^\dagger_{i,k} = \gamma_{i,-k} \Rightarrow u_{i,s,k} = -v^*_{i,s',k} \tag{2.32}$$

where $s, s' = \uparrow \ or \ \downarrow$ spin and are bind by the restriction in the above equation that they have to be different, i.e $s \neq s'$. Eq. (2.32) is the first restriction for our Unitary matrix elements. By taking the anti-commutation relations of eq. (2.30) we find that:

$$\Big\{\psi_{s,k}, \psi^\dagger_{s,k}\Big\} = 1 \Rightarrow \sum_{i=1,2}\big(|u_{i,s,k}|^2 + |v_{i,s,k}|^2\big) = 1 \tag{2.33}$$

and

$$\Big\{\gamma_{i,k}, \gamma^\dagger_{i,k}\Big\} = 1 \Rightarrow \sum_{s=\uparrow,\downarrow}\big(|u_{i,s,k}|^2 + |v_{i,s,-k}|^2\big) = 1 \tag{2.34}$$

These are the second and third restrictions. Let us write now explicitly the operators that we are going to use in order to define our Unitary matrix. We are going to need the operators:

$$\psi_{\uparrow,k} = \sum_{i=1,2} u_{i,\uparrow,k}\gamma_{i,k} + v^*_{i,\uparrow,k}\gamma^\dagger_{i,-k} = u_{1,\uparrow,k}\gamma_{1,k} + v^*_{1,\uparrow,k}\gamma^\dagger_{1,-k} + u_{2,\uparrow,k}\gamma_{2,k} + v^*_{2,\uparrow,k}\gamma^\dagger_{2,-k} \tag{2.35}$$

$$\psi_{\downarrow,k} = \sum_{i=1,2} u_{i,\downarrow,k}\gamma_{i,k} + v^*_{i,\downarrow,k}\gamma^\dagger_{i,-k} = u_{1,\downarrow,k}\gamma_{1,k} + v^*_{1,\downarrow,k}\gamma^\dagger_{1,-k} + u_{2,\downarrow,k}\gamma_{2,k} + v^*_{2,\downarrow,k}\gamma^\dagger_{2,-k} \tag{2.36}$$

$$\psi^\dagger_{\uparrow,-k} = \sum_{i=1,2} u^*_{i,\uparrow,-k}\gamma^\dagger_{i,-k} + v_{i,\uparrow,-k}\gamma_{i,k} = u^*_{1,\uparrow,-k}\gamma^\dagger_{1,-k} + v_{1,\uparrow,-k}\gamma_{1,k} + u^*_{2,\uparrow,-k}\gamma^\dagger_{2,-k} + v_{2,\uparrow,-k}\gamma_{2,k} \tag{2.37}$$

$$\psi^{\dagger}_{\downarrow,-k} = \sum_{i=1,2} u^{*}_{i,\downarrow,-k}\gamma^{\dagger}_{i,-k} + v_{i,\downarrow,-k}\gamma_{i,k} = u^{*}_{1,\downarrow,-k}\gamma^{\dagger}_{1,-k} + v_{1,\downarrow,-k}\gamma_{1,k} + u^{*}_{2,\downarrow,-k}\gamma^{\dagger}_{2,-k} + v_{2,\downarrow,-k}\gamma_{2,k} \quad (2.38)$$

The matrix form of our spinor in the Nambu space is defined by the Bogoliubov transformation that we introduced and has the form:

$$\begin{pmatrix} \psi_{\uparrow,k} \\ \psi_{\downarrow,k} \\ -\psi^{\dagger}_{\downarrow,-k} \\ \psi^{\dagger}_{\uparrow,-k} \end{pmatrix} = \begin{pmatrix} u_{1,\uparrow,k} & u_{2,\uparrow,k} & v^{*}_{1,\uparrow,k} & v^{*}_{2,\uparrow,k} \\ u_{1,\downarrow,k} & u_{2,\downarrow,k} & v^{*}_{1,\downarrow,k} & v^{*}_{2,\downarrow,k} \\ -v_{1,\downarrow,-k} & -v_{2,\downarrow,-k} & -u^{*}_{1,\downarrow,-k} & -u^{*}_{2,\downarrow,-k} \\ v_{1,\uparrow,-k} & v_{2,\uparrow,-k} & u^{*}_{1,\uparrow,-k} & u^{*}_{2,\uparrow,-k} \end{pmatrix} \begin{pmatrix} \gamma_{1,k} \\ \gamma_{2,k} \\ \gamma^{\dagger}_{1,-k} \\ \gamma^{\dagger}_{2,-k} \end{pmatrix} \quad (2.39)$$

Before we continue, it would be very helpful, in terms of notation, to write the positive energies as $\gamma_{1,k}$ and $\gamma_{2,k}$ (as it is), and the negative energies as $\gamma^{\dagger}_{1,-k} = \gamma_{4,k}$ ($\gamma_{1,k} = \gamma^{\dagger}_{4,-k}$) and $\gamma^{\dagger}_{2,-k} = \gamma_{3,k}$ ($\gamma_{2,k} = \gamma^{\dagger}_{3,-k}$). To have a more visual understanding of what this mapping means, one can take a look in the Fig.(2.2).

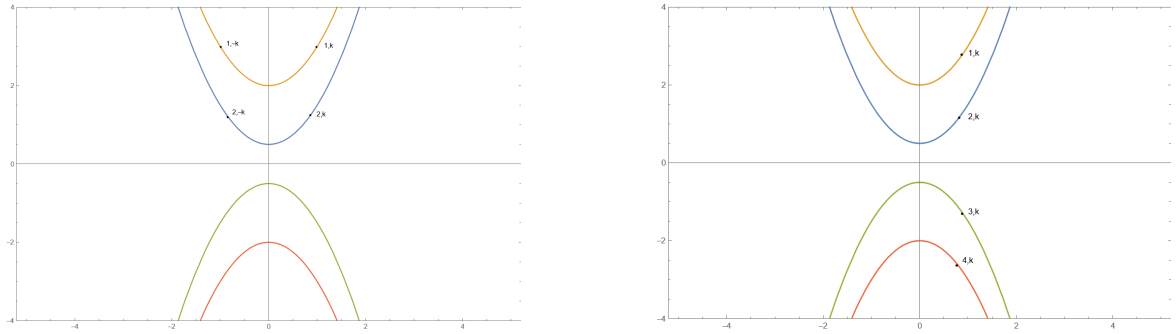

(a) First mapping of positive-negative energies (b) Second mapping of positive-negative energies

Figure 2.2: The above graphs corresponds to the four energy bands(2 for particles and 2 for holes) of the single particle system with $\mu \neq 0, \alpha = 0, \tilde{B} = 0$ and $\Delta = 0$. In the first image we see our original mapping of positive-negative energies. In the second image we see the mapping that we prefer to use.

Now we can diagonalize our Hamiltonian, by writing:

$$H_{SC} = \int dk \Psi^{\dagger}(H_{BdG})\Psi = \int dk \sum_{i=1}^{4} E_i \gamma^{\dagger}_{i,k}\gamma_{i,k} \quad (2.40)$$

To perform the diagonalization analytically is a "brutal" task. For that reason we use matlab to diagonalize it. To find the elements of this Unitary matrix we used the normalized eigenvectors of eq. (2.11) which they form a Unitary matrix by taking each column vector to represent each eigenenergy. Since the results were obtained in matlab (same in every program that can compute with symbolic

matrices), one must be very careful because once he calculates the normalized eigenvectors of our BdG Hamiltonian, these vectors will be represented in the diagonal basis, i.e in our case in the basis of eq. (2.26), (2.27). Thus, one needs to inverse the matrix in order to get our results. By comparing this unitary matrix with the results from matlab, we get the results:

$$u_{1,\uparrow,k} = \frac{\Delta a k(\tilde{B} - \xi)}{4iE_1 M_1} \tag{2.41}$$

$$u_{2,\uparrow,k} = \frac{\Delta \tilde{B}}{4M_1} + \frac{\Delta \tilde{B}^2(\Delta^2 + \xi^2 - M_1) + (\alpha k)^2 \xi^2}{16M_1^2} \tag{2.42}$$

$$v^*_{1,\uparrow,k} = \frac{-\alpha k \xi}{4iM_1} - \frac{4\alpha k \xi^2(\alpha^2 k^2 + \tilde{B}^2 + \Delta^2 - M_1)}{16iM_1^2 E_1} \tag{2.43}$$

$$v^*_{2,\uparrow,k} = \frac{M_1^2 E_1 + \tilde{B}\xi E_1(E_1^2\Delta^2 - (\alpha k)^2 - \tilde{B}^2) + 4M1(\tilde{B}\xi^2 + \tilde{B}^2\xi + (\alpha k)^2\xi + \tilde{B}\Delta^2 - \tilde{B} - \xi)}{16M_1^2 E_1} \tag{2.44}$$

These will be the terms that we are gonna be interested later.

2.3 Perturbation Theory

In order to find an effective description of the Quantum Hall edge modes, we will perform the perturbation theory assuming weak tunneling $\Delta \gg t$. Thus, we treat the tunneling Hamiltonian as a small perturbation to our system.

Before starting applying the perturbation theory in our system, we need to define the ground state of it. Let us take it to be equal with:

$$|\mathcal{GS}\rangle = |\Psi_{GS,QH}\rangle \otimes |\Psi_{BCS}\rangle \tag{2.45}$$

where $|\Psi_{GS,QH}\rangle$ is the IQH ground state. We start by calculating an effective Hamiltonian, $H^{eff}_{QH}(k)$. The idea is that we take a small window around μ_{QH} and we "forget" for now the $|\Psi_{GS,QH}\rangle$. This way, allows us to treat the $\psi_{QH,\uparrow,k,j}$ and $\psi^\dagger_{QH,\uparrow,k,j}$ operators as "constants", i.e that they have no effect on the $|\Psi_{BCS}\rangle$ but they still obey the fermionic rules of operators and one must keep track of the right signs. The BCS ground state is defined as the state where for $\forall$ positive energies γ_i and any momenta k

$$\gamma_{i,k} |\Psi_{BCS}\rangle = 0, \qquad i = 1, 2 \qquad \forall k \tag{2.46}$$

and are equivalent to (based on the new mapping):

$$\gamma_{4,k}^{\dagger}\left|\Psi_{BCS}\right\rangle = \gamma_{3,k}^{\dagger}\left|\Psi_{BCS}\right\rangle = 0, \qquad i = 1,2 \qquad \forall k \tag{2.47}$$

Note that the above relations are true for each k. In addition, states with negative energies $\gamma_{i,-k}^{\dagger}$ and $\gamma_{i,k}^{\dagger}$ create excitations:

$$\gamma_{i,k}^{\dagger}\left|\Psi_{BCS}\right\rangle = \left|i,k\right\rangle, \quad for \quad i = 1,2 \qquad \forall k \tag{2.48}$$

which are equivalent to:

$$\gamma_{3,-k}\left|\Psi_{BCS}\right\rangle = \gamma_{4,-k}\left|\Psi_{BCS}\right\rangle = \left|i,k\right\rangle, \quad for \quad i = 1,2 \qquad \forall k \tag{2.49}$$

where $\left|i,k\right\rangle$ is the new excited state. Furthermore, our definition implies the condition:

$$\gamma_{i,k}\gamma_{i,k}^{\dagger}\left|\Psi_{BCS}\right\rangle = \left|\Psi_{BCS}\right\rangle \tag{2.50}$$

One more important property of our definition of the BCS ground state that we are going to use later is that:

$$\begin{cases} \gamma_{j,q}\left|i,k\right\rangle = \delta_{i,j}\delta_{q,k}\left|\Psi_{BCS}\right\rangle \\ \gamma_{j,q}^{\dagger}\left|i,k\right\rangle \neq \left|\Psi_{BCS}\right\rangle \end{cases} \Rightarrow \left\langle\Psi_{BCS}\right|\gamma_{j,q}^{\dagger}\gamma_{i,k}^{\dagger}\left|\Psi_{BCS}\right\rangle = 0 \qquad (orthogonal) \tag{2.51}$$

which implies that later will take only the diagonal terms of the expectation value. The ground state $\left|\Psi_{BCS}\right\rangle$ is a superposition of states built up of Cooper pairs, i.e it obeys the bosonic commutation rules (since a Cooper pair is a composite boson with total spin 0 or 1 . This also means, that the wave functions are symmetric under particle interchange).

In order to apply perturbation theory in our model we write eq. (2.5) as:

$$\mathcal{H}(k) = \mathcal{H}_0(k) + \mathcal{H}_p(k) \tag{2.52}$$

where $\mathcal{H}_0(k) = H_{SC}(k) + H_{QH}(k)$ the unperturbed part of our Hamiltonian, and $\mathcal{H}_p(k) = H_t(k)$ the perturbation. Since we have a BCS ground state it is better to write $\mathcal{H}_p(k)$ in terms of the Bogoliubov quasiparticles. This means that we will replace the $\psi_{SC,\uparrow,k}^{\dagger}$ and $\psi_{SC,\uparrow,k}$ with the eq. (2.37) and (2.35) to get:

$$\mathcal{H}_p(k) = H_t(k) = -t\int dk \sum_{j=L,R} [\psi^\dagger_{QH,\uparrow,k,j}\psi_{SC,\uparrow,k} + \psi^\dagger_{SC,\uparrow,k}\psi_{QH,\uparrow,k,j}] =$$
$$-t\int dk \sum_{j=L,R} [\psi^\dagger_{QH,\uparrow,k,j}(u_{1,\uparrow,k}\gamma_{1,k} + v^*_{1,\uparrow,k}\gamma_{4,k} + u_{2,\uparrow,k}\gamma_{2,k} + v^*_{2,\uparrow,k}\gamma_{3,k}) +$$
$$(u^*_{1,\uparrow,k}\gamma^\dagger_{1,k} + v_{1,\uparrow,k}\gamma^\dagger_{4,k} + u^*_{2,\uparrow,k}\gamma^\dagger_{2,k} + v_{2,\uparrow,k}\gamma^\dagger_{3,k})\psi_{QH,\uparrow,k,j}] \tag{2.53}$$

We have now:

$$H^{eff}_{QH}(k) = \langle\Psi_{BCS}| H_p P_{exc.BCSstates}\frac{1}{E_{GS} - H_{BCS}}P_{exc.BCSstates}H_p |\Psi_{BCS}\rangle =$$
$$\langle\Psi_{BCS}| H_p \sum_{i''\in 1,2}\int_{-\infty}^{+\infty} dk'' |i''k''\rangle \langle i''k''| \frac{1}{E_{GS} - H_{BCS}} \sum_{i'\in 1,2}\int_{-\infty}^{+\infty} dk' |i'k'\rangle \langle i'k'| H_p |\Psi_{BCS}\rangle \tag{2.54}$$

where

$$P_{exc.BCSstates} = \sum_{n\in single\ \ exc.\ \ \ states} |n\rangle\langle n| = \sum_{i\in 1,2}\int_{-\infty}^{+\infty} dk\, |ik\rangle\langle ik| \tag{2.55}$$

is the projection on the BCS excited states. By performing these calculations (exact calculations can be found in (A.2)), we end up to an Effective description for the Quantum Hall edge modes of our system of the form:

$$H^{eff}_{QH}(k) = \int dk \sum_{i\in 1,2}\frac{t^2}{-E_i(k)}\Big(\psi^\dagger_{QH,\uparrow,k,L}\psi^\dagger_{QH,\uparrow,-k,L}(u_{i,\uparrow,k}v^*_{i,\uparrow,-k}) - \psi^\dagger_{QH,\uparrow,k,L}\psi_{QH,\uparrow,k,L}(u_{i,\uparrow,k}u^*_{i,\uparrow,k}) +$$
$$\psi^\dagger_{QH,\uparrow,k,L}\psi^\dagger_{QH,\uparrow,-k,R}(u_{i,\uparrow,k}v^*_{i,\uparrow,-k}) - \psi^\dagger_{QH,\uparrow,k,L}\psi_{QH,\uparrow,k,R}(u_{i,\uparrow,k}u^*_{i,\uparrow,k})$$
$$-\psi_{QH,\uparrow,-k,L}\psi^\dagger_{QH,\uparrow,-k,L}(v_{i,\uparrow,-k}v^*_{i,\uparrow,-k}) + \psi_{QH,\uparrow,-k,L}\psi_{QH,\uparrow,k,L}(v_{i,\uparrow,-k}u^*_{i,\uparrow,k})$$
$$-\psi_{QH,\uparrow,-k,L}\psi^\dagger_{QH,\uparrow,-k,R}(v_{i,\uparrow,-k}v^*_{i,\uparrow,-k}) + \psi_{QH,\uparrow,-k,L}\psi_{QH,\uparrow,k,R}(v_{i,\uparrow,-k}u^*_{i,\uparrow,k}) +$$
$$\psi^\dagger_{QH,\uparrow,k,R}\psi^\dagger_{QH,\uparrow,-k,L}(u_{i,\uparrow,k}v^*_{i,\uparrow,-k}) - \psi^\dagger_{QH,\uparrow,k,R}\psi_{QH,\uparrow,k,L}(u_{i,\uparrow,k}u^*_{i,\uparrow,k}) +$$
$$\psi^\dagger_{QH,\uparrow,k,R}\psi^\dagger_{QH,\uparrow,-k,R}(u_{i,\uparrow,k}v^*_{i,\uparrow,-k}) - \psi^\dagger_{QH,\uparrow,k,R}\psi_{QH,\uparrow,k,R}(u_{i,\uparrow,k}u^*_{i,\uparrow,k})$$
$$-\psi_{QH,\uparrow,-k,R}\psi^\dagger_{QH,\uparrow,-k,L}(v_{i,\uparrow,-k}v^*_{i,\uparrow,-k}) + \psi_{QH,\uparrow,-k,R}\psi_{QH,\uparrow,k,L}(v_{i,\uparrow,-k}u^*_{i,\uparrow,k})$$
$$-\psi_{QH,\uparrow,-k,R}\psi^\dagger_{QH,\uparrow,-k,R}(v_{i,\uparrow,-k}v^*_{i,\uparrow,-k}) + \psi_{QH,\uparrow,-k,R}\psi_{QH,\uparrow,k,R}(v_{i,\uparrow,-k}u^*_{i,\uparrow,k})\Big) \tag{2.56}$$

or in a composite form we can write the above equation as:

$$H^{eff}_{QH}(k) = \int dk \sum_{i\in 1,2}\sum_{\eta=L,R}\sum_{\eta'=L,R}\frac{t^2}{-E_i(k)}\Big(\psi^\dagger_{QH,\uparrow,k,\eta}\psi^\dagger_{QH,\uparrow,-k,\eta'}(u_{i,\uparrow,k}v^*_{i,\uparrow,-k}) - \psi^\dagger_{QH,\uparrow,k,\eta}\psi_{QH,\uparrow,k,\eta'}(u_{i,\uparrow,k}u^*_{i,\uparrow,k})$$
$$-\psi_{QH,\uparrow,-k,\eta}\psi^\dagger_{QH,\uparrow,-k,\eta'}(v_{i,\uparrow,-k}v^*_{i,\uparrow,-k}) + \psi_{QH,\uparrow,-k,\eta}\psi_{QH,\uparrow,k,\eta'}(v_{i,\uparrow,-k}u^*_{i,\uparrow,k})\Big) \tag{2.57}$$

where we have used the fact that $H_{BCS}\left|i,k\right\rangle = (E_{GS} + E_i)\left|i,k\right\rangle$ and from the particle-hole symmetry $E_i(k) = E_i(-k)$. The E_{GS} is considered to be the energy where every energy band is filled.

From the above expression, we are most interested in the terms that Induce Superconductivity. These terms are the ones that couples the chiral particles with different momentum (in order to have the desired momentum conservation on the axis) and have the form:

$$\int dk \sum_{i\in 1,2} \frac{t^2}{-E_i(k)} \psi^\dagger_{QH,\uparrow,k,L} \psi^\dagger_{QH,\uparrow,-k,R} (u_{i,\uparrow,k} v^*_{i,\uparrow,-k}) \tag{2.58}$$

where

$$\Delta_{ind} = \sum_{i\in 1,2} \frac{t^2 u_{i,\uparrow,k} v^*_{i,\uparrow,-k}}{-E_i(k)} \tag{2.59}$$

From the above calculations, we ended up to an Effective Hamiltonian describing our Quantum Hall system in the momentum space. Since we are interested to develop a theoretical model based on bosonization to describe our system, it is essential to perform a Fourier transformation to go to real space.

To do so, one should check if the integral over all k for the Δ_{ind}, eq. (2.58), is converging or not and it can be done by checking the dependence of k for each term, i.e that he checks what happens in big values for momentum. By taking all the dominants powers in k we can easily see that this integral converges. One more important thing before starting evaluating the integrals, is to check if it has poles. This can be done by checking the denominator of each term in eq. (2.59), where $u_{i,\uparrow,k}$ and $v^*_{i,\uparrow,k}$ are defined by eq. (2.41-2.44). Since these denominators are depend on $E_2^2 - E_1^2 = M_1^2$, M_1 and E_1, which are all quadratic functions of k, we can see by comparing the leading terms of the numerator and denominator that the integral of the induced gap as found in eq. (2.59) converges and by definition the e^{-kx} term of the Fourier transformation is convergent for $k \geq 0$.

To get an analytical result after the integration is very difficult, even with computational methods. What we can do however, is to take eq. (2.59) and Taylor expanded in to orders of Δ. This can be done, because we already made the assumption that $\Delta \gg t$ to use perturbation theory. Once we do so, we will find the Induced gap depends on Δ and the α, i.e $\Delta_{ind} \sim \alpha^2 t^2 \Delta$. This is a reasonable result, because if we set the value of $\Delta = 0$, we expect no induced gap to appear. What is also important here, is that the induce gap dependents on the Rashba coefficient α, which is also expected since we couple the edge modes with different spin. When the $\alpha = 0$ there is no induced gap in the system.

2.4 Feynman Path Integral Formalism

In this section we will try a different approach to our problem. Namely, we will try to integrate out the superconducting degrees of freedom of our system. To do so, we are going to use the Feynman Path Integral methods. In case one wants to know how to construct this path integral, he can check in [16] which is explained perfectly.

The system we are interested in is the same as before, i.e it will be described by eq. (2.5), where the Superconductor, the Quantum Hall and the Tunneling parts are described by eq. (2.6),(2.7),(2.8) respectively. We define now as Ψ and $\Psi^\dagger$ the nambu spinors of the Superconductor, and as Φ and $\Phi^\dagger$ the nambu spinors of the Quantum Hall, where

$$\overline{\Psi} = \left[\Psi_\uparrow^\dagger, \Psi_\downarrow^\dagger, -\Psi_\downarrow, \Psi_\uparrow\right] \tag{2.60}$$

and

$$\overline{\Phi} = \left[\Phi_\uparrow^\dagger, \Phi_\uparrow\right] \tag{2.61}$$

where the k dependence of the spinors is implied, i.e $\Psi = \Psi(k)$ and $\Phi = \Phi(k)$. Note, that these Nambu spinors will be treated as Grassmann variables for our purposes. We continue by writing the action of the full system. We have:

$$\mathcal{S} = S_{SC} + S_{QH} + S_t \tag{2.62}$$

where

$$S_{SC} = -\partial_\tau - H_{SC} = \int \frac{d\omega}{2\pi} \int dk\, \overline{\Psi} \tilde{H}_{SC} \Psi, \tag{2.63}$$

$$S_{QH} = -\partial_\tau - H_{QH} = \int \frac{d\omega}{2\pi} \int dk\, \overline{\Phi} \tilde{H}_{QH} \Phi, \tag{2.64}$$

$$S_t = \int dk\, \left(\overline{\Psi} T \Phi + \overline{\Phi} T^\dagger \Psi\right) \tag{2.65}$$

where $\tilde{H}_{SC} = i\omega - H_{SC}$, $\tilde{H}_{QH} = i\omega - H_{QH}$ and H_{SC}, H_{QH} the 4×4 matrix representation of the Superconductor and the 2×2 Quantum Hall respectively. Furthermore, T is the 4×2 tunneling coupling matrix and gets its form from the coupling between the nambu spinors, in particular:

$$T = \begin{pmatrix} -t & 0 \\ 0 & 0 \\ 0 & 0 \\ 0 & -t \end{pmatrix}. \tag{2.66}$$

In the above description, τ stands for the imaginary time and $i\omega$ is its Fourier transform in the

frequency space ($\partial_\tau \to -i\omega$) and since we are dealing with fermions we need to impose anti-periodic boundary conditions. Therefore, we need to set:

$$e^{i\omega\beta} = -1 \qquad or \qquad \omega = \omega_n = \frac{2n+1}{\beta} = (2n+1)T \tag{2.67}$$

where $\beta = \frac{1}{k_B T}$ with $k_B \to 1$ the Boltzmann constant and T the temperature.

The fermionic coherent state path integral representation for the partition function of this system is given by:

$$\mathcal{Z} = \int D[\overline{\Phi}, \Phi] \int D[\overline{\Psi}, \Psi] e^{-S_{SC}[\overline{\Psi},\Psi] - S_{QH}[\overline{\Phi},\Phi] - S_t[\overline{\Psi},\Psi,\overline{\Phi},\Phi]} \tag{2.68}$$

where $\overline{\Psi}, \Psi$ are the Grassmann variables corresponding to the superconducting fermionic fields $\Psi^\dagger, \Psi$ and $\overline{\Phi}, \Phi$ correspond to Quantum Hall fermionic fields $\Phi^\dagger, \Phi$ respectively and they are k dependant.

By manipulating the action in eq. (2.62) as shown in eq. (A.10), the path integral over superconducting fields takes the form of a Gaussian integral with exponent:

$$\begin{gathered} S_{SC}[\overline{\Psi}, \Psi] + S_{QH}[\overline{\Phi}, \Phi] + S_t[\overline{\Psi}, \Psi, \overline{\Phi}, \Phi] = \\ \int \frac{d\omega}{2\pi} \int dk \left[\left(\overline{\Psi} + \overline{\Phi} T^\dagger \tilde{H}_{SC}^{-1} \right) \tilde{H}_{SC} \left(\Psi + \tilde{H}_{SC}^{-1} T \Phi \right) + \overline{\Phi} \tilde{H}_{QH} \Phi - \overline{\Phi} T^\dagger \tilde{H}_{SC}^{-1} T \Phi \right] \end{gathered} \tag{2.69}$$

In this form we can integrate the superconducting degrees of freedom by using the property of the Grassmann variables:

$$\int d\eta^\dagger \int d\eta e^{-\eta^\dagger A \eta - \eta^\dagger J - J^\dagger \eta} = \int d\eta^\dagger \int d\eta e^{-(\eta^\dagger + J^\dagger A^{-1}) A (\eta + A^{-1} J) + J^\dagger A^{-1} J} \tag{2.70}$$

$$= det(A) e^{J^\dagger A^{-1} J} \tag{2.71}$$

where A is an $n \times n$ matrix, $\eta^\dagger, \eta$ the Grassmann variables and $J^\dagger, J$ the Grassmann source fields. Evaluating now the path integral with respect to the superconducting degrees of freedom we obtain the Effective Action:

$$S_{eff} = \int \frac{d\omega}{2\pi} \int dk \left[\overline{\Phi} \tilde{H}_{QH} \Phi - \overline{\Phi} T^\dagger \tilde{H}_{SC}^{-1} T \Phi \right] \tag{2.72}$$

and our partition function eq. (2.68), becomes:

$$\mathcal{Z} = \det\left(\tilde{H}_{SC}\right) \int D[\overline{\Phi}, \Phi] e^{-S_{eff}} = det(\tilde{H}_{SC}) \int D[\overline{\Phi}, \Phi] e^{-\overline{\Phi} \tilde{H}_{QH} \Phi + \overline{\Phi} T^\dagger \tilde{H}_{SC}^{-1} T \Phi} \tag{2.73}$$

where $\det\Big(\tilde{H}_{SC}\Big) = \det\big(\mathcal{G}_{SC}^{-1}\big) = \mathcal{Z}_{SC}$ is just the partition function and $\mathcal{G}_{SC} = \tilde{H}_{SC}^{-1} = \frac{1}{i\omega - H_{SC}}$ the Green function of our superconductor. Similarly we can define the Green function for the Quantum Hall as $\mathcal{G}_{QH} = \tilde{H}_{QH}^{-1} = \frac{1}{i\omega - H_{QH}}$. Our next step will be to find the matrix $\tilde{H}_{SC}^{-1}$. We can do this inversion analytical as we show in eq. (A.11). The result is:

$$\mathcal{G}_{SC} = \frac{((i\omega - \tilde{B}\sigma_z) + (\xi_k + \alpha k\sigma_y)\tau_z - \Delta\tau_x)((-\omega^2 - \xi_k^2 - (\alpha k)^2 + \tilde{B}^2 - \Delta^2) + 2i\omega\tilde{B}\sigma_z + 2\xi_k\alpha k\sigma_y)}{(-\omega^2 - \xi_k^2 - (\alpha k)^2 + \tilde{B}^2 - \Delta^2)^2 - (2i\omega\tilde{B})^2 - (2\xi_k\alpha k)^2} \tag{2.74}$$

In Appendix (A.3) one can find the analytical results (A.12 and A.13) of eq. (2.74).

By performing the same calculations computationally, i.e calcutaling the $\mathcal{G}_0 = \tilde{H}_{SC}^{-1} = \frac{1}{i\omega - H_{SC}}$ matrix in matlab, we got the same results for the numerator and the denominator of eq. (2.74) as in the analytical method which is a verification of what we calculate was correct.

The Emerging pairing that came from integrating out the superconducting degrees of freedom:

$$\mathcal{S}_{eff} = \int \frac{d\omega}{2\pi} \int dk \overline{\Phi} \mathcal{S}_{eff,pair}(k,\omega)\Phi = \int \frac{d\omega}{2\pi} \int dk \overline{\Phi} T^\dagger \tilde{H}_{SC}^{-1} T\Phi = \int \frac{d\omega}{2\pi} \int dk \overline{\Phi} \frac{-t^2}{\mathcal{D}} B\Phi \tag{2.75}$$

where we denote as B the matrix elements of the numerator of eq. (2.74). In particular, the matrix elements of B are:

$$\begin{aligned} B_{11} = i\omega^3 + \xi^3 + \tilde{B}^3 + \tilde{B}^2(i\omega - \xi_{k)} + \tilde{B}(\omega^2 - \xi_k^2 + (\alpha k)^2 - 2i\omega\xi_k - \Delta^2) + (\alpha k)^2(i\omega - \xi_k) \\ +\xi_k(\omega^2 + \Delta^2) + i\omega(\xi^2 + \Delta^2) \end{aligned} \tag{2.76}$$

$$\begin{aligned} B_{22} = i\omega^3 - \xi^3 - \tilde{B}^3 + \tilde{B}^2(i\omega + \xi_{k)} + \tilde{B}(-\omega^2 + \xi_k^2 - (\alpha k)^2 - 2i\omega\xi_k + \Delta^2) + (\alpha k)^2(i\omega + \xi_k) \\ -\xi_k(\omega^2 + \Delta^2) + i\omega(\xi^2 + \Delta^2) \end{aligned} \tag{2.77}$$

$$B_{12} = -2i\alpha k\Delta(\tilde{B} - \xi_k) \tag{2.78}$$

$$B_{21} = 2i\alpha k\Delta(\tilde{B} - \xi_k) \tag{2.79}$$

and

$$\mathcal{D} = (\omega^2 + E_1^2)(\omega^2 + E_2^2) \tag{2.80}$$

is the denominator. Note here, that the diagonal terms will give the Backscattering or Forwardscatter-

ing and the off-diagonal will give the Induced Superconductivity. Furthermore, the term

$$\mathcal{S}_{eff,pair}(k,\omega) = \int \frac{d\omega}{2\pi} \int dk \overline{\Phi} T^{\dagger} \mathcal{G}_0 T \Phi \tag{2.81}$$

can be viewed as the self-energy of our system. similar to [14].

What we want now to find now is the local term in time and space of eq. (2.75). For that purpose, we will perform Fourier transformation to this effective action. We define the Fourier transformation of the fermionic Quantum Hall fields as:

$$\overline{\Phi}(k,\omega) = \int \frac{dx_1 dt_1}{(2\pi)^2} \overline{\Phi}(x_1,t_1) e^{-ikx_1 + i\omega t_1} \tag{2.82}$$

$$\Phi(k,\omega) = \int \frac{dx_2 dt_2}{(2\pi)^2} \Phi(x_2,t_2) e^{ikx_2 - i\omega t_2} \tag{2.83}$$

We insert now eq. (2.82) inside eq. (2.75) and we get:

$$\mathcal{S}_{eff} = \int \frac{dk d\omega dx_1 dt_1 dx_2 dt_2}{(2\pi)^5} \overline{\Phi}(x_1,t_1) \mathcal{S}_{eff,pair}(k,\omega) e^{ik(x_2-x_1) - i\omega(t_2-t_1)} \Phi(x_2,t_2) \tag{2.84}$$

The first integration and most important will be the integration over the ω. To evaluate this integral we will use the Residue Theorem for every term in the $\mathcal{S}_{eff,pair}(k,\omega)$.

Here we will not present the analytical methods that were performed to evaluate these integrals. For more details, one can check in the Appendix (A.3).

We are interested in the terms that give the induced superconductivity, i.e the off-diagonal terms of the B matrix. The result for the off-diagonal term B_{12} (by taking also $x_2 = x_1$, local in space) is now:

$$\frac{-\pi B_{12}}{E_2 E_1 (E_2 + E_1)} \tag{2.85}$$

where in the above expression we replace the momentum k with $k_{f,QH}$. Next, we perform a Taylor expansion in the above expressions in terms of Δ, where we assume it weak, but still have in mind that we have weak tunneling $\Delta \gg t$.

As we can see from the result we have again:

$$\Delta_{ind} \propto \alpha^2 t^2 \Delta. \tag{2.86}$$

as was expected. Thus, so far we have found (not an analytical result) an approximation with 2 different methods on how to estimate the Induced gap of our system.

2.5 Integer Quantum Hall Description

Let us take a closer look at the Quantum Hall system. We mentioned in the previous section that we take a small window around the chemical potential μ_{QH}. Here we are going to analyze why we are interested in that small energy window. Now, we are considering that μ_{QH} can take values in the whole band area where the condition $\mu_{QH} \neq \mu_{SC}$ is still true. In the case where $\mu_{QH} = \mu_{SC}$ we have a resonance and we will discuss it a little bit in the Bosonization Chapter (3). As we said before, we have the Hamiltonian:

$$\begin{aligned} H_{QH}(k) = \frac{v}{2\pi}\int dk[(\psi^{\dagger}_{QH,\uparrow,k,L}(k)\psi_{QH,\uparrow,k,L} - \psi^{\dagger}_{QH,\uparrow,k,R}(k)\psi_{QH,\uparrow,k,R}) + \\ \mu_{QH}(\psi^{\dagger}_{QH,\uparrow,k,L}\psi_{QH,\uparrow,k,L} + \psi^{\dagger}_{QH,\uparrow,k,R}\psi_{QH,\uparrow,k,R}(k))] \end{aligned} \tag{2.87}$$

After the tunneling the Quantum Hall will be described by the Hamiltonian:

$$\mathcal{H}_{tot,QH}(k) = H_{QH}(k) + H^{eff}_{QH}(k) \tag{2.88}$$

where now the effective Hamiltonian of the Quantum Hall will have terms like:

$$H^{eff}_{QH}(k) : \begin{cases} \psi^{\dagger}_L(k)\psi^{\dagger}_R(-k), \psi^{\dagger}_R(k)\psi^{\dagger}_L(-k), \psi^{\dagger}_L(-k)\psi^{\dagger}_R(k), \psi^{\dagger}_R(-k)\psi^{\dagger}_L(k) \Rightarrow that\ induces\ SC \\ \psi^{\dagger}_L(k)\psi_L(k), \psi^{\dagger}_R(k)\psi_R(k), \psi^{\dagger}_L(-k)\psi_L(-k), \psi^{\dagger}_R(-k)\psi_R(-k) \Rightarrow that\ shifts\ \mu_{QH} \end{cases} \tag{2.89}$$

and terms like:

$$H^{eff}_{QH}(k) : \begin{cases} \psi^{\dagger}_L(k)\psi^{\dagger}_L(-k), \psi^{\dagger}_R(k)\psi^{\dagger}_R(-k), \psi^{\dagger}_L(-k)\psi^{\dagger}_L(k), \psi^{\dagger}_R(-k)\psi^{\dagger}_R(k) \Rightarrow more\ Energy\ costly \\ \psi^{\dagger}_L(k)\psi_R(k), \psi_L(-k)\psi^{\dagger}_R(-k), \psi^{\dagger}_R(k)\psi_L(k), \psi_R(-k)\psi^{\dagger}_L(-k) \Rightarrow gives\ \delta m\ terms \end{cases} \tag{2.90}$$

where the δm corresponds to backscattering procedure .Now, what we mean by more energy costly, is that we consider $|vk_F| \gg \Delta^j_{ind} = \Delta_{ind}$, for $j = RR, LL$ where Δ^j_{ind} is the coefficients in front of those pair terms.

The 2×2 $\mathcal{H}_{tot,QH}(k)$ Hamiltonian can be written now in the form:

$$\mathcal{H}_{2\times 2}(k) = vk\sigma_z + (-vk_F)\mathbb{I} + \delta m\sigma_x \tag{2.91}$$

where we can write the Bogoliubov de Gennes version of the Hamiltonian in the nambu spinor basis

as a 4×4 Hamiltonian:

$$\mathcal{H}_{tot,QH}(k) = \begin{pmatrix} \psi_R^\dagger(k) & \psi_L^\dagger(k) & \psi_R(-k) & \psi_L(-k) \end{pmatrix} \mathcal{H}_{BdG,QH}(k) \begin{pmatrix} \psi_R(k) \\ \psi_L(k) \\ \psi_R^\dagger(-k) \\ \psi_L^\dagger(-k) \end{pmatrix} \tag{2.92}$$

where we used the σ_z-basis for the nambu spinors, since the spin is polarized there, and

$$\mathcal{H}_{BdG,QH}(k) = \begin{pmatrix} v(k-k_F) & \delta m & 0 & \Delta_{ind} \\ \delta m & -v(k+k_F) & \Delta_{ind} & 0 \\ 0 & \Delta_{ind} & -v(-k-k_F) & -\delta m \\ \Delta_{ind} & 0 & -\delta m & v(-k+k_F) \end{pmatrix} \tag{2.93}$$

and $\psi_R^\dagger(k) = \psi_{QH,\uparrow,k,R}^\dagger(k)$ and $\psi_L^\dagger(k) = \psi_{QH,\uparrow,k,L}^\dagger(k)$ (similar of the Hermitian conjugate). In the above description, we included terms like $\delta m \psi_R^\dagger(k)\psi_R(k)$, $\delta m \psi_L^\dagger(k)\psi_L(k)$ and their H.c., where their values can be determined from one of the two above Effective descriptions. We expect that δm opens a normal gap at $k = 0$ and Δ_{ind} opens a BCS gap at $k = \pm k_F$ and this can be seen in the figure (2.3).

The eigenvalues of eq. (2.93) are found to be:

$$E_{QH}^2 = (vk)^2 + (vk_F)^2 + (\delta m)^2 + \Delta_{ind}^2 \pm 2\sqrt{(vk_F)^2\big((\delta m)^2 + (vk)^2\big)} \tag{2.94}$$

Note here, that in eq, (2.94), the δm terms will be important if we fix the Fermi level to a value that allows δm to be considerable to Δ_{ind} then we need to take them into consideration because it will also be a "battle" between those terms on whose gap will prevail. By taking $k = 0$ we found the relation:

$$|\Delta_{ind}| = \sqrt{\Big(vk_F + \delta m\Big)^2} \tag{2.95}$$

But we are not interested in this model on terms like these. In order to avoid them, we fix the chemical potential in a value such that the system does not allow these pairs of eq. (2.90) to be created, because it will be very costly in Energy. To give an idea of the values, the chemical potential will be $\mu \approx \frac{E_{QH}}{2}$, $E_{QH} \approx 10meV$ (very large for Integer Quantum Hall), $B_c \approx 8T$ (critical value of the magnetic field), the fermi momentum of Quantum Hall is $k_{QH,F} = \frac{\pi}{\alpha}$ with $\alpha = 4.391$Å the lattice spacing and $\Delta \approx 3\, meV$. More details about the the value of Δ are presented in the discussion after deriving eq. (3.129).

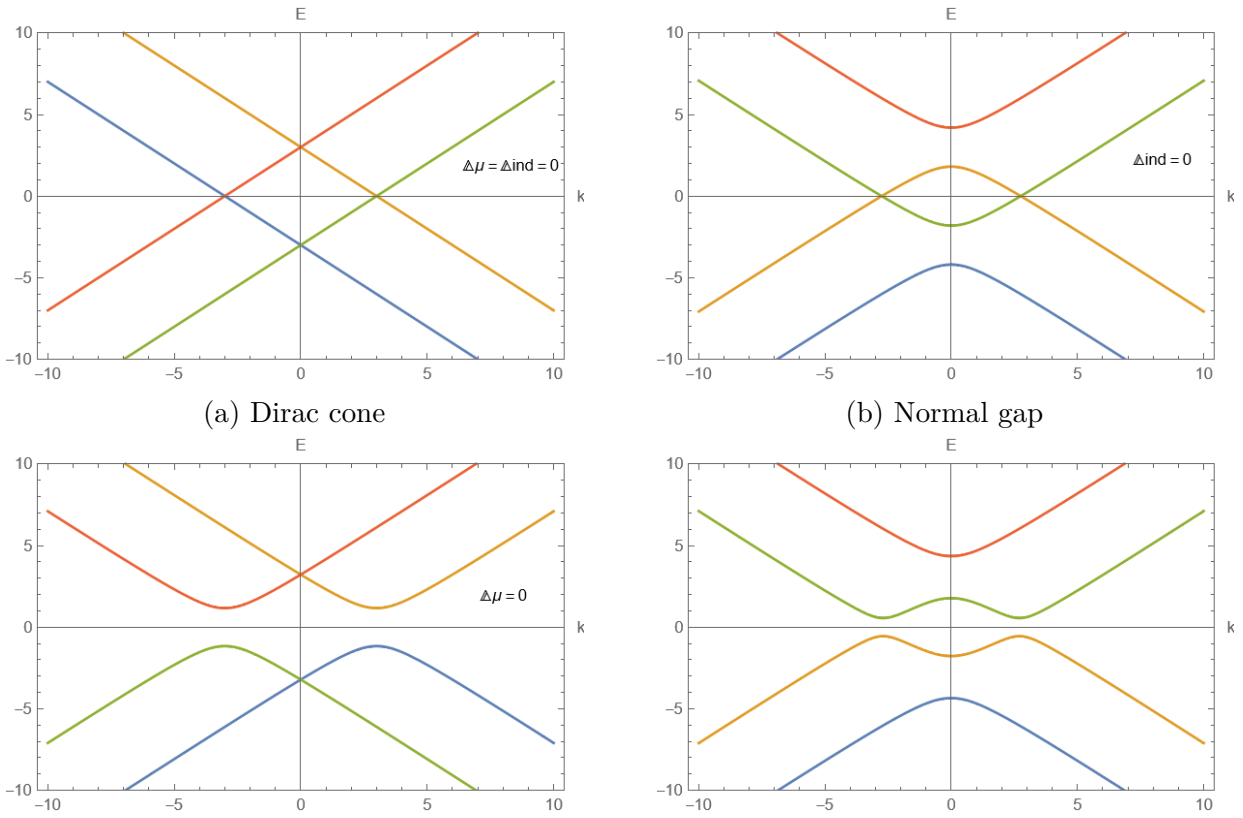

(a) Dirac cone

(b) Normal gap

(c) BCS gap

(d) Topological Phase

Figure 2.3: In the first image we see the Dirac cone of our Quantum Hall system. In the second Image we see that a normal gap opens (trivial phase transition) if we only have the $dm \neq 0$ terms and $\Delta_{ind} = 0$. In the third image we see that a BCS gap opens if we have $dm = 0$ terms and $\Delta_{ind} \neq 0$, i.e we have induced superconductivity (superconducting phase). Finally, in the fourth image we see that we have a topological phase transition if both terms are $dm \neq 0$ and $\Delta_{ind} \neq 0$.

2.6 Computational results

In this section we will show the plotting results of the Total system, eq. (2.5) without deriving an effective Hamiltonian. By writing the BdG form of the Total Hamiltonian ($\mathcal{H}_{BdG}(k)$), we get the matrix:

$$\begin{pmatrix} \xi_k + \tilde{B} & -i\alpha k & -\Delta & 0 & -t & -t & 0 & 0 \\ i\alpha k & \xi_k - \tilde{B} & 0 & -\Delta & 0 & 0 & 0 & 0 \\ -\Delta & 0 & -\xi_k + \tilde{B} & i\alpha k & 0 & 0 & 0 & 0 \\ 0 & -\Delta & -i\alpha k & -\xi_k - \tilde{B} & 0 & 0 & -t & -t \\ -t & 0 & 0 & 0 & v(k - k_F) & 0 & 0 & 0 \\ -t & 0 & 0 & 0 & 0 & -v(k + k_F) & 0 & 0 \\ 0 & 0 & 0 & -t & 0 & 0 & -v(-k - k_F) & 0 \\ 0 & 0 & 0 & -t & 0 & 0 & 0 & v(-k + k_F) \end{pmatrix} \tag{2.96}$$

Next, we present the results by plotting the eigenvalues of this 8×8 matrix.

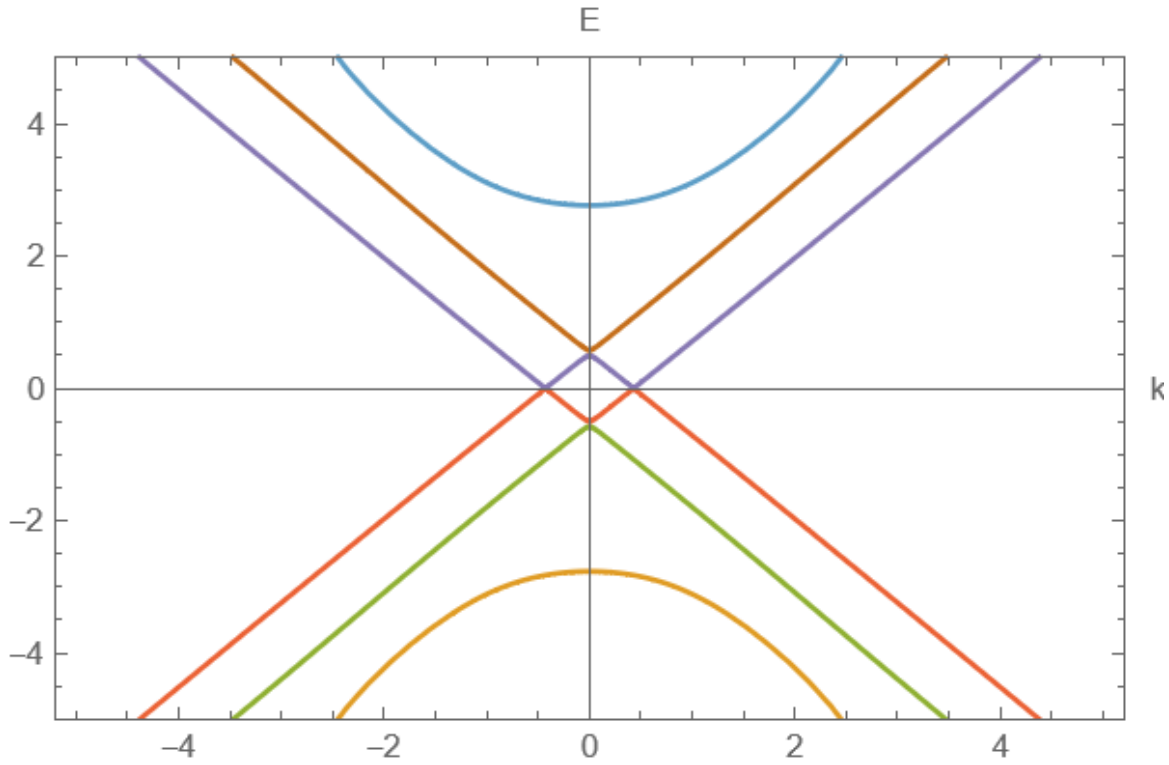

Figure 2.4: Trivial regime of the $\mathcal{H}_{BdG}(k)$.

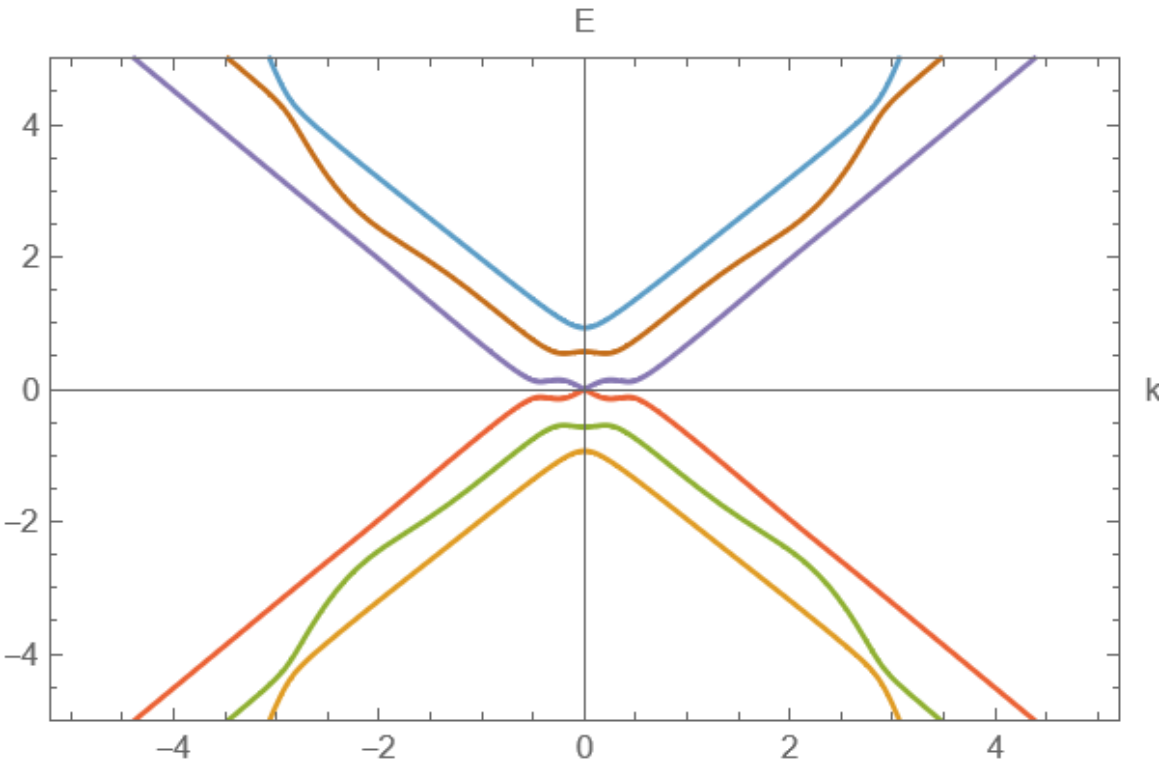

Figure 2.5: Phase transition of the $\mathcal{H}_{BdG}(k)$.

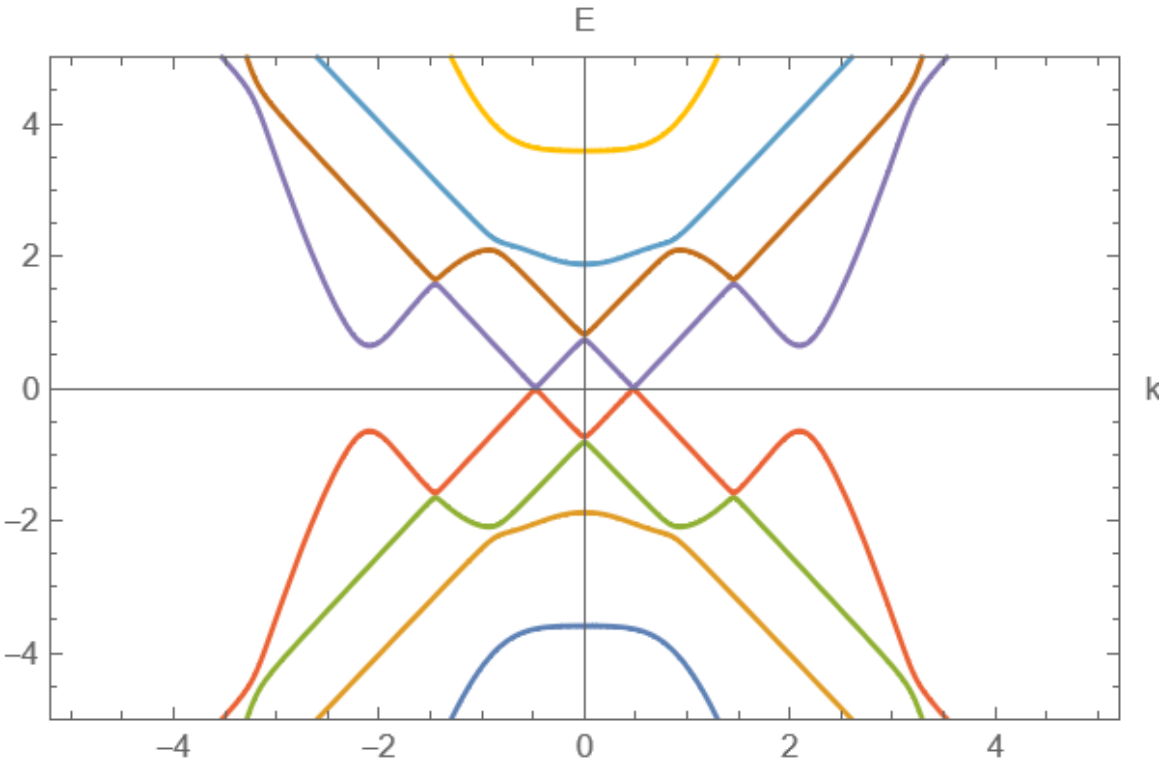

Figure 2.6: Topological regime of the $\mathcal{H}_{BdG}(k)$.

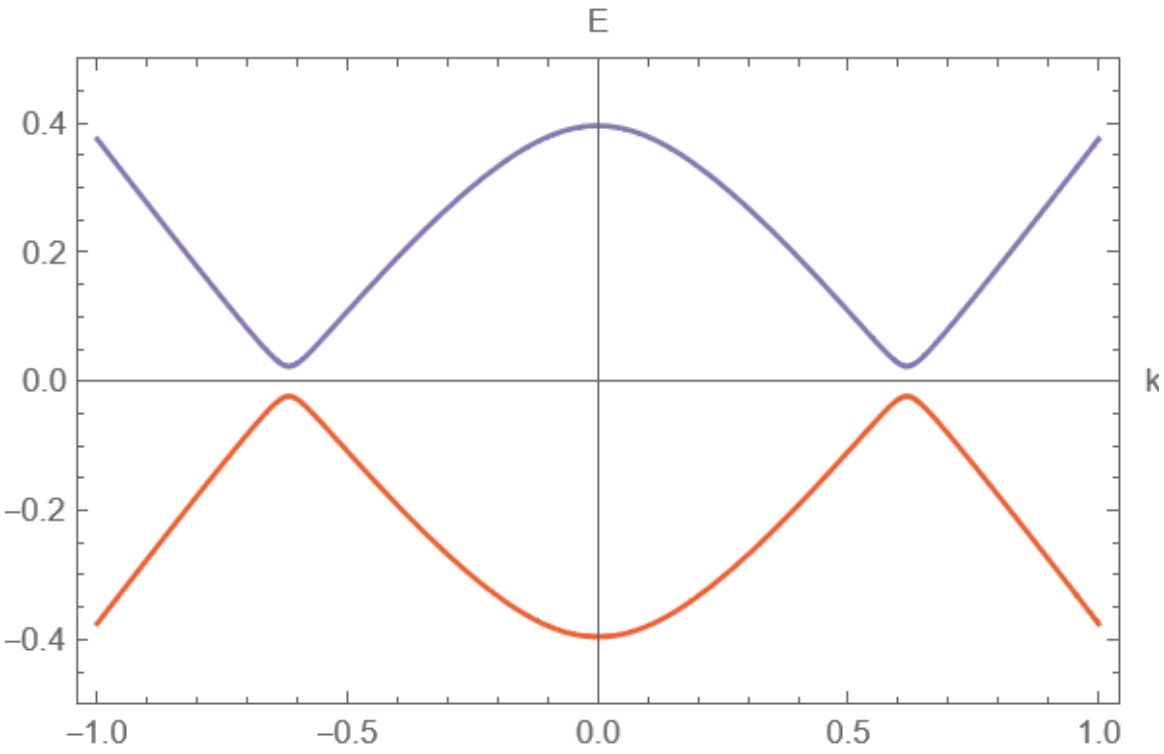

Figure 2.7: Induced Gap shown in topological regime of the $\mathcal{H}_{BdG}(k)$.

We start by showing the Trivial phase of our system in Fig. (2.4) where $\Delta > \tilde{B}_{cr}$. Next, we show in Fig. (2.5) we show that as we lower the value of Δ we are going to have a phase transition from the Normal to Topological state. In Fig. (2.6) our system is in the Topological state and if we zoom in in this plot, we can see as shown in Fig. (2.7) that a gap opens. This is the induced gap that we were trying to estimate in this Chapter. Note also, that in the above plots, the values that are indicated in the axis do not represent the true values of the terms but are some random (but they still follow the restrictions and the approximations we made so far) numerical values to check how our system behaves.

Chapter 3

Bosonization

In this section, we will be studying the bosonised description of our model. Our guide for this theory will be the lectures notes of [17]. As a starting point, we begin by introducing again the single particle Hamiltonian where we have now the pairing potential $\Delta = 0$:

$$H_{sp} = \xi_k + \alpha k \sigma_y + \tilde{B}\sigma_z \tag{3.1}$$

where again $\xi_k = \frac{k^2}{2m} - \mu$ is the kinetic term and the chemical potential μ sets the filling $\mu = \frac{k_{SC,F}^2}{2m^*}$ with m^* the effective mass, α is the strength of spin-orbit Rashba interaction and $\tilde{B} = g\mu_B B$ the Zeeman field with μ_B the Bohr magneton, g is the Landé g-factor, B the magnetic field and $\overrightarrow{\sigma} = (\sigma_x, \sigma_y, \sigma_z)$ the Pauli matrices. The spectrum can easily be found to be

$$E_\pm = \xi_k \pm \sqrt{\tilde{B}^2 + (\alpha k)^2} \tag{3.2}$$

and the corresponding eigenstates that belong in the σ_z-basis are

$$\psi = \begin{pmatrix} \psi_+ \\ \psi_- \end{pmatrix} = \begin{pmatrix} \frac{\left(\tilde{B}+\sqrt{\tilde{B}^2+(\alpha k)^2}\right)}{i\left(\left(\tilde{B}+\sqrt{\tilde{B}^2+(\alpha k)^2}\right)^2+(\alpha k)^2\right)^{1/2}} \\ \pm\frac{ak}{\left(\left(\tilde{B}+\sqrt{\tilde{B}^2+(\alpha k)^2}\right)^2+(\alpha k)^2\right)^{1/2}} \end{pmatrix} \tag{3.3}$$

If we want to project these states in the Bloch sphere, we have first for the state with the $+$ sign (the state of the upper band):

$$\left|\psi^+\right\rangle = \cos\frac{\vartheta}{2}\left|\uparrow\right\rangle + e^{i\phi}\sin\frac{\vartheta}{2}\left|\downarrow\right\rangle \tag{3.4}$$

and the state orthogonal to this one is the state of the lower band:

$$\left|\psi^{-}\right\rangle = \sin\frac{\vartheta}{2}\left|\uparrow\right\rangle - e^{i\phi}\cos\frac{\vartheta}{2}\left|\downarrow\right\rangle \tag{3.5}$$

where we showed in Chapter 1.6 that:

$$\cos\frac{\vartheta(k)}{2} = \frac{\left(\tilde{B}+\sqrt{\tilde{B}^2+(\alpha k)^2}\right)}{\left(\left(\tilde{B}+\sqrt{\tilde{B}^2+(\alpha k)^2}\right)^2+(\alpha k)^2\right)^{1/2}},\ \sin\frac{\vartheta(k)}{2} = \frac{-ak}{\left(\left(\tilde{B}+\sqrt{\tilde{B}^2+(\alpha k)^2}\right)^2+(\alpha k)^2\right)^{1/2}} \tag{3.6}$$

with $\phi = \frac{\pi}{2} = i$. Note here, that when the $\pm$ sign is being used like a superscript on the state it will denote that we are in the upper/lower band respectively. The lower band will be the most important, as will be shown later, and is the band that we keep the $-$ sign in $\sin\frac{\vartheta(k)}{2}$. It is quite easy to see that these two expressions have the usual trigonometric properties of $\cos\vartheta(k) = \cos\vartheta(-k)$ and $\sin\vartheta(-k) = -\sin\vartheta(k)$. We are going to make use of these properties when we try to derive the Bosonized description of our System. Furthermore, tt might be useful for future calculations to point out here that by replacing $\tilde{B} = 0$ in eq. (3.6), we find that:

$$\cos\frac{\vartheta(k)}{2} = \frac{1}{\sqrt{2}}, \quad and \quad \sin\frac{\vartheta(k)}{2} = \frac{-sign(\alpha k)}{\sqrt{2}} \tag{3.7}$$

which means that we get the eigenstates of z-basis.

Note here, that from now on, when we write $\sigma = \pm$ and $\sigma = \uparrow,\downarrow$ denotes the spin in σ_y and σ_z basis respectively.

Another way to consider the above is by writing eq. (3.1) in the form:

$$H = \xi_k + \alpha k\sigma_y + \tilde{B}\sigma_z = \xi_k\mathbb{I} + \overrightarrow{\eta}\cdot\overrightarrow{\sigma} \tag{3.8}$$

where $\overrightarrow{\eta} = \left(0, \alpha k, \tilde{B}\right)$ is a vector in the Bloch sphere and $\overrightarrow{\sigma} = \left(0, \sigma_y, \sigma_z\right)$ the Pauli matrices. In this representation is more clear to see that the angle ϑ in the Bloch sphere will get the values of:

$$\vartheta(k) = \frac{\alpha k}{\tilde{B}} \tag{3.9}$$

Here we need to consider 2 limits. The first one is when $\alpha k \to 0$. This gives us $\vartheta = 0$ which corresponds to $|\psi^{-}\rangle = |\uparrow\rangle$ (pollarized in spin $\uparrow$). The second limit is when $\tilde{B} \to 0$. This gives us $\vartheta = \pi/2$ which corresponds to $|\psi^{-}\rangle = \frac{1}{\sqrt{2}}|\uparrow\rangle + \frac{i}{\sqrt{2}}|\downarrow\rangle$ (the spin is conserved in the σ_y-basis). This is

in consistent with previous analysis and in particular we see that for $\tilde{B} = 0$ we get:

$$\begin{cases} |\psi^+\rangle = |+\rangle = \frac{|\uparrow\rangle - i|\downarrow\rangle}{\sqrt{2}}, & for \quad k < 0 \\ |\psi^-\rangle = |-\rangle = \frac{|\uparrow\rangle + i|\downarrow\rangle}{\sqrt{2}}, & for \quad k > 0 \end{cases} \tag{3.10}$$

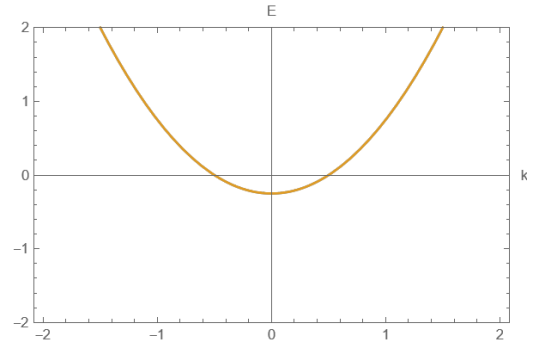

(a) Energy bands of the kinetic term only

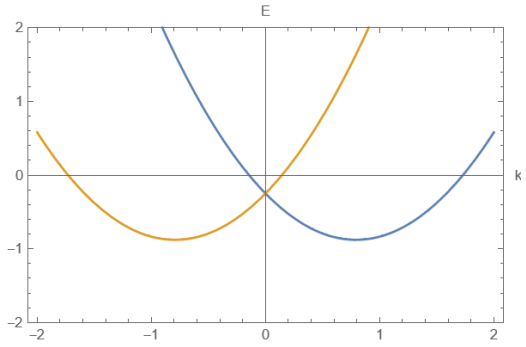

(b) Band splitting due to SOC

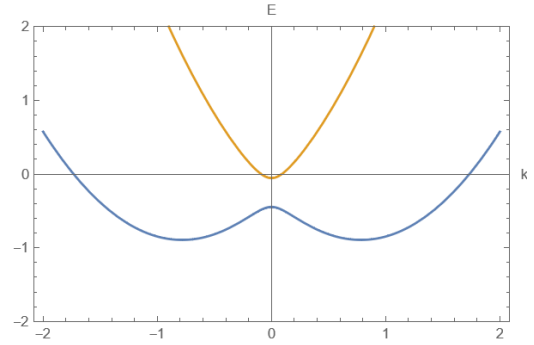

(c) Band splitting due to SOC and Zeeman splitting with small magnetic field

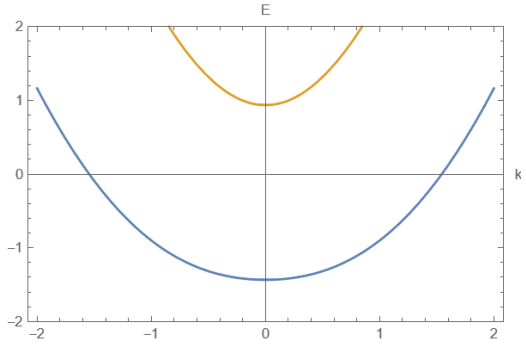

(d) Band splitting due to SOC and Zeeman splitting with bigger magnetic field

Figure 3.1: In the figure (a) we see the the energy spectrum of the kinetic term where we suppose $\alpha = 0, \tilde{B} = 0, \Delta = 0$. In Figure (b) we include the strong SOC and we see the bands split with spin $|\pm\rangle$. In the Figure (c), we open the magnetic field and keep it small. In the Figure (d), we raise the value of $\tilde{B}$ and see how the bands split.

In Figure (3.1) we said small magnetic field and bigger magnetic field. These terms will be clear in the next section where we analyze the Low-energy field approximation of our system.

3.1 Quantum Field Theory in Condensed Matter

The many-body problem in condensed matter physics generally relies on the machinery of perturbative quantum field theory to obtain solutions to model systems. Solutions to the field theories are obtained in terms of Greens functions, or equivalently, correlation functions. However, quantum fluctuations being at work on all length scales, a purely continuum theory makes no sense, and a

momentum cutoff has to be introduced in order to enable meaningful calculations. Such a regularization of the field theory invariably introduces a length scale Λ^{-1}, which is part of the definition of the theory as one of its parameters, along with various coupling constants, masses, and so on. A change in the cutoff Λ (through a trace over the high-momentum degrees of freedom) is accompanied by a modification of all other parameters of the theory. A field theory is then characterized not by a set of fixed parameter values, but by a Renormalization Group (RG) trajectory in parameter space, which traces the changing parameters of the theory as the cutoff is lowered.

Most important is the concept of fixed point, i.e., of a theory whose parameters are the same whatever the value of the cutoff. Most notorious are free particle theories (bosons or fermions), in which degrees of freedom at different momentum scales are decoupled, so that a partial trace in a momentum shell has no impact on the remaining degrees of freedom. Theories close (in a perturbative sense) to fixed points see their parameters fall into three categories: relevant, irrelevant and marginal. Relevant parameters grow algebraically under renormalization, irrelevant parameters decrease algebraically, whereas marginal parameters undergo logarithmic variations. The theory has no predictive power on its irrelevant parameters because if the the momentum cutoff is taken to infinity, then an arbitrary number of irrelevant parameters can be added to the theory without measurable effect on the low-energy properties determined from experiments. Thus, the cutoff Λ does not have to be taken to infinity, but has some natural value Λ_0, determined by a more microscopic theory (maybe even another field theory) which eventually supersedes the field theory considered at length scales smaller than Λ^{-1}. In condensed matter physics, the natural cutoff is the lattice spacing ($\approx 10 - 8$cm).

In practice, field theories should not be pushed too close to their natural cutoff Λ_0. It is expected that a large number (if not an infinity) of irrelevant couplings of order unity exist at that scale, and the theory then loses all predictive power. The general practice is to ignore irrelevant couplings altogether, and this is credible only well below the natural cutoff Λ^{-1}. The price to pay for this reduction in parameters is that the finite number of marginal or relevant parameters remaining cannot be quantitatively determined from the underlying microscopic theory (i.e., the lattice model). However, the predictions of the field theory can (in principle) be compared with experiments and the parameters of the theory be inferred.

Experiments on many-body electron systems normally measure properties at energy scales small compared to the Fermi energy. This means that only a few degrees of freedom in the system are excited, and only the low energy sector of a model need to be compared against experiment. The low energy, long distance physics also determines any long range order and cooperative phenomena present in a system. Divergences in certain correlation functions are indicative of the presence of ordering phase transitions in the system, such as ferromagnetic transitions or the Cooper pairing superconductivity phase transition. The field theory methodology has been extremely successful, with the properties of a number of simple metals accurately modeled by using Landaus Fermi liquid theory. However, many materials have emerged that have non-Fermi liquid properties and their behaviour can

be studied in 1D many body systems.

Normal perturbative methods of solution can no longer be justified in one dimension. This is because the non-interacting one dimensional fermion gas is unstable against the switching on of interactions. This is a form of the orthogonality catastrophe, where the interacting ground state is orthogonal to the non-interacting ground state.

3.1.1 Introduction to Bosonization

Bosonization of a quantum field theory describes a method by which fermionic operators in the theory, obeying anti-commutation relations, are replaced by bosonic operators obeying commutation relations. But the replacement of one field theory with another would appear to merely replace the problem of solving the original fermionic field theory with the problem of solving a bosonic field theory. The usefulness of this technique was realised when it was discovered that certain one dimensional interacting fermionic field theories, were equivalent to non-interacting bosonic field theories, i.e properties of the fermionic system can be described in terms of certain boson fields, whose properties are simpler to calculate than those of the original fermion fields.

Given the exact solution to the bosonic field theory, the properties of the fermionic theory can be calculated by use of a bosonization dictionary. For example, correlation functions in terms of fermionic operators can be re-written as expectations for bosonic operators, and solved.

Bosonization may be derived by defining a set of boson fields $\phi(x)$, and their conjugate momenta fields $\Pi(x)$, with given commutation relations, and then determining the commutation relations and Greens functions of the exponentials of these fields. The Greens functions and commutation relations are fermionic in nature, and an identity between the boson fields, $\phi(x)$ and $\Pi(x)$, and fermion fields $\psi(x)$ is made.

3.2 Low-Energy field approximation

We will now proceed to construct an effective low-energy theory. The low-energy theory is defined in terms of creation and annihilation operators in the vicinity of the Fermi points. In particular, we restrict ourselves to the modes of the momentum expansion in a $\pm$ neighborhood of $k_{SC,F}$ of width 2α, with α the Rashba spin-orbit coefficient.

For a starting point, we take the case where we include only the strong SOC in our system ($\tilde{B} = 0, \Delta = 0$). We see in Figure (3.2a) the 4 modes around $k_{SC,F}$ (lowest dotted lines) and this depends on where we set our Fermi level to be.

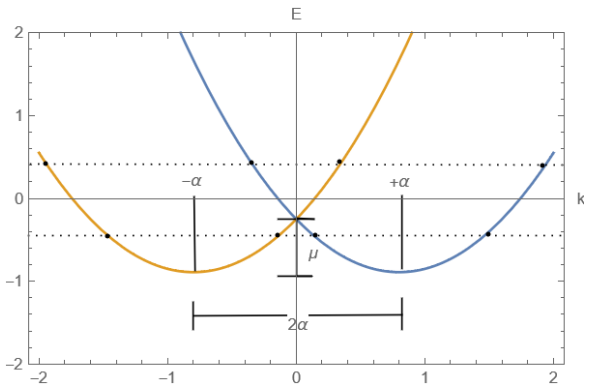

(a) Band splitting due to SOC for the 4 modes in both energy bands

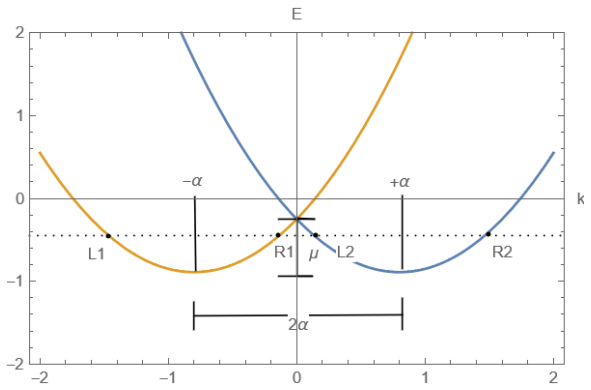

(b) Band splitting due to SOC only for the 4 modes in the lower energy band

Figure 3.2: In the figure (a) we see the the low-energy spectrum of the strong SOC and we see the bands split with spin $|\pm\rangle$. The dotes lines denotes the fermi level and the modes we have for each of our choice. In the Figure (b), we consider only the modes in the lower energy band since these are the ones we are interested. In both figures we have set $\tilde{B} = \Delta = 0$ and $\mu < \frac{\alpha^2}{2m}$.

If we set the chemical potential to start from the bottom of the lowest energy band and set $k = 0$, we see that the chemical potential should satisfy the relation $\mu < \frac{\alpha^2}{2m}$. When we turn on the magnetic field we are in the case that is depicted in Figures (3.1c 3.1d). These 2 cases are of big interest and worth analyze it further so we will label them as $\mathcal{I}$ and $\mathcal{II}$ correspondingly. In the low-energy field approximation we will have 4 modes only in the case $\mathcal{I}$. We will consider only the lower band which correspond to state $|\psi^-\rangle(k)$ because we are considering that $\mu < \frac{\alpha^2}{2m}$ and $\Delta, t, T < 2\tilde{B}$ where $2\tilde{B}$ is the gap between the 2 energy bands due to Zeeman splitting. In particular, in the case $\mathcal{I}$ (of Figure (3.1c)) we are treating the magnetic field as small perturbation and our states are represented in the σ_y-basis, i.e that the SOC is stronger than the magnetic field. The critical value for the magnetic field is found by taking the second derivative of eq. (3.2) equal to zero and setting $k = 0, \mu = \frac{\alpha^2}{2m}$ and is found equal with $\tilde{B}_{\mathcal{I},cr} = \frac{\alpha^2}{m}$. In the case $\mathcal{II}$, the spin is polarized in $\hat{z}$-direction and our states are represented in the σ_z-basis, but now we have 2-modes in the lower energy band. We can find the lowest point in the spectrum for case $\mathcal{II}$ by taking the second derivative of eq. (3.2) equal to zero and set $k = 0$. By doing so, we find $\tilde{B}_{\mathcal{II},cr} = \alpha^2 m$.

As we mentioned at the beginning of Chapter (2), we can integrate out the 2 dimensions and have an effective 1D theory. This will be the ideal case in which we built our model. It will be a good approximation for theoretical descriptions but it is not easy for experimental setups.

Since we consider a 1D quantum wire, we will assume that the electron density is such that the Fermi energy lies below the energy of the first excited state. The result is that the single-particle states with momenta in the range $-\alpha - k_{SC,F} < k < k_{SC,F} + \alpha$ are occupied and the states outside this range are empty. Thus the Fermi surface of this system reduces to four Fermi points at $\pm\alpha \pm k_{SC,F}$. We will also assume that the wire is long enough, $L \gg w$ (where L is the length and w the width of

the wire), so that the single particle states fill up densely the momentum axis, and that the density is high enough that $\Delta k = 2\pi\hbar/L \ll k_{SC,F}$. On the other hand, we will assume that the wire is narrow enough that the next band of (excited) states can effectively be neglected, $\epsilon_{SC,F} \ll \hbar^2/(2mw^2)$. At higher electronic densities, more than one band can intersect the Fermi energy. Each new partially occupied band is labeled by a pair of Fermi points. In practice we will work in a regime in which the following inequality holds:

$$\frac{L}{w} \gg 1 \gg \frac{w}{\lambda_{SC,F}} \tag{3.11}$$

where $\lambda_{SC,F} = \hbar/k_{SC,F}$ is the wavelength, and we have only four Fermi points.

Having set up the problem properly, it is time to make a very important observation. We saw that eq. (3.5) is written in the σ_z-basis. If we continue our analysis in this basis, we will encounter a difficulty in the Renormalization procedure. To be more specific, we will have to calculate 3_{rd} terms in order to estimate the gap. This can be avoided by changing the basis of the SC eigenstates from σ_z to σ_y -basis. This can be done by simple replacing the terms:

$$|\uparrow\rangle = \frac{|+\rangle + |-\rangle}{\sqrt{2}} \quad and \quad |\downarrow\rangle = \frac{|+\rangle - |-\rangle}{i\sqrt{2}} \tag{3.12}$$

in eq. (3.5). This will result to the lower band eigenstate in the σ_y-basis to be equal with:

$$\big|\psi^-(k)\big\rangle = \frac{1}{\sqrt{2}}\Big(\sin\frac{\vartheta(k)}{2} + \cos\frac{\vartheta(k)}{2}\Big)|+\rangle - \frac{1}{\sqrt{2}}\Big(\sin\frac{\vartheta(k)}{2} - \cos\frac{\vartheta(k)}{2}\Big)|-\rangle \tag{3.13}$$

In order to describe our original states in this low-energy field approximation, we perform first a Fourier transformation in our lower band state:

$$\big|\psi^-(x)\big\rangle = \int \frac{dk}{\sqrt{2\pi}} e^{ikx}\big|\psi^-(k)\big\rangle \tag{3.14}$$

where $\tilde{\alpha}$ is the lattice spacing and especially for NbN it is approximately $\tilde{\alpha} = 4.357\mathring{A}$. Next, we integrate in a very small window around fermi momentum and this will result to our 4-modes (2-Left and 2-Right) as shown in Figure (3.2b) with expressions in the bosonized picture of the form:

$$\begin{aligned}\psi_{L,1}(x) = \frac{1}{\sqrt{4\pi}} e^{i(-k_{SC,F}-\alpha)x}\Big[\mathrm{k}_+\frac{1}{\sqrt{2}}\Big(\sin\frac{\vartheta(-k_{SC,F}-\alpha)}{2} + \cos\frac{\vartheta(-k_{SC,F}-\alpha)}{2}\Big)e^{i(\phi_+(x)+\theta_+(x))} \\ -\mathrm{k}_-\frac{1}{\sqrt{2}}\Big(\sin\frac{\vartheta(-k_{SC,F}-\alpha)}{2} - \cos\frac{\vartheta(-k_{SC,F}-\alpha)}{2}\Big)e^{i(\phi_-(x)+\theta_-(x))}\Big]\end{aligned} \tag{3.15}$$

$$\psi_{R,1}(x) = \frac{1}{\sqrt{4\pi}} e^{i(k_{SC,F}-\alpha)x} \Big[\mathrm{k}_+ \frac{1}{\sqrt{2}} \Big(\sin\frac{\vartheta(k_{SC,F}-\alpha)}{2} + \cos\frac{\vartheta(k_{SC,F}-\alpha)}{2} \Big) e^{i(\phi_+(x)-\theta_+(x))} \\ -\mathrm{k}_- \frac{1}{\sqrt{2}} \Big(\sin\frac{\vartheta(k_{SC,F}-\alpha)}{2} - \cos\frac{\vartheta(k_{SC,F}-\alpha)}{2} \Big) e^{i(\phi_-(x)-\theta_-(x))} \Big] \quad (3.16)$$

$$\psi_{L,2}(x) = \frac{1}{\sqrt{4\pi}} e^{i(-k_{SC,F}+\alpha)x} \Big[\mathrm{k}_+ \frac{1}{\sqrt{2}} \Big(\sin\frac{\vartheta(-k_{SC,F}+\alpha)}{2} + \cos\frac{\vartheta(-k_{SC,F}+\alpha)}{2} \Big) e^{i(\phi_+(x)+\theta_+(x))} \\ -\mathrm{k}_- \frac{1}{\sqrt{2}} \Big(\sin\frac{\vartheta(-k_{SC,F}+\alpha)}{2} - \cos\frac{\vartheta(-k_{SC,F}+\alpha)}{2} \Big) + e^{i(\phi_-(x)+\theta_-(x))} \Big] \quad (3.17)$$

$$\psi_{R,2}(x) = \frac{1}{\sqrt{4\pi}} e^{i(k_{SC,F}+\alpha)x} \Big[\mathrm{k}_+ \frac{1}{\sqrt{2}} \Big(\sin\frac{\vartheta(k_{SC,F}+\alpha)}{2} + \cos\frac{\vartheta(k_{SC,F}+\alpha)}{2} \Big) e^{i(\phi_+(x)-\theta_+(x))} \\ -\mathrm{k}_- \frac{1}{\sqrt{2}} \Big(\sin\frac{\vartheta(k_{SC,F}+\alpha)}{2} - \cos\frac{\vartheta(k_{SC,F}+\alpha)}{2} \Big) e^{i(\phi_-(x)-\theta_-(x))} \Big] \quad (3.18)$$

or, we can write them in a more composite form like:

$$\psi_{\sigma,\eta,j} = \sum_{\sigma=\pm=\pm 1} \sum_{\eta=L/R=\pm 1} \sum_{j=1,2=\mp 1} \frac{1}{\sqrt{8\pi}} \mathrm{k}_\sigma \mathcal{C}_{\sigma,\eta,j} e^{i(-\eta k_{SC,F}+j\alpha)x} e^{i(\phi_\sigma(x)+\eta\theta_\sigma(x))} \quad (3.19)$$

where in the above description we defined as $\mathcal{C}_{+,\eta,j}(k) = \Big(\sin\frac{\vartheta(-\eta k_{SC,F}+j\alpha)}{2} + \cos\frac{\vartheta(-\eta k_{SC,F}+j\alpha)}{2} \Big)$ and $\mathcal{C}_{-,\eta,j}(k) = -\Big(\sin\frac{\vartheta(-\eta k_{SC,F}+j\alpha)}{2} + \cos\frac{\vartheta(-\eta k_{SC,F}+j\alpha)}{2} \Big)$. Also, in the above description $\sigma = \pm$ denotes the spin in the σ_y, $\eta = L/R = \pm 1$ denotes the Left and Right movers and $j = \mp 1 = 1, 2$ denotes the modes 1 or 2 and was chosen like this to always give the right sign for eq. (3.15-3.18). We should note here one important property for these coefficients that we are gonna use for later derivations, which is $\mathcal{C}_{+,\eta,-\sigma}(-k) = \mathcal{C}_{-,\eta,-\sigma}(-k)$ and is easy to check that it is true. Furthermore, we introduced the $k_\pm$ Klein factors. These operators are necessary because they ensure the proper fermionic anti-commutation relations between Right and Left-movers and have the properties:

$$\big\{ \mathrm{k}_{\sigma,\alpha}, \mathrm{k}_{\sigma',\beta} \big\} = 2\delta_{\sigma\sigma'}\delta_{\alpha\beta},\ \mathrm{k}^2_{\sigma,\alpha} = 1,\ \mathrm{k}_{\sigma,\alpha} = \mathrm{k}^\dagger_{\sigma,\alpha} = \mathrm{k}^{-1}_{\sigma,\alpha} \quad (3.20)$$

where $\alpha, \beta = SC, (F)QH$ here denotes the (F)QH or the SC. We have also introduced the bosonic

fields $\phi_\sigma(x), \theta_\sigma(x)$, with $\phi_\sigma(x) = \phi_\sigma^{SC}(x)$ and $\theta_\sigma(x) = \theta_\sigma^{SC}(x)$ which obey the commutation relations:

$$\left[\phi_\sigma^{SC}(x), \phi_{\sigma'}^{QH}(x)\right] = \left[\phi_\sigma^{SC}(x), \phi_{\sigma'}^{SC}(x')\right] = \left[\phi_\sigma^{QH}(x), \phi_{\sigma'}^{QH}(x')\right] = 0, \tag{3.21}$$

$$\left[\theta_\sigma^{SC}(x), \theta_{\sigma'}^{QH}(x)\right] = \left[\theta_\sigma^{SC}(x), \theta_{\sigma'}^{SC}(x')\right] = \left[\theta_\sigma^{QH}(x), \theta_{\sigma'}^{QH}(x')\right] = 0 \tag{3.22}$$

$$\left[\phi_\sigma^{SC}(x), \theta_{\sigma'}^{QH}(x')\right] = \left[\phi_\sigma^{QH}(x), \theta_{\sigma'}^{SC}(x')\right] = 0 \tag{3.23}$$

$$\left[\phi_\sigma^{SC}(x), \theta_{\sigma'}^{SC}(x')\right] = \left[\phi_\sigma^{QH}(x), \theta_{\sigma'}^{QH}(x')\right] = i\delta_{\sigma\sigma'}\pi\Theta(x - x') \tag{3.24}$$

where again $\sigma = \sigma' = \pm$ is the spin in the σ_y-basis when we are talking about our Superconductor and $\sigma' = \uparrow, \downarrow$ the spin in σ_z-basis when we refer to (Fractional or Integer) QH and

$$\Theta(x - x') = \begin{cases} \Theta(x - x' > 0) = 1 \\ \Theta(x - x' = 0) = \frac{1}{2} \quad for\ fermions \\ \Theta(x - x' < 0) = 0 \end{cases} \tag{3.25}$$

is the Heaviside step function. In above commutation relations for the Quantum Hall indices correspond to 1 electron. As we will see later for the case of FQH these relations will slightly change but will have a huge physical meaning. The expressions of the modes derived above are shown in the Figure (3.3).

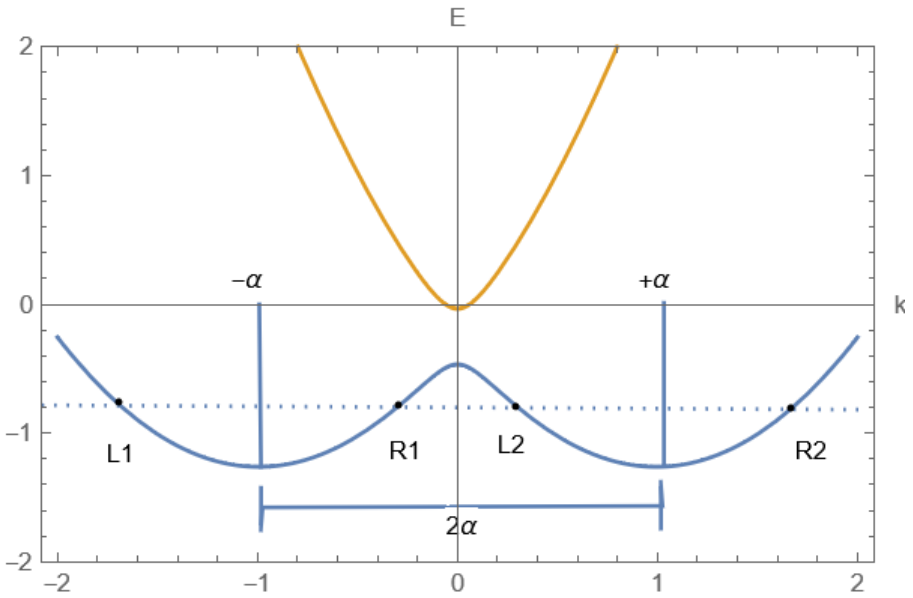

Figure 3.3: Here we see the 4 modes we are considering in the low-energy band where we include the strong SOC, the magnetic field is turned on ($\tilde{B} \neq 0$), the superconducting pairing potential $\Delta = 0$. When the momentum is fixed in the value $k = k_{SC,F}$ (dotted line), we are considering the low-energy approximation, which results to those 4 modes and their precise expressions found in eq. (3.15-3.18).

A more fundamental way to express the commutation relation (3.21) is to write it as:

$$\left[\frac{\partial_x \theta_{\sigma'}(x')}{\pi}, \phi_\sigma(x)\right] = -i\delta_{\sigma\sigma'}\delta(x-x') \tag{3.26}$$

It is an equal-time commutation relation, both the fields are here taken at the same time. It states indeed that $\partial_x\theta_{\sigma'}(x')$ is the canonically conjugate operator of ϕ, thus $\partial_x\theta_{\sigma'}(x') \propto \partial_t\phi_\sigma(t)$. To be more precise, in the above description when we defined the fields ϕ to be the dual field of θ, we mean that they must fulfill the following relations (which are valid for $\mathcal{K}=1$ only):

$$\partial_t\theta = v_F^e\partial_x\phi, \quad \partial_x\theta = \frac{\partial_t\phi}{v_F^e} \tag{3.27}$$

Based on equation (3.27) we encoded the chiral behaviour of our vortex operations in eq. (3.15-3.18) by defining the Left and Right bosonic fields as:

$$\phi_{L,\sigma} = \phi_\sigma + \theta_\sigma, \quad \phi_{R,\sigma} = \phi_\sigma - \theta_\sigma \tag{3.28}$$

where $\sigma = \pm$ is the spin.

In order to ensure that the above definitions of our Left and Right movers are well defined, we need to check that they obey the anti-commutation relations for fermions:

$$\left\{\psi_{x,\sigma}, \psi^\dagger_{x',\sigma'}\right\} = \frac{1}{2\pi\alpha}\delta_{\sigma\sigma'}\delta_{xx'}, \quad \left\{\psi_{x,\sigma}, \psi_{x',\sigma'}\right\} = \left\{\psi^\dagger_{x,\sigma}, \psi^\dagger_{x',\sigma'}\right\} = 0 \tag{3.29}$$

where after some simple calculations and apply the commutation relations of the bosonic fields $\phi(x)$ and $\theta(x)$ and considering the properties of Klein factors, we see that they obey eq. (3.29).

Here is a good point to introduce the charge (c) and spin (s) fields as follows:

$$\phi_c = \frac{\phi_+ + \phi_-}{\sqrt{2}}, \;\; \theta_c = \frac{\theta_+ + \theta_-}{\sqrt{2}} \tag{3.30}$$

$$\phi_s = \frac{\phi_+ - \phi_-}{\sqrt{2}}, \;\; \theta_s = \frac{\theta_+ - \theta_-}{\sqrt{2}} \tag{3.31}$$

The inverse relations that are going to be useful when we calculate the tunneling term are:

$$\phi_+^{SC} = \frac{\phi_c + \phi_s}{\sqrt{2}}, \quad \theta_+^{SC} = \frac{\theta_c + \theta_s}{\sqrt{2}} \tag{3.32}$$

$$\phi_-^{SC} = \frac{\phi_c - \phi_s}{\sqrt{2}}, \quad \theta_-^{SC} = \frac{\theta_c - \theta_s}{\sqrt{2}} \tag{3.33}$$

and $\phi_\pm^{SC}, \theta_\pm^{SC}$ have a periodicity of $\phi_\pm^{SC} = \phi_\pm^{SC} + 2\pi m$ and $\theta_\pm^{SC} = \theta_\pm^{SC} + 2\pi m$ respectively, where $m = 0, 1, 2, \ldots$ an integer number. By changing the basis we are rotating our original lattice space

by $45°$. In this basis our Hamiltonian should be diagonal. The spin and charge excitations will appear separately, therefore it is possible to regard the spin and charge particles as the new independent fundamental excitations instead of the old spin up and spin down particles. Indeed, because of the degeneracy of the spin up and spin down channel, we could have used any canonical rotation to define new particles, but spin and charge are particularly useful when interactions are present. This is intuitively clear because realistic interactions will couple total charge densities and thereby lift the degeneracy between the spin and the charge channel. With interactions, we are therefore forced to use the picture of spin and charge excitations, since the freedom of rotating degenerate channels is lost. Note however, that the spin and charge separation is not obeyed exactly for the particle numbers, because the new zero modes still must obey the old quantization formula. Both numbers must be integers, but cannot be changed independently. Adding a spin particle must always be accompanied by adding or removing a charge particle and vice versa, i.e. the total sum of spin and charge particles must always remain even. This just reflects the fact that we always have to add and remove real electrons, instead of spin/charge quasi-particles. We are gonna use these definitions in our next calculations.

By turning on the magnetic field, the system tends to couple the modes $\psi_{R,1}(x)$ and $\psi_{L,2}(x)$, in the point where the 2 parabolas are crossing in Figure(3.2b). Let's analyze this pairing term a bit. The magnetic pairing can be described in a Hamiltonian of the form:

$$H_{\tilde{B}} = \tilde{B}(\psi_+^\dagger(x)\psi_-(x) \ + \ H.C) = \\ \tilde{B}\Big(\big(\psi_{L,1}^\dagger(x) + \psi_{R,1}^\dagger(x)\big)\big(\psi_{L,2}(x) + \psi_{R,2}(x)\big) \ + \ H.C\Big) \tag{3.34}$$

We consider here the magnetic term as a small perturbation and by performing the calculations explicitly (check Appendix (B.2)), we find terms of the form:

- $\psi_{L,1}^\dagger(x)\psi_{L,2}(x) + \psi_{R,1}^\dagger(x)\psi_{R,2}(x) \ + \ H.C \sim \ e^{2i\alpha x} \ + \ H.C$
- $\psi_{L,1}^\dagger(x)\psi_{R,2}(x) + \psi_{R,1}^\dagger(x)\psi_{L,2}(x) \ + \ H.C \sim \ \big(e^{2i(k_{SC,F}+\alpha)x} + e^{2i(k_{SC,F}-\alpha)x}\big) \ + \ H.C$

For these terms it easily to see that they are Fast Oscillating (F.O), i,e they will be irrelevant at first order in the RG sense for our system and we can neglect them. Although, if we set the value of fermi momentum at $k_{SC,F} = \pm\alpha$ we get some relevant terms which will play an important role for future analysis. It is possible to get some exotic excitations in the final results and might be a good idea for future calculations, but for our case we consider that $k_{SC,F} \neq \alpha$, i.e we do not consider any resonance in the system. It of importance to note here that in the description the 4-modes in eq. (3.15-3.18) we have already included the magnetic field in our Hamiltonian in order to get a more rigorous picture of our system. One can set the $\tilde{B} = 0$ and will get the correct results as in the case of considering the Hamiltonian (3.1) without the Zeeman term. In case someone wonders about the critical value of magnetic $\tilde{B}_{cr}$ in which the superconductor remains in the topological regime, as in the previous analytical methods, we must note what we aim here is not consider if the SC is topological, but to

consider whether it induces a gap into the QH. The Majorana (or Parafermions) modes will come from the Integer (or Fractional) Quantum Hall in this case. If however the SC is in topological regime then we expect to have additional Majorana (or Parafermion) modes in our system. Finally, NbN is a Type-2 SC, this means the london penetration length λ_L and coherence length ξ should satisfy the relation $\lambda_L > \xi$ and in order to remain in the case $\mathcal{I}$ as mentioned before, we want the width w of the SC to be small. Typically, it should be $w \ll \lambda_L$.

Proceeding next, we turn on $\Delta \neq 0$, we are inducing superconductivity via an s-wave pairing to our system which takes the coupling between opposite spins in the modes (check Appendix (B.3)):

$$H_\Delta = -\Delta(\psi^\dagger_{L,1}(x)\psi^\dagger_{R,2}(x) + \psi^\dagger_{R,1}(x)\psi^\dagger_{L,2}(x) \; + \; H.C) = \\ i\mathrm{k}_+\mathrm{k}_-\frac{\Delta}{\pi}\Big(\mathcal{C}_{+,L,-1}\mathcal{C}_{-,L,-1} + \mathcal{C}_{+,R,+1}\mathcal{C}_{-,R,+1}\Big)\Big[\sin\big(\sqrt{2}(\phi_c(x) + \theta_s(x))\big) + \sin\big(\sqrt{2}(\phi_c(x) - \theta_s(x))\big)\Big] \tag{3.35}$$

where again we have here the prefactors $\mathcal{C}_{+,\eta,j} = \Big(\sin\frac{\vartheta(-\eta k_{SC,F}+j\alpha)}{2} + \cos\frac{\vartheta(-\eta k_{SC,F}+j\alpha)}{2}\Big)$ and $\mathcal{C}_{-,\eta,j} = -\Big(\sin\frac{\vartheta(-\eta k_{SC,F}+j\alpha)}{2} + \cos\frac{\vartheta(-\eta k_{SC,F}+j\alpha)}{2}\Big)$ and we see that appears 2 sine-Gordon terms. The operators $\phi_c(x)$ and $\theta_s(x)$ commute with each other, thus they can simultaneously minimized. This observation will be useful later. From these two terms we can see that:

$$\theta_s = 0 \Rightarrow \begin{cases} \mathrm{j}_c = 0 \\ \rho_s = 0 \end{cases} \tag{3.36}$$

where j_c is the charge density and ρ_s the spin density in the semiclassical picture.

The final step is to write the bosonized description of our tunneling Hamiltonian. Previously, we had:

$$H_t(x) = -t\int dx \sum_{j=L,R}[\psi^\dagger_{FQH,\uparrow,j}(x)\psi_{SC,\uparrow}(x) + \psi^\dagger_{SC,\uparrow}(x)\psi_{FQH,\uparrow,j}(x)] \tag{3.37}$$

It is worth noting again that due to the strong magnetic field, the spin of the Quantum Hall will be polarized in the $\hat{z}$-direction. So, we only consider the $\psi_{FQH,\uparrow,j}(x)$ states, for which we can neglect the spin indices but it will always be implied. Furthermore, in the previous methods we considered the Integer Quantum Hall and now since we do not want to calculate again the same things, we consider the Fractional Quantum Hall, hence the indices FQH in eq. (3.37).

Let's take a closer look to what we mean in this low-energy approximation description when we write $\psi_{SC,\uparrow}(x)$. We can write this term in real space by Fourier transforming as:

$$\psi_{SC,\uparrow}(x) = \int \frac{dk}{\sqrt{2\pi}}\big(\alpha(k)\psi^-_{SC}(k) + \beta(k)\psi^+_{SC}(k)\big)e^{ikx} \tag{3.38}$$

where the factors $\alpha(k), \beta(k)$ take the value of $\frac{1}{\sqrt{2}}$ when we consider $\tilde{B} = 0$. This also means that for $\tilde{B} = 0$ the bands are polarized along $\hat{y}$ and to be more presice, we get $|\uparrow\rangle_z = \frac{1}{\sqrt{2}}(|+\rangle_y + |-\rangle_y)$. From the above expression, we neglect the upper band ($\psi^+_{SC}(k)$) and take only the projection in the lower band. This means that our tunneling Hamiltonian eq. (3.37) becomes:

$$
\begin{aligned}
H_t(x) = -t \sum_{j=L,R} [\psi^\dagger_{FQH,\uparrow,j}(x)\psi_{SC,\uparrow}(x) + H.C] \approx \\
-t \int dx \sum_{j=L,R} [\psi^\dagger_{FQH,\uparrow,j}(x) \int \frac{dk}{\sqrt{2\pi}} \Big[\alpha(k)\psi^-_{SC}(k) + H.C\Big] \approx \\
-t \int dx \Big[\big(\psi^\dagger_{FQH,\uparrow,L}(x) + \psi^\dagger_{FQH,\uparrow,R}(x)\big)\big) \frac{1}{\sqrt{2\pi}} \big(\sum_{\sigma=\pm=\pm 1} \sum_{\eta=L,R} \sum_{j=1,2} \psi^-_{\sigma,\eta,j}(x)\big) + H.C\Big] = \\
\frac{-t}{\sqrt{2\pi}} \int dx \Big[\big(\psi^\dagger_{FQH,\uparrow,L}(x) + \psi^\dagger_{FQH,\uparrow,R}(x)\big)\big) \big(\sum_{\sigma=\pm=\pm 1} \sum_{\eta=L,R} \sum_{j=1,2} \psi^-_{\sigma,\eta,j}(x)\big) + H.C\Big]
\end{aligned}
\tag{3.39}
$$

where in above steps we considered the approximation that we take the projection only in the lower band and the low-energy approximation where we have 4-modes. Also the factor of $\alpha(k)$ was absorbed inside $\psi^-_{\eta,j}(x)$ so that we can take the general case with $\tilde{B} \neq 0$. In particular, we have:

$$
\begin{aligned}
\psi_{SC,\uparrow}(x) = \frac{1}{\sqrt{4\pi}} e^{i(-k_{SC,F}-\alpha)x} \Big[\mathrm{k}_{Sc,+} \mathcal{C}_{+,+1,-1} e^{i(\phi_+(x)+\theta_+(x))} - \mathrm{k}_- \mathcal{C}_{-,+1,-1} e^{i(\phi_-(x)+\theta_-(x))} \Big] \\
+ \frac{1}{\sqrt{4\pi}} e^{i(k_{SC,F}-\alpha)x} \Big[\mathrm{k}_{Sc,+} \mathcal{C}_{+,-1,-1} e^{i(\phi_+(x)-\theta_+(x))} - \mathrm{k}_- \mathcal{C}_{-,-1,-1} e^{i(\phi_-(x)-\theta_-(x))} \Big] \\
+ \frac{1}{\sqrt{4\pi}} e^{i(-k_{SC,F}+\alpha)x} \Big[\mathrm{k}_{Sc,+} \mathcal{C}_{+,+1,+1} e^{i(\phi_+(x)+\theta_+(x))} - \mathrm{k}_- \mathcal{C}_{-,+1,+1} e^{i(\phi_-(x)+\theta_-(x))} \Big] \\
+ \frac{1}{\sqrt{4\pi}} e^{i(k_{SC,F}+\alpha)x} \Big[\mathrm{k}_{Sc,+} \mathcal{C}_{+,-1,+1} e^{i(\phi_+(x)-\theta_+(x))} - \mathrm{k}_- \mathcal{C}_{-,-1,+1} e^{i(\phi_-(x)-\theta_-(x))} \Big]
\end{aligned}
\tag{3.40}
$$

where $\mathcal{C}_{\sigma,\eta,j}$ as defined before. In a more composite form, it can be written as:

$$
\psi^-_{\sigma,\eta,j} = \sum_{\sigma=\pm} \sum_{\eta=L/R=\pm 1} \sum_{j=\mp 1} \frac{1}{\sqrt{4\pi}} \mathrm{k}_\sigma \mathcal{C}_{\sigma,\eta,j} e^{i(-\eta k_{SC,F} + j\alpha)x} e^{i(\phi_\sigma(x) + \eta\theta_\sigma(x))} \tag{3.41}
$$

where $\mathcal{C}_{\sigma,\eta,j}$ coefficients were defined earlier but here we replaced j with $-\sigma$. It is important to note here that in eq. (3.41) the sign of the Fermi momentum is locked to the opposite sign of θ field, in particular, as will be shown later, in the sign of θ_c field and the sign of the Rashba coefficient it is locked to the the opposite sign of spin. In this way, when we consider the case $\tilde{B} = 0$, and by taking into consideration eq. (3.7) we will get the correct states. In the case where $\tilde{B} \neq 0$ the extra term will be considered as a small correction to the previous case. So far, we have defined every term in the bosonized picture except the FQH operators $\sum_{j=L,R} \psi_{FQH,\uparrow,j}(x)$. In the low-energy approximation,

we can write FQH operators as:

$$\psi_{FQH,\uparrow}(x) = \mathrm{k}_{FQH,\uparrow}\psi_{FQH,\uparrow,L}(x)e^{-ik_{FQH,F}x} + \mathrm{k}_{FQH,\uparrow}\psi_{FQH,\uparrow,R}(x)e^{ik_{FQH,F}x} \tag{3.42}$$

where we can write it in the bosonized picture as:

$$\psi_{FQH,\uparrow}(x) = \mathrm{k}_{FQH,\uparrow}\Big(e^{-ik_{FQH,F}x}e^{i(\phi_e(x)+\theta_e(x))} + e^{ik_{FQH,F}x}e^{i(\phi_e(x)-\theta_e(x))}\Big) \tag{3.43}$$

or in a composite form as :

$$\psi_{\eta'}(x) = \sum_{\eta'=L,R=\pm 1} \mathrm{k}_{FQH,\uparrow}\Big(e^{-\eta' ik_{FQH,F}x}e^{i(\phi_e(x)+\eta'\theta_e(x))}\Big) \tag{3.44}$$

where again, we see that the sign of the Fermi momentum $k_{FQH,F}$ is fixed to the opposite sign of θ_e. The bosonic fields for the FQH that we are going to use are $\phi'(x) \neq \phi_e(x)$ and $\theta'(x) = \theta_e(x)$, which means that one of them is different from the one in the IQH. Furthermore, for simplicity we will neglect the notation of FQH in the above bosonic fields and the spin $\uparrow$ polarization is implied. Let's try to make these definitions of the FQH bosonic fields more understandable.

We start by writing the wave function of a bare electron in edge state. This will be:

$$\psi_e = e^{i(\phi_e \pm \theta_e)}$$

where $\pm$ denotes left and right mover. By considering the composite fermion (i.e 1 electron + 2 magnetic flux) we are describing the Laughlin state of $\nu = 1/3$ and it can be described by:

$$\psi_{cf} = e^{i(3\phi_e \pm \theta_e)}$$

This means that our fractional quasiparticle can be described by the wave function:

$$\sqrt[3]{\psi_{cf}} = \psi_{qp} = e^{i(\phi' \pm \theta')}$$

Thus, the connection between FQH and the IQH bosonic fields is:

$$\phi'(x) = \frac{\phi_e(x)}{3} \;\; and \;\; \theta'(x) = \theta_e(x) \tag{3.45}$$

Since we are considering here the FQH of filling factor $\nu = \frac{1}{3}$, the FQH fields must obey the commu-

tation relations:

$$[\phi_{e,\sigma}(x), \theta_{e,\sigma'}(x')] = i\pi\delta_{\sigma\sigma'}\Theta(x-x') \iff \Big[3\phi_{\sigma}^{'FQH}(x), \theta_{\sigma'}^{'FQH}(x')\Big] = i\pi\delta_{\sigma\sigma'}\Theta(x-x')$$
$$\iff \Big[\phi_{\sigma}^{'FQH}(x), \theta_{\sigma'}^{'FQH}(x')\Big] = i\delta_{\sigma\sigma'}\frac{\pi}{3}\Theta(x-x') \tag{3.46}$$

The reason why they have this form is becoming more clear when we consider the interacting Luttinger liquid. Now, the role of interactions, is easily encoded the Luttinger parameter, which will be $\mathcal{K}_e = \frac{1}{3}$ (strong Coulomb interaction), and the Hamiltonian of the Luttinger liquid will be described in our case as:

$$H_{qp} = H_{FQH} = \frac{v_F^e}{2\pi}\int dx\Big(\mathcal{K}_e(\partial_x\phi_e(x))^2 + \frac{1}{\mathcal{K}_e}(\partial_x\theta_e(x))^2\Big) =$$
$$\frac{v_F^e}{2\pi}\int dx\Big(\mathcal{K}_e(3\partial_x\phi'(x))^2 + \frac{1}{\mathcal{K}_e}(\partial_x\theta'(x))^2\Big) = \frac{v_F^e}{2\pi}\int \frac{9}{3}(\partial_x\phi'(x))^2 + 3(\partial_x\theta'(x))^2 =$$
$$\frac{3v_F^e}{2\pi}\int dx\Big((\partial_x\phi'(x))^2 + (\partial_x\theta'(x))^2\Big) \tag{3.47}$$

where v_F^e is the Fermi velocity of the interacting system. That's why we chose this definition of the above fields. In more general case, one can define them as:

$$\phi'(x) = \mathcal{K}\phi_e(x) \;\; and \;\; \theta'(x) = \theta_e(x) \tag{3.48}$$

as was defined in our case.

What we managed so far, is that we mapped our original interacting Hamiltonian to a non-interacting. Furthermore, it is very important to note here that in this description basically the edge states of our Quantum Hall (Fractional or Integer) are being described by the Luttinger Liquid Hamiltonian. The transformation of the fields $\phi_e(x), \theta_e(x)$ to $\phi'(x), \theta'(x)$ respectively, implies that the commutation relations for these fields are not canonical any longer, and, for example, it modifies the definition of the duality relations:

$$\partial_t\theta' = \mathcal{K}v_F^e\partial_x\phi', \quad \partial_x\theta' = \frac{\mathcal{K}}{v_F^e}\partial_t\phi' \tag{3.49}$$

Let's take a moment here to remind ourselves some of the important physical meanings that the Luttinger parameter has to a system. For values of:

- $\mathcal{K} < 1$, we have an interacting system with repulsive interactions,
- $\mathcal{K} = 1$, we have a non-interacting system and for
- $\mathcal{K} > 1$ we have an interacting system with attractive interactions.

Going back to calculate the bosonized description of our tunneling Hamiltonian, we get the result in a composite form as:

$$H_t(x) = \frac{-t2i}{\sqrt{4\pi}} \int dx \sum_{\sigma=\pm} \sum_{\eta=L/R=\pm1} \sum_{\eta'=L/R=\pm1}$$
$$\Bigg(\mathrm{k}_{FQH,\uparrow}\mathrm{k}_{Sc,+}\mathcal{C}_{+,\eta} \sin\Big(3\phi(x) - \eta'\theta(x) - \frac{\phi_c+\phi_s}{\sqrt{2}} - \eta\frac{\theta_c+\theta_s}{\sqrt{2}} - \eta'(k_{FQH,F} - \eta\eta' k_{SC,F} - \sigma\alpha)x\Big)$$
$$-\mathrm{k}_{FQH,\uparrow}\mathrm{k}_{Sc,-}\mathcal{C}_{-,\eta} \sin\Big(3\phi(x) - \eta'\theta(x) - \frac{\phi_c-\phi_s}{\sqrt{2}} - \eta\frac{\theta_c-\theta_s}{\sqrt{2}} - \eta'(k_{FQH,F} - \eta\eta' k_{SC,F} - \sigma\alpha)x\Big)\Bigg) \tag{3.50}$$

where again in the above notation η and η' takes the values ±1 for L/R modes respectively and the term $\mathcal{C}_{\sigma,\eta}$ is similar to the $\mathcal{C}_{\sigma,\eta,j}$ by changing now $j = 1, 2 = -\sigma$ which denotes the modes. For simplicity, above we replaced $\phi'(x) = \phi(x)$ and $\theta'(x) = \theta(x)$ and we will keep these notations from now on. An important observation here is that in eq. (3.2) the sign of the $\theta(x)$ field is locked with the sign of $k_{FQH,F}$. This means that in second order of RG later we do not expect to have Slow Oscillating terms that depends on $\theta(x)$. If we did, these terms would represent back scattering terms. The analytic calculations of the above result can be found in the Appendix (B.4).

3.3 The Renormalization Group Analysis

The renormalization group is a central conceptual framework for understanding the behavior of strongly coupled and critical systems. It was originally formulated in the context of perturbative quantum field theory (particularly in relation to quantum electrodynamics), and found its crisper and most powerful realization in the explanation of critical phenomena in statistical physics. The most important ideas derived from the renormalization group are the concepts of a fixed point and universality. These ideas, due primarily to Wilson and Kadanoff, in turn provided a definition of a quantum field theory outside the framework of perturbation theory.

In its simplest representation the renormalization group is a transformation that maps a system with a set of coupling constants and a scale (representing the short-distance or high-energy cutoff) to another equivalent system with a different set of (renormalized) coupling constants and a different scale. This is done by a procedure known as a block-spin transformation (in the language of classical statistical mechanics), by which some of the degrees of freedom, representing the short-distance physics, are integrated out and a subsequent scale transformation is performed to restore the original scale (or units).

Both in classical statistical mechanics and in a quantum field theory we can formally represent the

system in terms of a path integral:

$$\mathcal{Z} = \int \mathcal{D}\phi e^{-\mathcal{S}(\phi)} \tag{3.51}$$

where the field ϕ may obey Fermi or Bose statistics, in which case it will be represented by a set of Grassmann or scalar (or vector) fields, depending on the case.

In our case, the quadratic terms of our Hamiltonian have the form of Luttinger liquids and are represented by:

$$\mathcal{H}_0 = \mathcal{H}_{FQH} + \mathcal{H}_c + \mathcal{H}_s \tag{3.52}$$

where

- The FQH hamiltonian is:

$$\mathcal{H}_{FQH} = \frac{3v_F^e}{2\pi} \int dx \Big((\partial_x \phi(x))^2 + (\partial_x \theta(x))^2 \Big) \tag{3.53}$$

- The charge Hamiltonian is:

$$\mathcal{H}_c = \frac{v_{F,c}^e}{2\pi} \int dx \Big(\mathcal{K}_c (\partial_x \phi_c(x))^2 + \frac{1}{\mathcal{K}_c} (\partial_x \theta_c(x))^2 \Big) \tag{3.54}$$

- and the spin Hamiltonian is:

$$\mathcal{H}_s = \frac{v_{F,s}^e}{2\pi} \int dx \Big(\mathcal{K}_s (\partial_x \phi_s(x))^2 + \frac{1}{\mathcal{K}_s} (\partial_x \theta_s(x))^2 \Big) \tag{3.55}$$

where usually $v_{F,c}^e \neq v_{F,s}^e$ and $\mathcal{K}_c \neq \mathcal{K}_s$. In the case however of a free fermion system the Luttinger parameters $\mathcal{K}_c = \mathcal{K}_s = 1$ and hence the charge and spin velocities are equal in that case , $v_{F,c}^e = v_{F,s}^e$. We replace the term $\partial_x \theta_s(x)$ by using the duality relation, eq. (3.49), and express the quadratic Hamiltonians in terms of ϕ fields. Moreover, we resort to Euclidean space, i.e., we use coordinates $z = (x, t \equiv i\tau)$, and we denote $d^2 z = dx d\tau$ such that the following duality relations hold:

$$\partial_\tau \theta_q = i v_{F,q}^e \mathcal{K}_q \partial_x \phi_q, \quad \partial_x \theta_q = i \frac{\mathcal{K}_q}{v_{F,q}^e} \partial_t \phi_q \tag{3.56}$$

where $q = FQH, s, c$ denotes the fields for the FQH, the spin and the charge components.

3.3.1 2-step RG

Many of the techniques that we are going to use form now on were based on lecture notes [17]. The way we will proceed with the RG analysis in our model, is by working on a 2-step RG procedure which is a simple way of improving the RG predictions. In the adoption of a two-step RG approach,

the flow is divided into separate parts, where each part is terminated when a coupling constant reaches a suitable upper threshold, which indicates when a given interaction semiclassically pins the related fields. After each separate flow, an effective Hamiltonian for the remaining unpinned sectors is considered. In particular, this means that we will divide the flow in two different steps. In the first one, we will consider the unperturbed action of our system as the one that includes only the quadratic terms (Luttinger liquids). This means that we have:

$$\mathcal{S}_0 = \mathcal{S}_{Luttinger} = \frac{1}{2\pi}\int d^2z\Big[\sum_{q=FQH,s,c}\frac{\mathcal{K}_q}{v^e_{F,q}}(\partial_\tau\phi_q(z))^2 + v^e_{F,q}\mathcal{K}_q(\partial_x\phi_q(z))^2\Big] \tag{3.57}$$

Then, we let the parameters or coupling constants flow until a parameter reaches the threshold (cutoff) or all of the parameters flow below some minimum for which a gapless phase is expected. By doing so, we will find that at first-order perturbation that the Δ term will be most relevant and so will pin the fields ϕ_c and θ_s to zero and our system is now gapped (or massive), or equivalent that the Δ term is strong and relevant, thus we open the Δ gap. The second step is to find the relevant terms in 2nd-order perturbation and from there we let our parameters flow again until the threshold where we will find a different parameter. By solving next the RG flow equations we will be in position to determine the induced gap. The role of the perturbative action will play the tunneling action and the Δ term, and it is equal to:

$$\begin{aligned}
&\mathcal{S}_I = \mathcal{S}_\Delta + \mathcal{S}_t = \\
&i\mathrm{k}_+\mathrm{k}_-\frac{\Delta}{\pi}\Big(\mathcal{C}_{+,L,-1}\mathcal{C}_{-,L,-1}+\mathcal{C}_{+,R,+1}\mathcal{C}_{-,R,+1}\Big)\int d^2z\Bigg[\Big[\sin\big(\sqrt{2}(\phi_c(z)+\theta_s(z))\big)+ \\
&\sin\big(\sqrt{2}(\phi_c(z)-\theta_s(z))\big)\Big]\Bigg] + \frac{2it}{\sqrt{2\pi}}\int dx\sum_{\eta=L/R=\pm1}\sum_{\eta'=L/R=\pm1} \\
&\Bigg(\mathrm{k}_{FQH,\uparrow}\mathrm{k}_{Sc,+}\mathcal{C}_{+,\eta}\sin\Big(3\phi(x)-\eta'\theta(x)-\frac{\phi_c+\phi_s}{\sqrt{2}}-\eta\frac{\theta_c+\theta_s}{\sqrt{2}}-\eta'(k_{FQH,F}-\eta\eta' k_{SC,F}-\sigma\alpha)x\Big) \\
&-\mathrm{k}_{FQH,\uparrow}\mathrm{k}_{Sc,-}\mathcal{C}_{-,\eta}\sin\Big(3\phi(x)-\eta'\theta(x)-\frac{\phi_c-\phi_s}{\sqrt{2}}-\eta\frac{\theta_c-\theta_s}{\sqrt{2}}-\eta'(k_{FQH,F}-\eta\eta' k_{SC,F}-\sigma\alpha)x\Big)\Bigg)
\end{aligned} \tag{3.58}$$

One could also define the perturbative action to be only the tunneling term, but in this case the definition of the correlation functions change (since we include a massive term) of eq. (3.64), (3.65) and it makes it more complicated to to define the function $\mathcal{C}(r)$, but not impossible.

The idea behind the Wilsonian renormalization group is the following. For each of the bosonic fields, we distinguish fast and slow modes, separated by an effective cutoff in momentum space, which we define as $\tilde{\Lambda} = \Lambda e^{-l}$ (or $\tilde{\Lambda} = \Lambda/b$ with $b > 1$). Furthermore, we introduce an ultraviolet momentum

cutoff $\Lambda > \tilde{\Lambda}$ (the new short distance cutoff is $\alpha' = b\alpha$). Thus, we need to rescale the lengths and the time in order to restore the units ($x' = x/b$ or $k' = kb$). The fast oscillating modes are characterized by $\tilde{\Lambda} < k < \Lambda$ and we are interested in the limit $\tilde{\Lambda}/\Lambda = 1 - dl$ (or equivalent $\Lambda/\tilde{\Lambda} = 1 + dl$), with dl infinitesimal. The bosonic fields can thus decomposed to the following:

$$\phi_q(z) = \phi_{\mathbf{s},q}(z) + \phi_{\mathbf{f},q}(z) \tag{3.59}$$

$$\theta_q(z) = \theta_{\mathbf{s},q}(z) + \theta_{\mathbf{f},q}(z) \tag{3.60}$$

where again $q = FQH, s, c$ and $\mathbf{s}, \mathbf{f}$ denotes the slow and fast modes respectively. These transformations must obey some basic principles. The most important one is that this procedure should be compatible with the underlying symmetries of the physical system. We will assume that the rescaling is isotropic both in space and in space-time. Thus, we are assuming that there will be an effective Lorentz invariance in the system of interest.

The full action of our system is written as:

$$\mathcal{S} = \mathcal{S}_0 + \mathcal{S}_t \tag{3.61}$$

To understand the renormalization flow, we must derive and effective action for the slow modes only, by averaging over the fast modes. Thus, by integrating out the fast degrees of freedom we obtain:

$$\mathcal{S}_{eff}(\tilde{\Lambda}) = \mathcal{S}_0(\phi_{\mathbf{s}}) - \ln\langle e^{-\mathcal{S}_t(\phi_{\mathbf{s}}+\phi_{\mathbf{f}})}\rangle_{\mathbf{f}} \approx$$
$$\mathcal{S}_0(\phi_{\mathbf{s}}) + \underbrace{\left\langle \mathcal{S}_t(\phi_{\mathbf{s}}+\phi_{\mathbf{f}})\right\rangle_{\mathbf{f}}}_{\mathcal{A}} - \frac{1}{2}\left(\underbrace{\left\langle \mathcal{S}_t^2(\phi_{\mathbf{s}}+\phi_{\mathbf{f}})\right\rangle_{\mathbf{f}}}_{\mathcal{B}} - \underbrace{\left\langle \mathcal{S}_t(\phi_{\mathbf{s}}+\phi_{\mathbf{f}})\right\rangle_{\mathbf{f}}^2}_{\mathcal{A}^2} \right) + \dots \tag{3.62}$$

where the expectation values are taken on the (fast) Gaussian action only, and we identified the effective action at the second order of perturbation theory. In the following we make extensive use of the following well-known key property of Gaussian integrals:

$$\left\langle e^{i\sum_k \alpha_k \phi_k} \right\rangle = e^{-\frac{1}{2}\sum_{k,k'} \alpha_k \alpha_{k'} \langle \phi_k \phi_{k'} \rangle} \tag{3.63}$$

with ϕ the fields over which the integration is carried out and α_k here are the coefficients in front of the ϕ fields. Consider the following relations:

$$\left\langle \phi_{\mathbf{f},q}(z_1)\phi_{\mathbf{f},q}(z_2)\right\rangle_{\mathbf{f}} = \int_{\tilde{\Lambda}}^{\Lambda} \frac{dk}{2} \frac{J_0(kr)}{\mathcal{K}_q k} = \frac{C_q(r)}{2\mathcal{K}_q} \ln \frac{\Lambda}{\tilde{\Lambda}} \tag{3.64}$$

$$\left\langle \theta_{\mathbf{f},q}(z_1)\theta_{\mathbf{f},q}(z_2)\right\rangle_{\mathbf{f}} = \frac{C_q(r)\mathcal{K}_q}{2}\ln\frac{\Lambda}{\tilde{\Lambda}} \tag{3.65}$$

where $q = e, c, s$ and the logarithm captures the scaling behaviour, and $C(r)$ is a short-range function of $r = \sqrt{v_{F,q}^2(\tau_1-\tau_2)^2 + (x_1-x_2)^2}$ such that $C(0) = 1$. In the following we will consider $C_q(r)$ to be suitably short-ranged; in the case of a sharp cutoff, $C_q(r) = J_0(\Lambda r)$ and the Bessel function J_0 does not satisfactorily fulfill this assumption, but $C_q(r)$ can be made sufficiently short-ranged with more refined cutoffs.

Before we proceed any further, we will introduce first the vertex operators that is a shorthand notation for the corresponding sine-Gordon terms that appear in our Interacting action. In particular, we denote as:

$$\mathcal{O}^{\nu}_{\Delta,\pm} = e^{i\nu\sqrt{2}(\phi_c(z)\pm\theta_s(z))} \tag{3.66}$$

the operator that describes the Δ sine-Gordon terms with $\nu = \pm$ to get the operator and its Hermitian Conjugate. For the tunneling term, we set:

$$\mathcal{O}^{\nu}_{t,\sigma,\eta,\eta',\pm} = e^{i\nu\left((3\phi-\eta'\theta-\frac{\phi_c\pm\phi_s}{\sqrt{2}}-\eta\frac{\theta_c\pm\theta_s}{\sqrt{2}}-\eta'(k_{FQH,F}-\eta\eta' k_{SC,F}-\sigma\alpha)x\right)} \tag{3.67}$$

Let's proceed by evaluating in first order the Δ term. We have now for the first $\sin$ term that:

$$\begin{gathered}
\left\langle 2i\sin\sqrt{2}(\phi_c(z)+\theta_s(z))\right\rangle = \left\langle \mathcal{O}^{+}_{\Delta,+} - \mathcal{O}^{-}_{\Delta,+}\right\rangle \\
\left\langle e^{i\sqrt{2}(\phi_c(z)+\theta_s(z))} - e^{-i\sqrt{2}(\phi_c(z)+\theta_s(z))}\right\rangle = \\
\left\langle e^{i\sqrt{2}(\phi_{\mathbf{s},c}(z)+\phi_{\mathbf{f},c}(z)+\theta_{\mathbf{s},s}(z))+\theta_{\mathbf{f},s}(z))} - e^{-i\sqrt{2}(\phi_{\mathbf{s},c}(z)+\phi_{\mathbf{f},c}(z)+\theta_{\mathbf{s},s}(z))+\theta_{\mathbf{f},s}(z))}\right\rangle = \\
e^{i\sqrt{2}(\phi_{\mathbf{s},c}(z)+\theta_{\mathbf{s},s}(z))}\left\langle e^{\sqrt{2}(\phi_{\mathbf{f},c}(z)+\theta_{\mathbf{f},s}(z))}\right\rangle_{\mathbf{f}} - e^{-i\sqrt{2}(\phi_{\mathbf{s},c}(z)+\theta_{\mathbf{s},s}(z))}\left\langle e^{\sqrt{2}(\phi_{\mathbf{f},c}(z)+\theta_{\mathbf{f},s}(z))}\right\rangle_{\mathbf{f}} = \\
e^{i\sqrt{2}(\phi_{\mathbf{s},c}(z)+\theta_{\mathbf{s},s}(z))}e^{-2(\langle\phi^2_{\mathbf{f},c}(z)\rangle_{\mathbf{f}}+\langle\theta^2_{\mathbf{f},s}(z)\rangle_{\mathbf{f}})} - e^{-i\sqrt{2}(\phi_{\mathbf{s},c}(z)+\theta_{\mathbf{s},s}(z))}e^{-2(\frac{1}{2}\langle\phi^2_{\mathbf{f},c}(z)\rangle_{\mathbf{f}}+\frac{1}{2}\langle\theta^2_{\mathbf{f},s}(z)\rangle_{\mathbf{f}})} = \\
2i\sin\left(\sqrt{2}(\phi_{\mathbf{s},c}(z)+\theta_{\mathbf{s},s}(z))\right)e^{-2\frac{1}{2}(\frac{1}{2\mathcal{K}_c}+\frac{\mathcal{K}_s}{2})\ln\frac{\Lambda}{\tilde{\Lambda}}} = 2i\sin\left(\sqrt{2}(\phi_{\mathbf{s},c}(z)+\theta_{\mathbf{s},s}(z))\right)\left(1-(\frac{1}{2\mathcal{K}_c}+\frac{\mathcal{K}_s}{2})dl\right)
\end{gathered} \tag{3.68}$$

and similar for the terms $\mathcal{O}^{\nu}_{\Delta,-}$. From here it is easy to see that the scaling dimensions of the above operators are $\mathcal{D}_\Delta = \frac{1}{2\mathcal{K}_c}+\frac{\mathcal{K}_s}{2}$. We consider now the Non-Interacting (N-I) case by choosing the values $\mathcal{K}_c = \mathcal{K}_s = 1$ for the Luttinger parameters of the charge and spin sector. This results to the scaling dimension of the Δ term to be equal to $\mathcal{D}_\Delta = 1$, thus it is relevant. What this means for our 2-step RG procedure is that for the $\mathcal{I}$-step we consider our pairing potential Δ to scale as $\Delta' \sim \Delta(l=0)e^l$, where $\Delta(l=0) = const.$ is the value that we choose for the pairing potential similar to our previous methods. Since Δ' grows exponential ($\mathcal{D}_\Delta = 1$), means that at $\mathcal{I}$-step it opens gap.

Let us now calculate the first part of the tunneling first-order term $\mathcal{A}_{t,1}$:

$$\mathcal{A}_{t,1} = t\frac{\mathrm{k}_{FQH,\uparrow}\mathrm{k}_{Sc,+}}{\sqrt{2\pi}}\mathcal{C}_{+,\eta}$$
$$\sum_{\eta=L/R=\pm1}\sum_{\eta'=L/R=\pm1}\sum_{\sigma=\pm1}\Big\langle e^{i\Big((3\phi-\eta'\theta-\frac{\phi_s+\phi_c}{\sqrt{2}}-\eta\frac{\theta_s+\theta_c}{\sqrt{2}}-\eta'(k_{FQH,F}-\eta\eta' k_{SC,F}-\sigma\alpha)x\Big)}$$
$$-e^{-i\Big((3\phi-\eta'\theta-\frac{\phi_s+\phi_c}{\sqrt{2}}-\eta\frac{\theta_s+\theta_c}{\sqrt{2}}-\eta'(k_{FQH,F}-\eta\eta' k_{SC,F}-\sigma\alpha)x\Big)}\Big\rangle_{\mathbf{f}} \sim$$
$$e^{i\Big((3\phi_{\mathbf{s}}-\eta'\theta_{\mathbf{s}}-\frac{\phi_{\mathbf{s},s}+\phi_{\mathbf{s},c}}{\sqrt{2}}-\eta\frac{\theta_{\mathbf{s},s}+\theta_{\mathbf{s},c}}{\sqrt{2}}-\eta'(k_{FQH,F}-\eta\eta' k_{SC,F}-\sigma\alpha)x\Big)}\Big\langle e^{i\Big((3\phi_{\mathbf{f}}-\eta'\theta_{\mathbf{f}}-\frac{\phi_{\mathbf{f},s}+\phi_{\mathbf{f},c}}{\sqrt{2}}-\eta\frac{\theta_{\mathbf{f},s}+\theta_{\mathbf{f},c}}{\sqrt{2}}\Big)}\Big\rangle_{\mathbf{f}}$$
$$-e^{-i\Big((3\phi_{\mathbf{s}}-\eta'\theta_{\mathbf{s}}-\frac{\phi_{\mathbf{s},s}+\phi_{\mathbf{s},c}}{\sqrt{2}}-\eta\frac{\theta_{\mathbf{s},s}+\theta_{\mathbf{s},c}}{\sqrt{2}}-\eta'(k_{FQH,F}-\eta\eta' k_{SC,F}-\sigma\alpha)x\Big)}\Big\langle e^{-i\Big((\frac{9}{2}\phi_{\mathbf{f}}-\eta'\theta_{\mathbf{f}}-\frac{\phi_{\mathbf{f},s}+\phi_{\mathbf{f},c}}{\sqrt{2}}-\eta\frac{\theta_{\mathbf{f},s}+\theta_{\mathbf{f},c}}{\sqrt{2}}\Big)}\Big\rangle_{\mathbf{f}} =$$
$$e^{i\Big((3\phi_{\mathbf{s}}-\eta'\theta_{\mathbf{s}}-\frac{\phi_{\mathbf{s},s}+\phi_{\mathbf{s},c}}{\sqrt{2}}-\eta\frac{\theta_{\mathbf{s},s}+\theta_{\mathbf{s},c}}{\sqrt{2}}-\eta'(k_{FQH,F}-\eta\eta' k_{SC,F}-\sigma\alpha)x\Big)}e^{-\Big((\frac{9}{2}\langle\phi_{\mathbf{f}}^2\rangle_{\mathbf{f}}+\frac{1}{2}\langle\theta_{\mathbf{f}}^2\rangle_{\mathbf{f}}+\frac{\langle\phi_{\mathbf{f},s}^2\rangle_{\mathbf{f}}+\langle\phi_{\mathbf{f},c}^2\rangle_{\mathbf{f}}}{4}+\frac{\langle\theta_{\mathbf{f},s}^2\rangle_{\mathbf{f}}+\langle\theta_{\mathbf{f},c}^2\rangle_{\mathbf{f}}}{4}\Big)}$$
$$-e^{-i\Big((3\phi_{\mathbf{s}}-\eta'\theta_{\mathbf{s}}-\frac{\phi_{\mathbf{s},s}+\phi_{\mathbf{s},c}}{\sqrt{2}}-\eta\frac{\theta_{\mathbf{s},s}+\theta_{\mathbf{s},c}}{\sqrt{2}}-\eta'(k_{FQH,F}-\eta\eta' k_{SC,F}-\sigma\alpha)x\Big)}e^{-\Big((\frac{9}{2}\langle\phi_{\mathbf{f}}^2\rangle_{\mathbf{f}}+\frac{1}{2}\langle\theta_{\mathbf{f}}^2\rangle_{\mathbf{f}}+\frac{\langle\phi_{\mathbf{f},s}^2\rangle_{\mathbf{f}}+\langle\phi_{\mathbf{f},c}^2\rangle_{\mathbf{f}}}{4}+\frac{\langle\theta_{\mathbf{f},s}^2\rangle_{\mathbf{f}}+\langle\theta_{\mathbf{f},c}^2\rangle_{\mathbf{f}}}{4}\Big)} =$$
$$e^{i\Big((3\phi_{\mathbf{s}}-\eta'\theta_{\mathbf{s}}-\frac{\phi_{\mathbf{s},s}+\phi_{\mathbf{s},c}}{\sqrt{2}}-\eta\frac{\theta_{\mathbf{s},s}+\theta_{\mathbf{s},c}}{\sqrt{2}}-\eta'(k_{FQH,F}-\eta\eta' k_{SC,F}-\sigma\alpha)x\Big)}e^{-\Big((\frac{9}{12}+\frac{1}{12}+\frac{\frac{1}{2\mathcal{K}_s}+\frac{1}{2\mathcal{K}_c}}{4}+\frac{\frac{\mathcal{K}_s}{2}+\frac{\mathcal{K}_c}{2}}{4}\Big)\ln\frac{\Lambda}{\tilde{\Lambda}}}$$
$$-e^{-i\Big((3\phi_{\mathbf{s}}-\eta'\theta_{\mathbf{s}}-\frac{\phi_{\mathbf{s},s}+\phi_{\mathbf{s},c}}{\sqrt{2}}-\eta\frac{\theta_{\mathbf{s},s}+\theta_{\mathbf{s},c}}{\sqrt{2}}-\eta'(k_{FQH,F}-\eta\eta' k_{SC,F}-\sigma\alpha)x\Big)}e^{-\Big((\frac{9}{12}+\frac{1}{12}+\frac{\frac{1}{2\mathcal{K}_s}+\frac{1}{2\mathcal{K}_c}}{4}+\frac{\frac{\mathcal{K}_s}{2}+\frac{\mathcal{K}_c}{2}}{4}\Big)\ln\frac{\Lambda}{\tilde{\Lambda}}} =$$
$$-2i\sin\Big(3\phi_{\mathbf{s}}-\eta'\theta_{\mathbf{s}}-\frac{\phi_{\mathbf{s},s}+\phi_{\mathbf{s},c}}{\sqrt{2}}-\eta\frac{\theta_{\mathbf{s},s}+\theta_{\mathbf{s},c}}{\sqrt{2}}-\eta'(k_{FQH,F}-\eta\eta' k_{SC,F}-\sigma\alpha)x\Big)$$
$$(\frac{\tilde{\Lambda}}{\Lambda})^{\frac{9}{12}+\frac{1}{12}+\frac{1}{8\mathcal{K}_s}+\frac{1}{8\mathcal{K}_c}+\frac{\mathcal{K}_s}{8}+\frac{\mathcal{K}_c}{8}} =$$
$$-2i\sin\Big(3\phi_{\mathbf{s}}-\eta'\theta_{\mathbf{s}}-\frac{\phi_{\mathbf{s},s}+\phi_{\mathbf{s},c}}{\sqrt{2}}-\eta\frac{\theta_{\mathbf{s},s}+\theta_{\mathbf{s},c}}{\sqrt{2}}-\eta'(k_{FQH,F}-\eta\eta' k_{SC,F}-\sigma\alpha)x\Big)$$
$$\Big(1-\Big(\frac{9}{12}+\frac{1}{12}+\frac{1}{8\mathcal{K}_s}+\frac{1}{8\mathcal{K}_c}+\frac{\mathcal{K}_s}{8}+\frac{\mathcal{K}_c}{8}\Big)dl\Big) \tag{3.69}$$

where in the above calculations, we used the fact that the correlation functions for the FQH are given by:

$$\langle\phi_e(x)\phi_e(y)\rangle \approx -\frac{1}{\mathcal{K}_e}\ln(x-y) \iff 9\langle\phi(x)\phi(y)\rangle = -\frac{1}{2\mathcal{K}_e}\ln(x-y)$$
$$\langle\phi(x)\phi(y)\rangle = -\frac{1}{6}\ln(x-y) \tag{3.70}$$

$$\langle\theta(x)\theta(y)\rangle = -\frac{1}{6}\ln(x-y) \tag{3.71}$$

with $\mathcal{K}_e = \frac{1}{3}$. Similar, we get the results for the other $\sin$ term. We thus obtain the first-order

contribution:

$$\mathcal{A} = -t2i \sum_{\eta=L/R=\pm1} \sum_{\eta'=L/R=\pm1} \sum_{\sigma=\pm1}$$
$$\left(\frac{\mathrm{k}_{FQH,\uparrow}\mathrm{k}_{Sc,+}}{\sqrt{2\pi}} \sin\frac{\vartheta(-\eta k_{SC,F}+j\alpha)}{2} \int d^2z' \left(1+\left(2-\left(\frac{9}{12}+\frac{1}{12}+\frac{1}{8\mathcal{K}_s}+\frac{1}{8\mathcal{K}_c}+\frac{\mathcal{K}_s}{8}+\frac{\mathcal{K}_c}{8}\right)\right)dl\right)\right.$$
$$\left. \sin\left(3\phi_{\mathbf{s}} - \eta'\theta_{\mathbf{s}} - \frac{\phi_{\mathbf{s},s}+\phi_{\mathbf{s},c}}{\sqrt{2}} - \eta\frac{\theta_{\mathbf{s},s}+\theta_{\mathbf{s},c}}{\sqrt{2}} - \eta'(k_{FQH,F}-\eta\eta' k_{SC,F}-\sigma\alpha)x\right)\right. -$$
$$\frac{\mathrm{k}_{FQH,\uparrow}\mathrm{k}_{Sc,-}}{\sqrt{2\pi}} \cos\frac{\vartheta(-\eta k_{SC,F}+j\alpha)}{2} \int d^2z' \left(1+\left(2-\left(\frac{9}{12}+\frac{1}{12}+\frac{1}{8\mathcal{K}_s}+\frac{1}{8\mathcal{K}_c}+\frac{\mathcal{K}_s}{8}+\frac{\mathcal{K}_c}{8}\right)\right)dl\right)$$
$$\sin\left(3\phi_{\mathbf{s}} - \eta'\theta_{\mathbf{s}} - \frac{\phi_{\mathbf{s},c}-\phi_{\mathbf{s},s}}{\sqrt{2}} - \eta\frac{\theta_{\mathbf{s},c}+\theta_{\mathbf{s},s}}{\sqrt{2}} - \eta'(k_{FQH,F}-\eta\eta' k_{SC,F}-\sigma\alpha)x\right) \tag{3.72}$$

where $\mathcal{D}_t = \frac{9}{12}+\frac{1}{12}+\frac{1}{8\mathcal{K}_s}+\frac{1}{8\mathcal{K}_c}+\frac{\mathcal{K}_s}{8}+\frac{\mathcal{K}_c}{8}$ is the scaling dimension of the tunneling part and we included also the rescaling term $d^2z = (1+2dl)d^2z'$. Note also, that in the above calculations appears also a term $\left\langle \phi_{\mathbf{f},q}(z)\theta_{\mathbf{f},q}(z')\right\rangle_{\mathbf{f}} = i\frac{\pi}{2}\Theta(x-x')$ (if q=FQH appears an extra term of $\frac{1}{3}$). This correlation does not carry much information though, but the usual commutation relation between θ and ϕ. One can for practical purposes ignore it after considering the right phase given by the CBH formula. For that reason we choose to ignore it from our expressions and not carrying it around but if someone wants to be as rigorous as possible he should include it. Finally, we are using that in $1+1D$ the rescalling of the slow components of the fields is remaining the same, i.e that $\phi'_{\mathbf{s},q} = \phi_{\mathbf{s},q}$ and $\theta'_{\mathbf{s},q} = \theta_{\mathbf{s},q}$.

From now on, when we want to calculate the scaling dimensions of an operator $\mathcal{O}$ we will use the relation

$$\langle \mathcal{O}(x)\mathcal{O}(y)\rangle \sim \frac{1}{|x-y|^{2\mathcal{D}_\mathcal{O}}} \tag{3.73}$$

and we will drop the notation of $\mathbf{s}$ and $\mathbf{f}$ for the slow and fast oscillating fields respectively, for the sake of saving space but it will always be implied that we average on fast oscillating fields and what remains are the slow oscillating. As we can easily see, the first-order contribution $\mathcal{A}$ of the interacting action provides the standard dependence from the scaling dimensions of the RG equations and is also a F.O. term due the dependence of the Fermi momentum. At this point we should make a very important observation. Our Superconductor here is 3-D. By integrating out the 2 dimensions it is like giving the $k_{SC,F}$ a distribution for its values. Now if at some point the value of $k_{SC,F}$ is such that $\eta'(k_{FQH,F}-\eta\eta' k_{SC,F}-\sigma\alpha) = 0$, then at first-order of RG, the terms in eq. (3.72) become relevant, cause we do not have any F.O. term when we are tuning to this special case. This will result in having in our system different quasiparticles and therefore different phases of matter. This might be very interesting to work with and one can find amazing results. But for the purposes of our project we consider that we are not in this special case (in this resonance) and we take the integral over the

average positions x this term is "dying" fast and thus is considered F.O. term.

To get more information of the system, we must focus in the second-order contributions and, in particular, on the non-trivial terms appearing in $\mathcal{B}$ term. In particular, we have:

$$\mathcal{B} = \left\langle \mathcal{S}_t^2(\phi_{\mathbf{s}} + \phi_{\mathbf{f}}) \right\rangle_{\mathbf{f}} = \left\langle \big(\mathcal{S}_t(\phi_{\mathbf{s}}(z_1) + \phi_{\mathbf{f}}(z_1)\big)\big(\mathcal{S}_t(\phi_{\mathbf{s}}(z_2) + \phi_{\mathbf{f}}(z_2)\big) \right\rangle_{\mathbf{f}} \tag{3.74}$$

To calculate all these terms is a very painful procedure for that reason we need to make some observations that will make our lives easier. Again here is it very easy to see that we are going to have many F.O terms which are going to be irrelevant in the RG sense. For that reason, we focus only on terms that are relevant. To distinguish these terms from our expression of the perturbative Hamiltonian, one must find the combinations between the terms

$$\left\langle \big(\mathcal{S}_t(\phi_{\mathbf{s}}(z_1) + \phi_{\mathbf{f}}(z_1)\big)\big(\mathcal{S}_t(\phi_{\mathbf{s}}(z_2) + \phi_{\mathbf{f}}(z_2)\big) \right\rangle_{\mathbf{f}}$$

that "kills" the F.O terms, i.e the terms that depend on the position x. We can combine these terms by writing them in a composite form like:

$$\left\langle \mathcal{O}^{\nu}_{t,\eta,\eta',\sigma,\pm} \mathcal{O}^{\nu'}_{t,\eta,\eta',\sigma,\pm} \right\rangle_{\mathbf{f}} \tag{3.75}$$

where here we are taking the combinations where $\eta \neq \eta'$, $j \neq j'$ and $\nu = \nu'$. In this way we emphasize the fact that the S.O (Slow Oscillating) terms will appear by coupling Left- and Right-movers with different energy modes.

The interesting part about the S.O. terms of eq. (3.75) is that we get 2 kinds of S.O. In particular, we get terms of form:

$$\left\langle \mathcal{O}^{\nu}_{t,\eta,\eta',j,\pm} \mathcal{O}^{\nu'}_{t,\eta,\eta',j',\pm} \right\rangle_{\mathbf{f}} \sim \begin{cases} e^{i\nu(6\phi - \sqrt{2}(\phi_c + \mu\theta_s))} \\ e^{i\nu(6\phi - \sqrt{2}(\phi_c + \mu\phi_s)))} \end{cases} \tag{3.76}$$

We will not proceed by calculating explicitly these 2nd-order terms but we will benefit from this quick analysis in the $\mathcal{II}$-step RG.

Let us recall again our analysis so far. In the $\mathcal{I}$-step of RG, we started from the Interacting action of eq. (3.58) where in 1st-order of perturbation we found that the Δ term opens a gap. This means that we can minimize the fields ϕ_c and θ_s simultaneously since the commute with each other. We choose then to pin their value to their minimum, thus we choose:

$$\phi_c = const. \qquad \theta_s = const. \tag{3.77}$$

This also implies that the fields ϕ_s and θ_c are flat and can take any value. This is an important

observation and will be very useful in the $\mathcal{II}$-step of RG. It will be useful at this point to calculate these minima. We have that:

$$\sin\left(\sqrt{2}(\phi_c+\theta_s)\right)+\sin\left(\sqrt{2}(\phi_c-\theta_s)\right)=$$
$$\sin\left(\sqrt{2}\phi_c\right)\cos\left(\sqrt{2}\theta_s\right)+\cos\left(\sqrt{2}\phi_c\right)\sin\left(\sqrt{2}\theta_s\right)+\sin\left(\sqrt{2}\phi_c\right)\cos\left(\sqrt{2}\theta_s\right)-\cos\left(\sqrt{2}\phi_c\right)\sin\left(\sqrt{2}\theta_s\right)=$$
$$2\sin\left(\sqrt{2}\phi_c\right)\cos\left(\sqrt{2}\theta_s\right) \tag{3.78}$$

From here it is easy to see that we have different combinations for the minima. Namely, we have:

1. For $\sin\left(\sqrt{2}\phi_c\right)=-1$ and $\cos\left(\sqrt{2}\theta_s\right)=1$, we get:

$$\phi_c=\frac{4\pi\eta-\pi}{2\sqrt{2}}\quad or\quad \phi_c=\frac{4\pi\eta+3\pi}{2\sqrt{2}},\quad and\quad \theta_s=\sqrt{2}\pi\eta,\qquad \eta\in\mathbb{Z} \tag{3.79}$$

2. For $\sin\left(\sqrt{2}\phi_c\right)=1$ and $\cos\left(\sqrt{2}\theta_s\right)=-1$, we get:

$$\theta_s=\frac{2\pi\eta-\pi}{2\sqrt{2}}\quad or\quad \theta_s=\frac{2\pi\eta+\pi}{2\sqrt{2}},\quad and\quad \phi_c=\frac{4\pi\eta+\pi}{2\sqrt{2}},\qquad \eta\in\mathbb{Z} \tag{3.80}$$

These minima will be useful in later calculations.

Proceeding now to the $\mathcal{II}$-step of RG we will consider now an effective Interacting action of the remaining fields but we will include also an extra term. So, our Effective Interaction has the form:

$$\mathcal{S}^{\mathcal{II}}_{I,eff}=\mathcal{S}_t+\mathcal{S}_h \tag{3.81}$$

This extra term will include all the relevant terms that we would expect to find in the second order of perturbation if we were following the standard methods in RG and it has the form (check Appendix (B.5) for more details):

$$\mathcal{S}_h=\mathrm{k}_{Sc,+}\mathrm{k}_{Sc,-}\int d^2z\sum_{\mu=\pm1}\left(h_\mu\cos\left(6\phi-\sqrt{2}(\phi_c+\mu\theta_s)\right)\right)+h'_\mu\cos\left(6\phi-\sqrt{2}(\phi_c+\mu\phi_s)\right)\Big) \tag{3.82}$$

where h_μ and h'_μ is used to distinguish the two different kind of S.O terms that appear. If we take again the 1st-order of perturbation for this term, we will see that we have:

$$\left\langle h'_\mu\cos\left(6\phi-\sqrt{2}(\phi_c+\mu\phi_s)\right)\right\rangle_{\mathbf{f}}=0 \tag{3.83}$$

and the reason is that we are averaging over all the fields ϕ_s which as we said earlier are flat and

therefore they have zero average contribution. This will leave us only with the terms:

$$\mathcal{S}_h = \int d^2z \sum_{\mu=\pm 1} \mathrm{k}_{Sc,+}\mathrm{k}_{Sc,-} h_\mu \cos\Big(6\phi - \sqrt{2}(\phi_c + \mu\theta_s)\Big)\Big) \tag{3.84}$$

From now on we drop the μ subscript from h_μ for simplicity. Now, at first-order of perturbation we just get the rescaling of it and we found it equal with:

$$\mathcal{S}_h = h\bigg(1 + \Big(2 - \frac{6\cdot 6}{6\cdot 2} - \frac{1}{2\mathcal{K}_c} - \frac{\mathcal{K}_s}{2}\Big)dl\bigg) \int d^2z' \sum_{\mu=\pm 1} \mathrm{k}_{Sc,+}\mathrm{k}_{Sc,-} \cos\Big(6\phi - \sqrt{2}(\phi_c + \mu\theta_s)\Big)\Big) \tag{3.85}$$

where the scaling dimension of the term $\mathcal{S}_h$ is $\mathcal{D}_h = 3 + \frac{1}{2\mathcal{K}_c} + \frac{\mathcal{K}_s}{2}$. At this point we need to distinguish two cases for the scaling dimension $\mathcal{D}_h$ which corresponds to the 1st and the 2nd step of RG. In particular we will get:

$$\mathcal{D}_h = \begin{cases} 3 + \frac{1}{2\mathcal{K}_c} + \frac{\mathcal{K}_s}{2} = 3 + \frac{1}{2} + \frac{1}{2} = 4, & for \;\; \mathcal{I} - step \;\; of \;\; RG \\ 3 + \frac{1}{2\mathcal{K}_c} + \frac{\mathcal{K}_s}{2} = 3 + 0 + 0 = 3, & for \;\; \mathcal{II} - step \;\; of \;\; RG \end{cases} \tag{3.86}$$

From here it easy to see that we get the first-order RG flow equations for the parameter h_μ to be equal with:

$$\frac{dh_\mu}{dl} = \Big(2 - 3 - \frac{1}{2\mathcal{K}_c} - \frac{\mathcal{K}_s}{2}\Big)h_\mu = \begin{cases} -2h_\mu, & for \;\; \mathcal{I} - step \;\; of \;\; RG \\ -h_\mu, & for \;\; \mathcal{II} - step \;\; of \;\; RG \end{cases} \tag{3.87}$$

These corresponds to the equations:

$$h_\mu(l) = \begin{cases} h_{\mu,0}e^{-2l}, & for \;\; \mathcal{I} - step \;\; of \;\; RG \\ h_{\mu,0}e^{-l}, & for \;\; \mathcal{II} - step \;\; of \;\; RG \end{cases} \tag{3.88}$$

here $h_\mu(l = 0) = h_{\mu,0}$ corresponds to the bare value of l and we take it to be equal with the result of the $\mathcal{II}$-order in perturbation theory that we calculated in Section (2.3). The above results tells us that in 1st order of perturbation at $\mathcal{I}$-step of RG the h term is strongly irrelevant. Furthermore, at $\mathcal{II}$-step of RG (still in 1st order of perturbation) it remains irrelevant and we do not open a gap, as shown in Fig. (3.4). Thus, in order to get any extra information and how to open a gap, we need to investigate further orders. For that purpose, to get a more realistic scenario we will investigate the 2nd order in perturbation in $\mathcal{II}$-step of RG where the fields ϕ_c and θ_s are pinned. This means that we

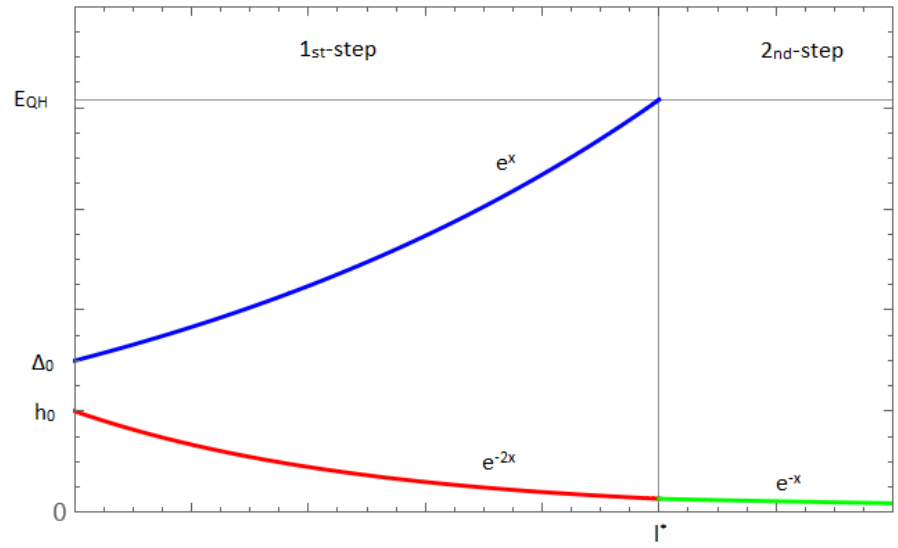

Figure 3.4: Here we see the schematic representation of steps $\mathcal{I}$ and $\mathcal{I}$ of RG in the 1st order. We see that the Δ term is relevant at $\mathcal{I}$-step (blue line) and it grows until it reaches the threshold at l^* where it pins the ϕ_c and θ_s fields. The red line represents the h term at $\mathcal{I}$-step where we can see that it is irrelevant. When the h term reaches the end of the $\mathcal{I}$-step at l^* we see that the scaling dimensions changes at $\mathcal{I}\mathcal{I}$-step and it scales as $h(l^*)e^{-l}$, where $h(l^*) = h_0 e^{-2l^*}$, where we can see that it is still irrelevant.

can manipulate a bit further eq. (3.84). We can write it as:

$$\mathcal{S}_h = \int d^2z \sum_{\mu=\pm1} i\mathrm{k}_{Sc,+}\mathrm{k}_{Sc,-}h_\mu \cos\Big(6\phi - \sqrt{2}(\phi_c + \mu\theta_s)\Big) =$$

$$\int d^2z \sum_{\mu=\pm1} i\mathrm{k}_{Sc,+}\mathrm{k}_{Sc,-}h_\mu \Big(\cos(6\phi)\cos\Big(-\sqrt{2}(\phi_c + \mu\theta_s)\Big) + \sin(6\phi)\sin\Big(-\sqrt{2}(\phi_c + \mu\theta_s)\Big)\Big) =$$

$$\int d^2z \sum_{\mu=\pm1} i\mathrm{k}_{Sc,+}\mathrm{k}_{Sc,-}h_\mu \Big(\cos(6\phi)\cos\Big(\sqrt{2}(\phi_c + \mu\theta_s)\Big) - \sin(6\phi)\sin\Big(\sqrt{2}(\phi_c + \mu\theta_s)\Big)\Big) \quad (3.89)$$

From here it easy to see that by choosing one of the combinations of eq. (3.79) or (3.80) for determining the minima we get:

$$\cos\Big(\sqrt{2}(\phi_c + \mu\theta_s)\Big) = 0, \qquad \sin\Big(\sqrt{2}(\phi_c + \mu\theta_s)\Big) = -1 \quad (3.90)$$

Thus, we end up with the sine-Gordon term:

$$\mathcal{S}_h = 2i\mathrm{k}_{Sc,+}\mathrm{k}_{Sc,-}\int d^2z\, h\sin(6\phi) \quad (3.91)$$

where the additional factor of 2 comes from the fact that we get the same contribution regardless of the value of μ. From here, we can manipulate the last equation a bit more. We can introduce a gauge transformation that shifts the ϕ field by $\pi/2$. In particular we get:

$$\mathcal{S}_h = 2i\mathrm{k}_{Sc,+}\mathrm{k}_{Sc,-}\int d^2z\, h\sin\left(6(\phi+\frac{\pi}{12})\right) = 2i\mathrm{k}_{Sc,+}\mathrm{k}_{Sc,-}\int d^2z\, h\cos\left(6\phi\right) \tag{3.92}$$

We define now the operators:

$$\mathcal{O}_h^{\nu}(z) = e^{i\nu(6\phi(z))} \tag{3.93}$$

where again $\nu = \pm 1$. In this way we can write the $\mathcal{S}_h$ as:

$$\mathcal{S}_h = \frac{h}{2i}\mathrm{k}_{Sc,+}\mathrm{k}_{Sc,-}\int d^2z \sum_{\nu=\pm 1}\mathcal{O}_h^{\nu}(z) \tag{3.94}$$

We will begin our analysis by focusing on the non-trivial terms $\mathcal{B}$ of eq. (3.3.1) by using the effective Interacting action of eq. (3.81) that we introduced in $\mathcal{II}$-step of RG. This means that we have now:

$$\left\langle \mathcal{S}_{I,eff}^{\mathcal{II}}(z_1)\mathcal{S}_{I,eff}^{\mathcal{II}}(z_2)\right\rangle_{\mathbf{f}} \tag{3.95}$$

where it is easy to see that all the mixed terms of form:

$$\left\langle \mathcal{S}_t(z_1)\mathcal{S}_h(z_2)\right\rangle_{\mathbf{f}} \tag{3.96}$$

will be F.O terms and so we can neglect them since they will be irrelevant in the RG sense. For the terms of the form:

$$\left\langle \mathcal{S}_t(z_1)\mathcal{S}_t(z_2)\right\rangle_{\mathbf{f}} \tag{3.97}$$

we will end up to a similar analysis like the one we made for eq. (3.76) where now the fields ϕ_c and θ_s are pinned. The most important terms will be the ones we introduced in the $\mathcal{II}$-step of RG:

$$\left\langle \mathcal{S}_h(z_1)\mathcal{S}_h(z_2)\right\rangle_{\mathbf{f}} \tag{3.98}$$

In particular, we see that we have terms like:

$$\left\langle \mathcal{S}_h(z_1)\mathcal{S}_h(z_2)\right\rangle_{\mathbf{f}} = \frac{h^2}{(2i)^2}\int d^2z \sum_{\nu=\pm 1}\sum_{\nu'=\pm 1}\left\langle \mathcal{O}_h^{\nu}(z)\mathcal{O}_h^{\nu'}(z)\right\rangle \tag{3.99}$$

where these terms can be written as:

$$\Big\langle \mathcal{O}_h^{\nu}(z_1)\mathcal{O}_h^{\nu'}(z_2)\Big\rangle_{\mathbf{f}} = \Big\langle e^{i\nu(6\phi(z_1))}e^{i\nu'(6\phi(z_2))}\Big\rangle_{\mathbf{f}} = e^{i(6(\nu\phi(z_1)+\nu'\phi(z_2)))}\Big(1-\big(6\nu\nu'\mathcal{C}(z_1-z_2)+6\big)dl\Big) \tag{3.100}$$

In total we will get in second-order for the non-trivial term $\mathcal{B}$ for $\mathcal{S}_h$ that:

$$\begin{aligned}\Big\langle \mathcal{S}_h(z_1)\mathcal{S}_h(z_2)\Big\rangle_{\mathbf{f}} &= \frac{h^2}{(2i)^2}\int d^2z \sum_{\nu=\pm1}\sum_{\nu'=\pm1}\Big\langle \mathcal{O}_h^{\nu}(z_1)\mathcal{O}_h^{\nu'}(z_2)\Big\rangle = -\frac{h^2}{4}\int d^2z_1'd^2z_2' \\ &\Bigg(\underbrace{\Big\langle \mathcal{O}_h^{+}(z_1)\mathcal{O}_h^{+}(z_2)\Big\rangle}_{\nu=\nu'=+1}+\underbrace{\Big\langle \mathcal{O}_h^{-}(z_1)\mathcal{O}_h^{-}(z_2)\Big\rangle}_{\nu=\nu'=-1}+\underbrace{\Big\langle \mathcal{O}_h^{-}(z_1)\mathcal{O}_h^{+}(z_2)\Big\rangle}_{\nu=-1,\nu'=+1}+\underbrace{\Big\langle \mathcal{O}_h^{+}(z_1)\mathcal{O}_h^{-}(z_2)\Big\rangle}_{\nu=+1,\nu'=-1}\Bigg) = \\ &-\frac{h^2}{2}\int d^2z_1'd^2z_2'\Big(1+\Big(4-\big(6\mathcal{C}(z_1'-z_2')+6\big)\Big)dl\Big)\cos\big(6(\phi_1+\phi_2)\big) \\ &+\Big(1+\Big(4-\big(-6\mathcal{C}(z_1'-z_2')+6\big)\Big)dl\Big)\cos\big(6(\phi_1-\phi_2)\big)\end{aligned} \tag{3.101}$$

where we wrote the fields as $\phi(z_1')=\phi_1$ and $\phi(z_2')=\phi_2$. By taking the square of the first-order result we get in second order the terms $\mathcal{A}^2$:

$$\begin{aligned}\Big\langle \mathcal{S}_h(z)\Big\rangle_{\mathbf{f}}^2 = \Big\langle \mathcal{S}_h(z_1)\Big\rangle_{\mathbf{f}}\Big\langle \mathcal{S}_h(z_2)\Big\rangle_{\mathbf{f}} &= \frac{h^2}{(2i)^2}\int d^2z_1'd^2z_2' \sum_{\nu=\pm1}\sum_{\nu'=\pm1}\Big\langle \mathcal{O}_h^{\nu}(z_1)\Big\rangle_{\mathbf{f}}\Big\langle \mathcal{O}_h^{\nu'}(z_2)\Big\rangle_{\mathbf{f}} = \\ &-\frac{h^2}{4}\int d^2z_1'd^2z_2'\Bigg(\underbrace{\Big\langle \mathcal{O}_h^{+}(z_1)\Big\rangle_{\mathbf{f}}\Big\langle \mathcal{O}_h^{+}(z_2)\Big\rangle_{\mathbf{f}}}_{\nu=\nu'=+1}+\underbrace{\Big\langle \mathcal{O}_h^{-}(z_1)\Big\rangle_{\mathbf{f}}\Big\langle \mathcal{O}_h^{-}(z_2)\Big\rangle_{\mathbf{f}}}_{\nu=\nu'=-1} \\ &+\underbrace{\Big\langle \mathcal{O}_h^{-}(z_1)\Big\rangle_{\mathbf{f}}\Big\langle \mathcal{O}_h^{+}(z_2)\Big\rangle_{\mathbf{f}}}_{\nu=-1,\nu'=+1}+\underbrace{\Big\langle \mathcal{O}_h^{+}(z_1)\Big\rangle_{\mathbf{f}}\Big\langle \mathcal{O}_h^{-}(z_2)\Big\rangle_{\mathbf{f}}}_{\nu=+1,\nu'=-1}\Bigg) = \\ -\frac{h^2}{2}\big(1+(4-6)dl\big)&\int d^2z_1'd^2z_2'\Big(\cos\big(6(\phi_1+\phi_2)\big)+\cos\big(6(\phi_1-\phi_2)\big)\Big)\end{aligned} \tag{3.102}$$

Now it is very easy to see that by combining these terms we left with:

$$\begin{aligned}\mathcal{B}-\mathcal{A}^2 = -\frac{h^2}{2}\int d^2z_1'd^2z_2'\Bigg(&\Big(1-6\mathcal{C}(z_1'-z_2')dl\Big)\cos\big(6(\phi_1+\phi_2)\big) \\ &-\Big(1+6\mathcal{C}(z_1'-z_2')dl\Big)\cos\big(6(\phi_1-\phi_2)\big)\Bigg)\end{aligned} \tag{3.103}$$

Let us note here, that we can get the same results if we decide to carry around the ϕ_c and θ_s fields as shown in Appendix (B.5). To evaluate these terms, we will use the approximation that the function

$\mathcal{C}(z_1 - z_2)$ is assumed to have a short-range character and for that reason it can be made very localized by using a suitable cutoff. In this situation we will consider that $z_1 - z_2 < \bar{a}$. This constrains the two points to be in a neighbourhood of size $dz \approx (\bar{a}, \bar{a}/v_q)$ from each other, where $\bar{a}$ can be considered of the order of the Quantum Hall energy v_F^e/E_{QH}.

Let us analyze now the first term of equation (B.36). We will use the substitution of $\mathcal{C}(z_1' - z_2') \approx \gamma\delta(z_1 - z_2)$, with $\gamma \approx \bar{a}^2/v_q$. This means that $\phi(z_1') = \phi(z_2')$ and in particular we will have that:

$$-\frac{h^2}{2}\int d^2z_1' d^2z_2' \Big(1 - 6\mathcal{C}(z_1' - z_2')dl\Big) \cos\big(6(\phi_1 + \phi_2)\big) \approx -\frac{h^2}{2}\int d^2z' \Big(1 - 6\gamma dl\Big) \cos\big(12\phi(z')\big) \tag{3.104}$$

At second order, we see that emerges the operator $\cos\big(12\phi(z')$. If we follow again the same procedure of the second step in RG, i.e if we introduce a new effective action which will contain now this new operator that emerged and has the form:

$$\mathcal{S}_{h_{new}} = \int d^2z h_{new} \cos\big(12\phi(z')\big) \tag{3.105}$$

we will see that by finding its RG equation in first order we will get:

$$\frac{dh_{new}}{dl} = h_{new}(2 - \mathcal{D}_{h_{new}}) \tag{3.106}$$

where its scaling dimension is $\mathcal{D}_{h_{new}} = 12$. This means that it will be highly irrelevant.

Let us continue our analysis with the second term of eq. (B.36). If we take again the same approximation as for the first term, where we approximate the short-range function with a δ-function, $\mathcal{C}(z_1' - z_2') \approx \gamma\delta(z_1' - z_2')$, we do not get anything. The most relevant term must therefore be obtained by considering a better expansion for the localized function $\mathcal{C}(z_1' - z_2')$. The way of dealing with this is to change variables from z_1 and z_2' to center of mass (z_R') and relative coordinate (z_r'):

$$z_R' = \frac{z_1' + z_2'}{2}, \qquad z_r' = z_1' - z_2' \tag{3.107}$$

The correlation function $\mathcal{C}(z_1' - z_2')$ depends only on $|z_r'|$ and we may assume that it is non-negligible only in a neighborhood of size $\bar{a}$ around $|z_r' = 0|$. We observe that $\bar{a}$ is in general a non-universal quantity of the system (might miss a factor) and depends on the microscopic behavior of the model, although we can set the length scale of $\bar{a} = v_F^e/E_{QH}$ for practical purposes. Based on this observation,

and assuming that $\bar{a}$ is small, we can approximate:

$$\frac{h^2}{2}\int d^2z_1' d^2z_2' 6\mathcal{C}(z_1'-z_2')dl\cos\big(6(\phi_1-\phi_2)\big) \approx \frac{h^2}{2}\int d^2z_R' d^2z_r' 6\mathcal{C}(|z_r'|dl\cos\big(6(\phi_1-\phi_2)\big) \approx$$
$$\frac{6h^2}{2}\frac{\bar{a}^2}{v_q}dl\int d^2z_R'\cos\big(6(\underbrace{z_1'-z_2'}_{\bar{a}})\partial_{z_R'}\phi(\frac{z_1'+z_2'}{2})\big) = \frac{6h^2}{2}\frac{\bar{a}^2}{v_q}dl\int d^2z_R'\cos\big(6(\underbrace{z_1'-z_2'}_{\bar{a}})\partial_{z_R'}\phi(z_R')\big) \tag{3.108}$$

here we got the term $\frac{\bar{a}^2}{u_q}$ by integrating out the relative coordinates. In order to continue from here, we make the assumption that $\bar{a}\partial_{z_R'}\phi(\frac{z_1'+z_2'}{2}) \ll 1$ and we Taylor expand it around the minima. Of course we can not expand it around all minima, and for that reason we will choose one of the minima of eq. (3.79) (does not matter which one). By Taylor expanding eq. (3.108) around $\theta_s = 0$ (good choice in case someone follows the procedure shown to derive eq. (B.36)) and ignoring the constant term, we get:

$$2\frac{6h^2}{2}\frac{\bar{a}^2}{v_q}dl\int d^2z_R'\cos\big(6(\underbrace{z_1'-z_2'}_{\bar{a}})\partial_{z_R'}\phi(z_R')\big) \approx$$
$$-6h^2\frac{6^2\bar{a}^4}{2v_q}dl\int d^2z_R'\big(\partial_{z_R'}\phi(z_R')\big)^2 = -6^3h^2\frac{\bar{a}^4}{2v_q}dl\int d^2z'\Big[\big(\partial_{z'}\phi(z')\big)^2+\frac{1}{v_q^2}\big(\partial_{\tau'}\phi(z')\big)^2\Big] \tag{3.109}$$

where here $v_q = v_F^e$, the velocity of the FQH particles. We can see that the term in eq. (3.109) modifies the quadratic part of the Hamiltonian. In particular, if we neglect the operator in eq. (3.104), we obtain in second order:

$$\frac{\mathcal{A}^2-\mathcal{B}}{2} \approx \frac{6^3h^2}{4}\frac{\bar{a}^4}{v_F^e}dl\int d^2z'\Big[\big(\partial_{z'}\phi(z')\big)^2+\frac{1}{v_F^{e2}}\big(\partial_{\tau'}\phi(z')\big)^2\Big] \tag{3.110}$$

At this point it would be useful to go back into the description of the bare electron instead of continuing with our quasiparticle description. The reason is that we will be able to write that way the Kosterlitz and Thouless equations for the Luttinger parameter $\mathcal{K}_e$. This can easily be done by reversing eq. (3.70). Thus, eq. (3.110) can be written as:

$$\frac{\mathcal{A}^2-\mathcal{B}}{2} \approx \frac{2^4h^2}{4}\frac{\bar{a}^4}{2\mathcal{K}_e v_F^e}dl\int d^2z'\Big[\big(\partial_{z'}\phi_e(z')\big)^2+\frac{1}{v_F^{e2}}\big(\partial_{\tau'}\phi_e(z')\big)^2\Big] \tag{3.111}$$

The factor of 2^4 comes form the fact that the sine-Gordon term is written as $\cos(6\phi) = \cos(2\phi_e)$. We are now in position to write the effective action with the contributions from 1st and 2nd order for the $\mathcal{II}$-step of RG. In particular, we get:

$$\mathcal{S}_{eff}^{\mathcal{II}}(\tilde{\Lambda}) = \mathcal{S}_0 + \mathcal{A} + \frac{\mathcal{A}^2-\mathcal{B}}{2} \tag{3.112}$$

But as it was shown before, at 1st order the $\mathcal{S}_h$ term is still irrelevant, thus we can neglect it. Also, in the $\mathcal{II}$-step of RG, the $\mathcal{S}_0$ will include only the quadratic terms for FQH because the ϕ_c and θ_s fields are fields. And so, we are left with:

$$\mathcal{S}_{eff}^{\mathcal{II}}(\tilde{\Lambda}) \approx \mathcal{S}_0 + \frac{\mathcal{A}^2 - \mathcal{B}}{2} =$$
$$\int d^2z' \left[\left(\frac{\mathcal{K}_e v_F^e}{2\pi} + \frac{2^4 h^2 \bar{a}^4}{8\mathcal{K}_e v_F^e} dl \right) \left(\partial_{z'} \phi_e(z')\right)^2 + \left(\frac{\mathcal{K}_e}{2\pi v_F^e} + \frac{2^4 h^2 \bar{a}^4}{8\mathcal{K}_e v_F^{e^3}} dl \right) \left(\partial_{\tau'} \phi_e(z')\right)^2 \right] \tag{3.113}$$

Differentiating $\mathcal{S}_{eff}^{\mathcal{II}}$ we can derive the RG equations for the Luttinger parameter. In particular we obtain:

$$\frac{\mathcal{K}_e'}{2\pi} = \sqrt{\left(\frac{\mathcal{K}_e v_F^e}{2\pi} + \frac{2^4 h^2 \bar{a}^4}{8\mathcal{K}_e v_F^e} dl \right) \left(\frac{\mathcal{K}_e}{2\pi v_F^e} + \frac{2^4 h^2 \bar{a}^4}{8\mathcal{K}_e v_F^{e^3}} dl \right)} \approx \frac{\mathcal{K}_e}{2\pi} + \frac{1}{2\pi} \frac{\pi 2^4 h^2 \bar{a}^4}{4\mathcal{K}_e v_F^{e^2}} dl \tag{3.114}$$

where $\mathcal{K}_e'$ is the new rescaled Luttinger parameter of our $\mathcal{S}_{eff}^{\mathcal{II}}$ action. Similarly, we get the velocity $v_F^{e\,\prime} = 1$. We can calculate now the RG equation for the Luttinger parameter and the velocity, and we find them to be equal with:

$$\frac{d\mathcal{K}_e}{dl} = \frac{2^4 h^2 \bar{a}^4 \pi}{4\mathcal{K}_e v_F^{e^2}} \tag{3.115}$$

and

$$\frac{dv_F^{e\,\prime}}{dl} = 0 \tag{3.116}$$

and means that the velocity does not change under the RG flow, which is consistent with the Lorentz invariance of the system. At first order, we found the scaling dimension for h to be equal with:

$$\mathcal{D}_h = \frac{2^2}{4\mathcal{K}_e} = \frac{1}{\mathcal{K}_e} \tag{3.117}$$

and the corresponding RG equation for h at first order was:

$$\frac{dh}{dl} = h \frac{d\Big(1 + \big(2 - \frac{1}{\mathcal{K}_e}\big) dl\Big)}{dl} \Rightarrow \frac{dh}{dl} = h\Big(2 - \frac{1}{\mathcal{K}_e}\Big) dl \tag{3.118}$$

To summarize the RG equations of the system at second order are:

$$\frac{d\mathcal{K}_e}{dl} = \frac{2^4 h^2 \bar{a}^4 \pi}{4\mathcal{K}_e v_F^{e^2}}, \qquad \frac{dh}{dl} = h\Big(2 - \frac{1}{\mathcal{K}_e}\Big) \tag{3.119}$$

and from eq. (3.118) we can see that the critical point corresponds to the value $\mathcal{K}_e = \frac{1}{2}$.

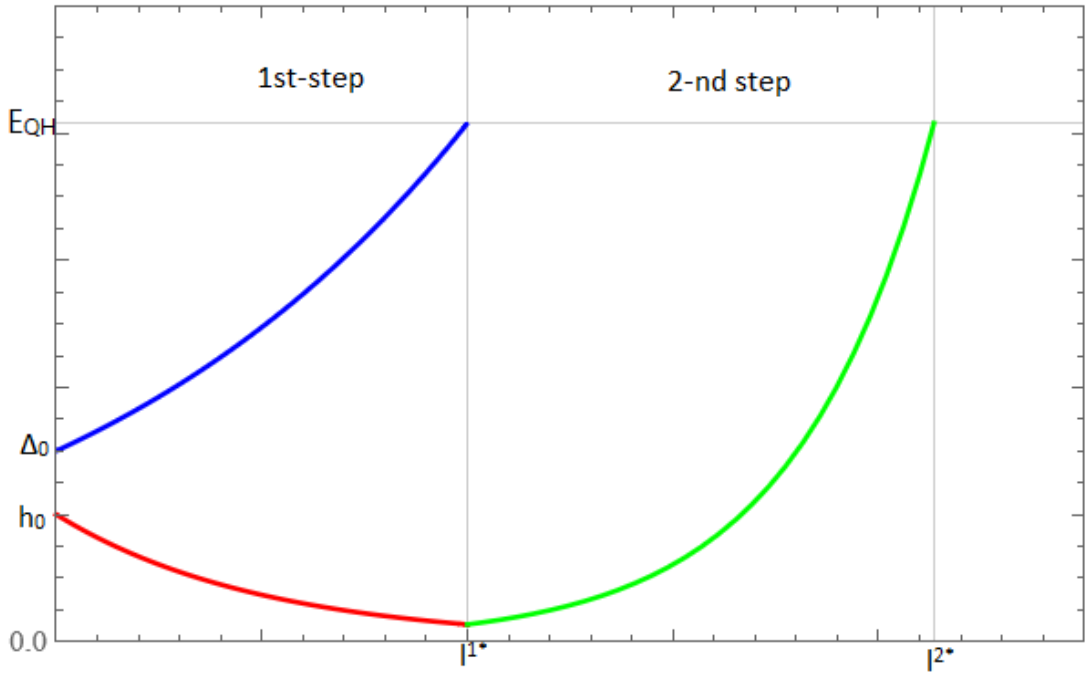

Figure 3.5: Here we see the schematic representation of steps $\mathcal{I}$ and $\mathcal{I}$ of RG in the 2nd-order. We see that the Δ term is relevant at $\mathcal{I}$-step (blue line) and it grows until it reaches the threshold at l^* where it pins the ϕ_c and θ_s fields. The red line represents the h term at $\mathcal{I}$-step where we can see that it is irrelevant (same as before in Figure 3.4). When the h term reaches the end of the $\mathcal{I}$-step at l^{1^*} we see that the scaling dimensions changes at $\mathcal{I}\mathcal{I}$-step and it scales as $h(l^{1^*})e^{cl^{1^*}}$, where $h(l^*) = h_0 e^{-2l^{1^*}}$, where we can see that it is relevant for the values of the prefactor $c - 2 > 0$.

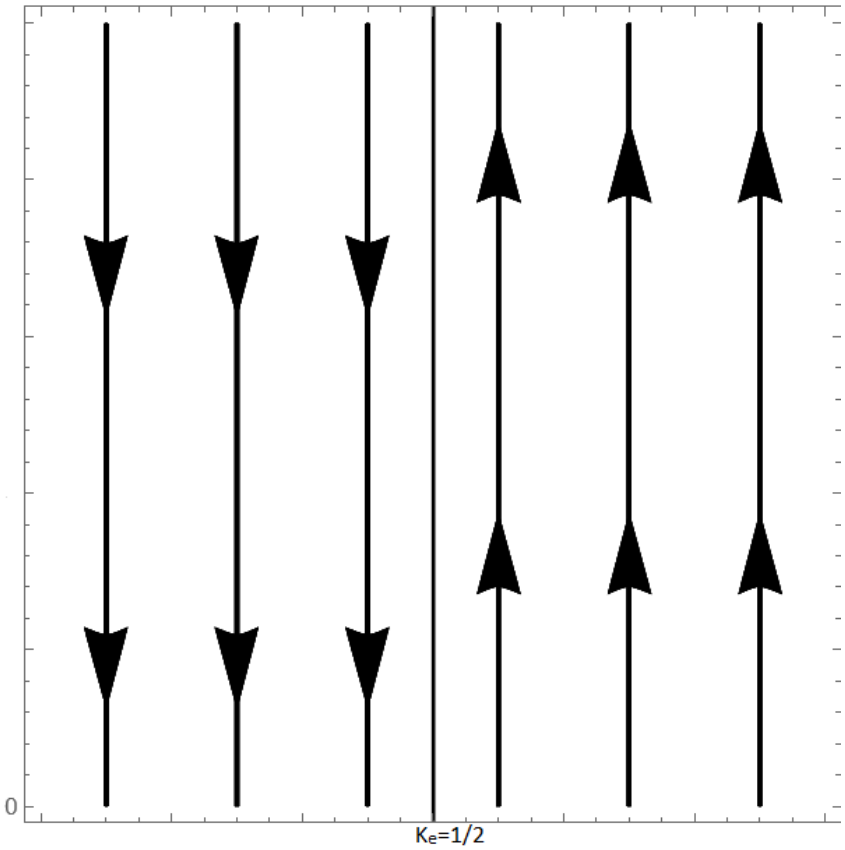

Figure 3.6: Here we see the RG flow at 1st-order. As it represented, the flow is only relevant when the Luttinger parameter takes the value $\mathcal{K}_e = \frac{1}{2}$.

We are interested now in the behavior close to the phase transition that occurs at $\mathcal{D}_h = \frac{1}{2}$, thus $\mathcal{K}_e = \frac{1}{2}$, therefore we define the small parameter t' and the effective coupling constant y' which are associated with $\frac{dh}{dl}$ and $\frac{d\mathcal{K}'_e}{dl}$ respectively. In particular, we define them as:

$$t' = \mathcal{K}_e - \frac{1}{2}, \qquad y = \frac{2^2\bar{a}^2\sqrt{\pi}}{v_F^e}\frac{h}{\mathcal{K}_e} \tag{3.120}$$

In this way, when we differentiate t', it will be inconsistent with:

$$\frac{dt'}{dl} = \frac{d\mathcal{K}'_e}{dl} = \frac{2^4h^2\bar{a}^4\pi}{4\mathcal{K}_e v_F^{e^2}} = \frac{Ah^2}{\mathcal{K}_e} \tag{3.121}$$

where $A = \frac{2^2\bar{a}^4\pi}{v_F^{e^2}}$ and for $\mathcal{K}_e = \frac{1}{2}$, we get:

$$\frac{dt'}{dl} = \frac{d\mathcal{K}'_e}{dl} = 2Ah^2 = y^2 \tag{3.122}$$

By taking now the derivative for the coupling constant y we find that:

$$\frac{dy}{dl} = \frac{2^2\bar{a}^2\sqrt{\pi}}{v_F^e}\frac{1}{\mathcal{K}_e}\frac{dh}{dl} = \Big(2 - \frac{1}{\mathcal{K}_e}\Big)y = \Big(2 - \frac{1}{t' + \frac{1}{2}}\Big)y = 2\Big(1 - \frac{1}{2t' + 1}\Big)y \approx 2\Big(1 - (1 - 2t')\Big)y = 4t'y \tag{3.123}$$

To summarize, we have delivered the Kosterlitz and Thouless equations:

$$\frac{dt'}{dl} = y^2, \qquad \frac{dy}{dl} = 4t'y \tag{3.124}$$

The first step to solve them is to realize that $\mu = 4t^2 - y^2$ is invariant under the RG flow defined by these equations. Therefore the flow trajectories in the plane (t, y) are always hyperboles and $y = \pm 2t$ are the separatrices defininig the critical lines.

We can now choose the value of $\mathcal{K}_e = \frac{1}{3}$ which corresponds to Laughlin state $\nu = \frac{1}{3}$, to estimate at which point we are going to have phase transition. We find that corresponds to the critical values of:

$$t'(\mathcal{K}_e = \frac{1}{3}) = -\frac{1}{6}, \qquad y_{cr} = -2t = \frac{1}{3} \tag{3.125}$$

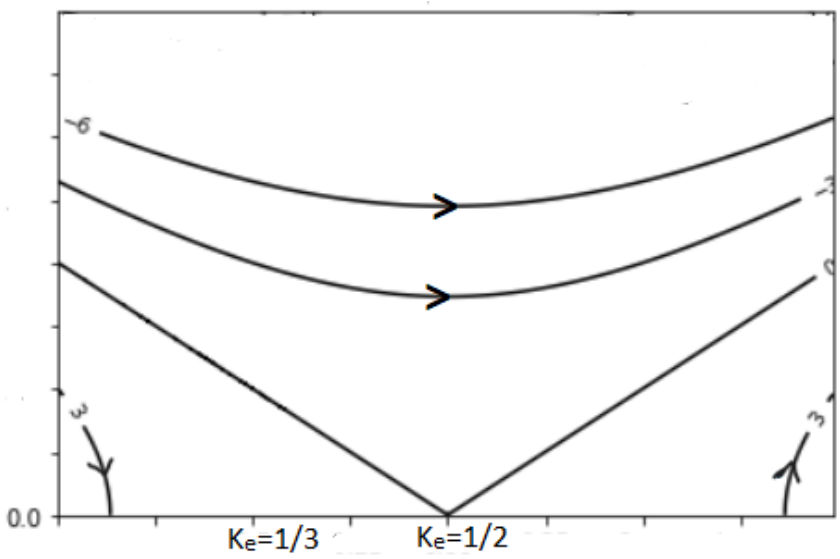

Figure 3.7: Here we see the RG flow at 2nd-order after the linearization. As it is represented, the flow is only relevant when the parameters take the values that are above the critical values that found on eq. (3.125).

Gap estimation

Based on the RG equations and on the conservation of the parameter μ under the RG flow, it is also possible to refine the estimate of the gap. As we said before, at the beginning of $\mathcal{I}$-step of RG we start

from an initial value for $\Delta = \Delta(l=0) = \Delta_0 = const.$. We set the UV cutoff to be given by the QH gap E_{QH}, where after that value, our RG procedure breaks down. We denote as l_1^* the value in which the our pairing potential scales to reach the UV cutoff. This means that at the l_1^* we will have:

$$E_{QH} = \Delta_0 e^{l_1^*} \Rightarrow \frac{E_{QH}}{\Delta_0} = e^{l_1^*} \Rightarrow l_1^* = \ln \frac{E_{QH}}{\Delta_0} \tag{3.126}$$

where to get the scaling dimensions of the Δ term we have assumed that $\mathcal{K}_c = \mathcal{K}_s = 1$ and results to $\mathcal{D}_\Delta = 1$. Then, for the parameter $h(l)$, by starting from an initial value of $h(l=0) = h_0 = const.$, we find that at the end of $\mathcal{I}$-step, or equivalent at the beginning of $\mathcal{II}$-step, it has a value of:

$$h(l_1^*) = h_0 e^{-2l_1^*} = h_0 e^{\left(-2\ln\frac{E_{QH}}{\Delta_0}\right)} = h_0 e^{\left(\ln\left(\frac{E_{QH}}{\Delta_0}\right)^{-2}\right)} \Rightarrow h(l_1^*) = h_0 \Big(\frac{\Delta_0}{E_{QH}}\Big)^2 \tag{3.127}$$

This is the value at the beginning of $\mathcal{II}$-step of RG and this is the one that we will put inside the Kosterlitz and Thouless equations. By substituting the value of $\bar{a} = v_F^e/E_{QH}$ and eq. (3.127) into eq. (3.125) we find that;

$$y = h_0 \Big(\frac{\Delta_0}{E_{QH}}\Big)^2 \Big(\frac{v_F^e}{E_{QH}}\Big)^2 \frac{2^2\sqrt{\pi}}{v_F^e \mathcal{K}_e} = 4\sqrt{\pi} h_0 v_F^e \frac{\Delta_0^2}{E_{QH}^4} \frac{1}{\mathcal{K}_e} \tag{3.128}$$

Thus, the constrain in order for h to flow to strong coupling, is:

$$y > y_{cr} \rightarrow y > \frac{1}{3} \Rightarrow h_0 > \frac{\mathcal{K}_e}{12\sqrt{\pi} v_F^e} \frac{E_{QH}^4}{\Delta_0^2} \tag{3.129}$$

According to, [18], typically, the FQH bulk energy gap is $E_{QH} \sim 0.016 e^2/\epsilon l_B \sim 1.7 meV$ in graphene setups where $\epsilon \approx 1$ is the dielectric constant in suspended graphene and l_B is the magnetic length. The velocity of the edge modes is equal to $v_F^e = 10^5 m/s$. They also state, that for strong induced pairing ($\Delta \rightarrow E_{QH}$), and sufficiently long islands, Δ_e (quasielectron gap) grows much beyond E_C (charging energy of the island). In this case, the system is deeply in the topological regime and coherent tunnelling mediated by parafermions is the dominant transport channel.

Let us take a moment here to discuss what eq. (3.129) means to us. Till now, we mentioned all the parameters expect one, the value of the superconducting gap Δ for NbN which in typical graphene setups it is usually $\Delta \geq E_{QH}$.

According to [19] and [20] they say that the superconducting energy gap is $\Delta_0 \approx 3\, meV$ at zero magnetic field. If we consider this value for the RG procedure we see that we have $\Delta > E_{QH}$ which means that the whole RG procedure was for nothing, since we considered the UV cutoff to be the E_{QH}, and after that value the Bosonization breaks down. In this situation, we can take $\Delta \approx E_{QH}$ and

this will have as a result to get:

$$h_0 > \frac{\mathcal{K}_e E_{QH}^2}{12\sqrt{\pi} v_F^e} \tag{3.130}$$

This means that our RG procedure starts from the $\mathcal{II}$-step without having a step $\mathcal{I}$.But the exact value of Δ depends on many factors, for example depends on the value of the magnetic field, on magnetic flux vortices into the system or from the fabrication of the Superconductor.

What is more encouraging is that in [1] they do not take a particular value for Δ, but rather it varies uniformly in the range $[-\Delta, \Delta]$ over distances comparable to the minimum coherence length $\xi_0 \sim \frac{u_f}{\Delta}$. Although, as they state, this is a heuristic ansatz for an actual experimental setup, they motivate their model by noting that the leading order effect of having finite chemical potential disorder within the superconductor or near the junction and the presence of magnetic flux vortices within the superconductor cause variations in the induced pairing in the edge modes. In this case, we will have $\Delta \leq E_{QH}$ and the Bosonization and the RG procedure will still be valid. Thus, our field theoretical model can still give an estimate result for the gap.

Let's try now to give an estimate value of the Induced Gap, based on true values of the parameters. To do so, we must first check the dimensions of the parameter h_0. In order for eq. (3.130) to hold, we see that h_0 should have dimensions $Energy/length$. Our guess is that it should be associated with the QH. When we were constructing the step $\mathcal{I}$ and step $\mathcal{II}$ of the RG procedure, we said that we take energy scale of h_0 to be the value of Δ_{ind} that we calculated previously in Ch. 2. Since we also need a length scale it makes sense to assume that h_0 depends on the lattice spacing of the QH α_{QH} and we take it to be equal to $\alpha_{QH} = v_F^e / E_{QH}$, because α_{QH} will be the Ultraviolet cutoff (the length scale) for the edge modes. By replacing the above in eq. (3.130), we get:

$$\Delta_{ind} > \frac{\mathcal{K}_e E_{QH}}{12\sqrt{\pi}} \Rightarrow \Delta_{ind} > 0,2664 \ meV \tag{3.131}$$

This is the numerical result that we estimate from the RG procedure for the Induced Gap in graphene.

At this point there is another question that may rise. As we said before, one factor that may affect the value of Δ are vortices. How sure are we that in our system we will not have vortices? Preliminary work [21] shows that the high magnetic fields required to sustain the FQH state clash with superconductivity. This leads to a proliferation of Abrikosov vortices in the superconductor supplying the proximity coupling with in-gap states residing in the vortex cores. Thus, we can not say for sure that in our system we will not have vortices. This is an open question for us and can motivate us for future work.

Chapter 4

Conclusion and Outlook

In this thesis, we studied an (Integer, Fractional) Quantum Hall/superconductor hybrid device with the sole purpose to derive an effective field theory based on Bosonization to describe it. An important factor that enabled the study of such a system was the choice of the Superconductor, the NbN. This special Superconductor, as was already mentioned, keeps his superconductivity in very high magnetic field, and high magnetic are needed for Fractional Quantum Hall system to thrive. Another equally important property is the large spin-orbit coupling in NbN superconductor, which provides a necessary ingredient for a spin-flip process allowing for a pairing between electrons with the same spin polarization.

At first, there was made an attempt to find an effective description of the Induced gap that appears from the same spin electron pairings to describe the counter propagating edge modes for the Integer Quantum Hall case. This attempt was made by using 2nd-order Perturbation Theory and the Feynman Path Integral method for field theories. In both these approaches, the results were a successful. Both of them provided an effective description of approximating the Induced gap in momentum space. For this project however, it is important to be able to translate these results in real space, because then it will be possible to compare them with the result of the Bosonized description. As was already seen, due to the complicated form of the Induced gap, in both approaches, it was not possible to provide an analytical result for the Δ_{ind} in real space.

Next, there was made the Bosonized description for this Quantum Hall/superconductor hybrid device. This method, has the advantage that the mapping to the Integer or to the Fractional Quantum Hall case can be very easily. The reason is, because the chiral edge state of the Quantum Hall can be described from the Luttinger Liquid Hamiltonian. In this description, the Interactions (FQH) are hidden in the Luttinger parameter. For the IQH which is non-Interacting, the Luttinger parameter takes the value $\mathcal{K}_e = 1$ and for the FQH takes the value of the laughlin state. In this particular case the value is $\mathcal{K}_e = \frac{1}{3}$ ($\nu = \frac{1}{3}$). Furthermore, in this description it is not required for the Superconductor to be in the topological phase in order to acquire the zero modes at the edges. It was taken in the trivial phase, because these modes are expected to appear due to Quantum Hall. If the Superconductor was

taken to be in the topological state, there might another pair of exotic particles that appear in the edges of the Quantum wire. This is probably a good starting point for future research.

Finally, after the Bosonized description of the system in established, an estimation of the Induced gap is pursued via Renormalization Group methods. A 2-step RG procedure is concluded to be well defined in order to reach a result. In this way, the flow is divided into separate parts, where each part is terminated when a coupling constant reaches a suitable upper threshold, which indicates when a given interaction semiclassically pins the related fields. In the $\mathcal{I}$-step of RG, it is found that a Superconducting gap opens by the Δ term until it reaches the threshold which is taken to be the E_{QH}. After the related fields are pinned (ϕ_C and θ_s), it is found that all the other terms are irrelevant at first order, thus, a 2nd-order term is calculated. After that, the Kosterlitz and Thouless equations are derived and an estimation about the gap is being made. It is concluded that in order to open a gap Δ and E_q must be comparable, which for NbN it might not always be the case because the value of Δ depends on many factors.

In conclusion, based on the Bosonized description of the Fractional Quantum Hall/superconductor hybrid device, one could use our result to make an approximation about the gap. As was shown, even in the case of NbN, which is a very disordered SC, these description might give encouraging results. But it can also be used in case another Superconductor with the same properties is studied. Last but not least, in the Bosonized description, there were encountered 2 different resonances. In case of these values for the Fermi momentum a further investigation could occur, which will probably result to more exotic particles. Future work must also include the study of transport phenomena and the construction of a Bosonized description for them. As one continues to investigate such systems more and more questions will arise and he can never be sure of how rich the physics behind such devices is.

List of Figures

Bibliography

[1] Önder Gül et al., *Andreev Reflection in the Fractional Quantum Hall State*, Phys. Rev. X **12, 021057 (2022)**.

[2] Fradkin Eduardo, *Field Theories of Condensed Matter Physics*, 2nd ed. Cambridge: Cambridge University Press (2013).

[3] David Tong, *Lectures on the Quantum Hall Effect*, arXiv:1606.06687 (2016).

[4] Martin Leijnse and Karsten Flensberg, *Introduction to topological superconductivity and Majorana fermions*, Semicond. Sci. Technol. **27, 124003 (2012)**.

[5] Jason Alicea, *New directions in the pursuit of Majorana fermions in solid state systems*, Reports on Progress in Physics, Rep. Prog. Phys. **75 076501 (2012)**.

[6] Simon, Steven H, *The Oxford Solid State Basics*, First edition, Oxford University Press (2013).

[7] K. v. Klitzing, G. Dorda, and M. Pepper, *New Method for High-Accuracy Determination of the Fine-Structure Constant Based on Quantized Hall Resistance*, Phys. Rev. Lett. **45,494 (1980)**.

[8] Ciftja, Orion, *Detailed solution of the problem of Landau states in a symmetric gauge*, Eur. J. Phys. **41 035404 (2020)**.

[9] R. B. Laughlin, *Anomalous Quantum Hall Effect: An Incompressible Quantum Fluid with Fractionally Charged Excitations*, Phys. Rev. Lett. **50, 1395 (1983)**.

[10] M. O. Goerbig, *Electronic properties of graphene in a strong magnetic field*, Rev. Mod. Phys. **83, 1193 (2011)**.

[11] Lee, GH., Huang, KF., Efetov, D. et al., *Inducing Superconducting Correlation in Quantum Hall Edge States*, Nature Phys **13, 693698 (2017)**.

[12] Clarke, D., Alicea, J. Shtengel, K., *Exotic non-Abelian anyons from conventional fractional quantum Hall states*, Nat Commun **4, 1348 (2013)**.

[13] Andreas B. Michelsen, Patrik Recher, Bernd Braunecker, and Thomas L. Schmidt, *Supercurrent enabled Andreev reflection in a chiral quantum Hall edge state*, arXiv:2203.13384v2 (2022).

[14] Christopher Reeg, Jelena Klinovaja, and Daniel Loss, *Destructive interference of direct and crossed Andreev pairing in a system of two nanowires coupled via an s-wave superconductor*. Phys. Rev. B **96, 081301(R) (2017)**.

[15] Michele Burrello, Mauro Iazzi, and Andrea Trombettoni, *Notes about a spin-orbit superconductor* (2011).

[16] A. Altland and B. D. Simons, *Condensed Matter Field Theory*, 2nd ed. Cambridge: Cambridge University Press (2010).

[17] M Burrello, *Introduction to one-dimensional models* (2022).

[18] Ida E. Nielsen, Karsten Flensberg, Reinhold Egger, and Michele Burrello, *Readout of Parafermionic States by Transport Measurements*, Phys. Rev. Lett. **129, 037703 (2022)**.

[19] Shailesh Kalal et al., *Effect of disorder on superconductivity of NbN thin films studied using x-ray absorption spectroscopy*, J. Phys.: Condens. Matter **33 305401 (2021)**.

[20] K. S. Keskar, Tsutomu Yamashita, and Yutaka Onodera, *Superconducting Transition Temperatures of R. F. Sputtered NbN Films*, Jpn. J. Appl. Phys. 10 370 (1971).

[21] Schiller, N., Katzir, B. A. et al., *Interplay of superconductivity and dissipation in quantum Hall edges*, arXiv:2202.10475 (2022).

Chapter 5

Appendices

A Appendix

A.1 Supplementary for the Superconductor

In this Appendix, we present a way to calculate analytically the eigenvalues of the Hamiltonian of eq. (2.12). This can be done by taking the square of eq. (2.12):

$$\begin{aligned} H_{BdG} = \xi_k\tau_z + \alpha k\sigma_y\tau_z + \tilde{B}\sigma_z - \Delta\tau_x \Rightarrow H_{BdG}^2 = \left(\xi_k\tau_z + \alpha k\sigma_y\tau_z + \tilde{B}\sigma_z - \Delta\tau_x\right)^2 \Rightarrow \\ H_{BdG}^2 = \xi_k^2 + (\alpha k)^2 + \tilde{B}^2 + \Delta^2 + 2\xi\alpha k\sigma_y + 2\xi\tilde{B}\tau_z\sigma_z - 2\tilde{B}\Delta\sigma_z\tau_x - \\ \xi\Delta\underbrace{\{\tau_z,\tau_x\}}_{=0} + \alpha k\tilde{B}\underbrace{\{\sigma_y,\sigma_z\}}_{=0}\tau_z - \alpha k\Delta\sigma_y\underbrace{\{\tau_z,\tau_x\}}_{=0} \Rightarrow \\ H_{BdG}^2 - \xi_k^2 - (\alpha k)^2 - \tilde{B}^2 - \Delta^2 = 2\xi\alpha k\sigma_y + 2\xi\tilde{B}\tau_z\sigma_z - 2\tilde{B}\Delta\sigma_z\tau_x \end{aligned} \tag{A.1}$$

Here we square it again and collecting the terms to make the anti-commutation relation as before, we get:

$$\begin{aligned} \left(H_{BdG}^2 - \xi_k^2 - (\alpha k)^2 - \tilde{B}^2 - \Delta^2\right)^2 = \left(2\xi\alpha k\sigma_y + 2\xi\tilde{B}\tau_z\sigma_z - 2\tilde{B}\Delta\sigma_z\tau_x\right)^2 \Rightarrow \\ \left(H_{BdG}^2 - \xi_k^2 - (\alpha k)^2 - \tilde{B}^2 - \Delta^2\right)^2 = 4\xi_k^2\tilde{B}^2 + 4\xi_k^2(\alpha k)^2 + 4\tilde{B}^2\Delta^2 \Rightarrow \\ H_{BdG}^2 - \xi_k^2 - (\alpha k)^2 - \tilde{B}^2 - \Delta^2 = \pm 2\sqrt{\xi_k^2\left((\alpha k)^2 + \tilde{B}^2\right) + \tilde{B}^2\Delta^2} \Rightarrow \\ H_{BdG}^2 = \xi_k^2 + (\alpha k)^2 + \tilde{B}^2 + \Delta^2 \pm 2\sqrt{\xi_k^2\left((\alpha k)^2 + \tilde{B}^2\right) + \tilde{B}^2\Delta^2} \end{aligned} \tag{A.2}$$

where $H^2_{BdG} = E^2_{BdG,\pm}$ and we used the anti-commutation relations of the Pauli matrices $\{\sigma_i, \sigma_j\} = 2\delta_{i,j}$. Similar for the τ matrices.

A.2 Supplementary for the Perturbation theory

In this Appendix we present the exact calculations we performed to derive a final result for the Perturbation Theory approach. By starting from eq. (2.3), we try to calculate each term separately.

- We start the calculations from:

$$H_p \left|\Psi_{BCS}\right\rangle = -t \int dk \sum_{j=L,R} [\psi^\dagger_{QH,\uparrow,k,j}\psi_{SC,\uparrow,k} + \psi^\dagger_{SC,\uparrow,k}\psi_{QH,\uparrow,k,j}] \left|\Psi_{BCS}\right\rangle =$$
$$-t \int dk \sum_{j=L,R} [\psi^\dagger_{QH,\uparrow,k,j}(u_{1,\uparrow,k}\gamma_{1,k} + v^*_{1,\uparrow,k}\gamma_{4,k} + u_{2,\uparrow,k}\gamma_{2,k} + v^*_{2,\uparrow,k}\gamma_{3,k}) -$$
$$\psi_{QH,\uparrow,k,j}(u^*_{1,\uparrow,k}\gamma^\dagger_{1,k} + v_{1,\uparrow,k}\gamma^\dagger_{4,k} + u^*_{2,\uparrow,k}\gamma^\dagger_{2,k} + v_{2,\uparrow,k}\gamma^\dagger_{3,k})] \left|\Psi_{BCS}\right\rangle =$$
$$-t \int dk \sum_{j=L,R} [\psi^\dagger_{QH,\uparrow,k,j} v^*_{1,\uparrow,k} \left|1,-k\right\rangle + v^*_{2,\uparrow,k} \left|2,-k\right\rangle) - \psi_{QH,\uparrow,k,j} u^*_{1,\uparrow,k} \left|1,k\right\rangle + u^*_{2,\uparrow,k} \left|2,k\right\rangle)] =$$
$$-t \int dk \sum_{i=1,2} \sum_{j=L,R} [\psi^\dagger_{QH,\uparrow,k,j}(v^*_{i,\uparrow,k}) \left|i,-k\right\rangle - \psi_{QH,\uparrow,k,j}(u^*_{i,\uparrow,k}) \left|i,k\right\rangle] \tag{A.3}$$

- For the next term, we are not interested for extra excitation but we want to end up back in the BCS ground state. That means that the operators with negative energy will obey $\gamma_{3,k} \left|2,k\right\rangle = \gamma_{4,k} \left|1,k\right\rangle \neq 0$ (create extra excitations) but $\left\langle\Psi_{BCS}\right| \gamma_{3,k} \left|2,k\right\rangle = \left\langle\Psi_{BCS}\right| \gamma_{4,k} \left|1,k\right\rangle 0$. Thus, we neglect them in the next calculation for the simplicity not to carry them around. We have:

$$H_p \left|i'',k''\right\rangle = -t \int dk''' \sum_{j=L,R} [\psi^\dagger_{QH,\uparrow,k''',j}\psi_{SC,\uparrow,k'''} + \psi^\dagger_{SC,\uparrow,k'''}\psi_{QH,\uparrow,k''',j}] \left|i'',k''\right\rangle =$$
$$-t \int dk''' \sum_{j=L,R} [\psi^\dagger_{QH,\uparrow,k''',j}(u_{1,\uparrow,k}\gamma_{1,k'''} + v^*_{1,\uparrow,k'''}\gamma_{4,k'''} + u_{2,\uparrow,k'''}\gamma_{2,k'''} + v^*_{2,\uparrow,k'''}\gamma_{3,k'''}) \left|i'',k''\right\rangle -$$
$$\psi_{QH,\uparrow,k''',j}(u^*_{1,\uparrow,k'''}\gamma^\dagger_{1,k'''} + v_{1,\uparrow,k'''}\gamma^\dagger_{4,k'''} + u^*_{2,\uparrow,k'''}\gamma^\dagger_{2,k'''} + v_{2,\uparrow,k'''}\gamma^\dagger_{3,k'''}) \left|i'',k''\right\rangle] =$$
$$-t \int dk''' \sum_{j=L,R} [\psi^\dagger_{QH,\uparrow,k''',j}(u_{1,\uparrow,k'''}\delta_{1,i''}\delta_{k''',k''} \left|\Psi_{BCS}\right\rangle + u_{2,\uparrow,k'''}\delta_{2,i''}\delta_{k''',k''} \left|\Psi_{BCS}\right\rangle) -$$
$$\psi_{QH,\uparrow,k''',j}(v_{1,\uparrow,k'''}\delta_{1,i''}\delta_{-k''',k''} \left|\Psi_{BCS}\right\rangle + v_{2,\uparrow,k'''}\delta_{2,i''}\delta_{-k''',k''} \left|\Psi_{BCS,}\right\rangle] =$$
$$-t \int dk''' \sum_{i'''=1,2} \sum_{j=L,R} [\psi^\dagger_{QH,\uparrow,k''',j}(u_{i''',\uparrow,k'''})\delta_{i''',i''}\delta_{k''',k''} \left|\Psi_{BCS}\right\rangle -$$
$$\psi_{QH,\uparrow,k''',j}(v_{i''',\uparrow,k'''})\delta_{i''',i''}\delta_{-k''',k''} \left|\Psi_{BCS}\right\rangle] \tag{A.4}$$

We want now to put these terms in our relation for $H_{QH}^{eff}(k)$, but first let's try to simplify it a bit. We take:

$$\langle i',k'|\, H_p\, |\Psi_{BCS}\rangle = -t\,\langle i',k'|\int dk \sum_{i=1,2}\sum_{j=L,R}[\psi^{\dagger}_{QH,\uparrow,k,j}(v^{*}_{i,\uparrow,k})\,|i,-k\rangle - \psi_{QH,\uparrow,k,j}(u^{*}_{i,\uparrow,k})\,|i,k\rangle] =$$
$$-t\int dk \sum_{i=1,2}\sum_{j=L,R}[\psi^{\dagger}_{QH,\uparrow,k,j}(v^{*}_{i,\uparrow,k})\,\langle i',k'|i,-k\rangle - \psi_{QH,\uparrow,k,j}(u^{*}_{i,\uparrow,k})\,\langle i',k'|i,k\rangle =$$
$$-t\int dk \sum_{i=1,2}\sum_{j=L,R}[\psi^{\dagger}_{QH,\uparrow,k,j}(v^{*}_{i,\uparrow,k})\delta_{-k,k'}\delta_{i,i'} - \psi_{QH,\uparrow,k,j}(u^{*}_{i,\uparrow,k})\delta_{k,k'}\delta_{i,i'}] \tag{A.5}$$

The second terms that we simplify are:

$$\sum_{i'\in 1,2}\langle i'',k''|\,\frac{1}{E_{GS}-H_{BCS}(k')}\,|i',k'\rangle = \sum_{i'\in 1,2}\langle i'',k''|\,\frac{1}{E_{GS}-(E_{GS}+E_{i'}(k'))}\,|i',k'\rangle =$$
$$\sum_{i'\in 1,2}\frac{1}{-E_{i'}(k')}\,\langle i'',k''|i',k'\rangle = \sum_{i'\in 1,2}\frac{1}{-E_{i'}(k')}\delta_{i'',i'}\delta_{k'',k'} \tag{A.6}$$

Finally, the last term will be:

$$\langle \Psi_{BCS}|\, H_p\, |i'',k''\rangle = \tag{A.7}$$
$$-t\,\langle\Psi_{BCS}|\int_{-\infty}^{+\infty}dk''\int dk'''\sum_{i'''=1,2}\sum_{j=L,R}\Big(\psi^{\dagger}_{QH,\uparrow,k''',j}(u_{i''',\uparrow,k'''})\delta_{i''',i''}\delta_{k''',k''}\,|\Psi_{BCS}\rangle -$$
$$\psi_{QH,\uparrow,k''',j}(v_{i''',\uparrow,k'''})\delta_{i''',i''}\delta_{-k''',k''}\,|\Psi_{BCS}\rangle\Big) =$$
$$-t\,\langle\Psi_{BCS}|\int dk''\sum_{i''=1,2}\sum_{j=L,R}\Big(\psi^{\dagger}_{QH,\uparrow,k'',j}(u_{i'',\uparrow,k''})\,|\Psi_{BCS}\rangle - \psi_{QH,\uparrow,-k'',j}(v_{i'',\uparrow,-k''}\,|\Psi_{BCS}\rangle\Big) =$$
$$-t\int dk''\sum_{i''=1,2}\sum_{j=L,R}\Big(\psi^{\dagger}_{QH,\uparrow,k'',j}(u_{i'',\uparrow,k''})\delta_{i'',i}\delta_{k'',k} - \psi_{QH,\uparrow,-k'',j}(v_{i'',\uparrow,-k''})\delta_{i'',i}\delta_{k'',k}\Big) =$$
$$-t\int dk\sum_{i=1,2}\sum_{j=L,R}\Big(\psi^{\dagger}_{QH,\uparrow,k,j}(u_{i,\uparrow,k}) - \psi_{QH,\uparrow,-k,j}(v_{i,\uparrow,-k})\Big) \tag{A.8}$$

Putting all these terms back together, we get:

$$H_{QH}^{eff}(k) =$$

$$\langle\Psi_{BCS}| H_p \sum_{i''\in 1,2}\int_{-\infty}^{+\infty} dk'' \, |i''k''\rangle \langle i''k''| \frac{1}{E_{GS}-H_{BCS}} \sum_{i'\in 1,2}\int_{-\infty}^{+\infty} dk' \, |i'k'\rangle \langle i'k'| H_p |\Psi_{BCS}\rangle =$$

$$\left(t\int dk'' \sum_{i''=1,2}\sum_{j=L,R}[\psi^\dagger_{QH,\uparrow,k'',j}(u_{i'',\uparrow,k''})\delta_{i'',i}\delta_{k'',k} - \psi_{QH,\uparrow,-k'',j}(v_{i'',\uparrow,-k''}\delta_{i'',i}\delta_{k'',k}]\right)$$

$$\int_{-\infty}^{+\infty} dk' \sum_{i'\in 1,2}\frac{1}{-E_{i'}(k')}\delta_{i'',i'}\delta_{k'',k'}$$

$$\left(t\int dk \sum_{i=1,2}\sum_{j=L,R}[\psi^\dagger_{QH,\uparrow,k,j}(v^*_{i,\uparrow,k})\delta_{-k,k'}\delta_{i,i'} - \psi_{QH,\uparrow,k,j}(u^*_{i,\uparrow,k})\delta_{k,k'}\delta_{i,i'}]\right) =$$

$$\left(t\int dk \sum_{i=1,2}\sum_{j=L,R}\frac{1}{-E_i(k)}[\psi^\dagger_{QH,\uparrow,k,j}(u_{i,\uparrow,k}) - \psi_{QH,\uparrow,-k,j}(v_{i,\uparrow,-k})]\right)$$

$$\left(t\int dk \sum_{i=1,2}\sum_{j=L,R}[\psi^\dagger_{QH,\uparrow,-k,j}(v^*_{i,\uparrow,-k}) - \psi_{QH,\uparrow,k,j}(u^*_{i,\uparrow,k})]\right) =$$

$$\int dk \sum_{i\in 1,2}\frac{t^2}{-E_i(k)}\left(\psi^\dagger_{QH,\uparrow,k,L}(u_{i,\uparrow,k}) - \psi_{QH,\uparrow,-k,L}(v_{i,\uparrow,-k}) + \psi^\dagger_{QH,\uparrow,k,R}(u_{i,\uparrow,k}) - \psi_{QH,\uparrow,-k,R}(v_{i,\uparrow,-k})\right)$$

$$\left(\psi^\dagger_{QH,\uparrow,-k,L}(v^*_{i,\uparrow,-k}) - \psi_{QH,\uparrow,k,L}(u^*_{i,\uparrow,k}) + \psi^\dagger_{QH,\uparrow,-k,R}(v^*_{i,\uparrow,-k}) - \psi_{QH,\uparrow,k,R}(u^*_{i,\uparrow,k})\right) =$$

$$\int dk \sum_{i\in 1,2}\frac{t^2}{-E_i(k)}\Big(\psi^\dagger_{QH,\uparrow,k,L}\psi^\dagger_{QH,\uparrow,-k,L}(u_{i,\uparrow,k}v^*_{i,\uparrow,-k}) - \psi^\dagger_{QH,\uparrow,k,L}\psi_{QH,\uparrow,k,L}(u_{i,\uparrow,k}u^*_{i,\uparrow,k}) +$$

$$\psi^\dagger_{QH,\uparrow,k,L}\psi^\dagger_{QH,\uparrow,-k,R}(u_{i,\uparrow,k}v^*_{i,\uparrow,-k}) - \psi^\dagger_{QH,\uparrow,k,L}\psi_{QH,\uparrow,k,R}(u_{i,\uparrow,k}u^*_{i,\uparrow,k})$$

$$-\psi_{QH,\uparrow,-k,L}\psi^\dagger_{QH,\uparrow,-k,L}(v_{i,\uparrow,-k}v^*_{i,\uparrow,-k}) + \psi_{QH,\uparrow,-k,L}\psi_{QH,\uparrow,k,L}(v_{i,\uparrow,-k}u^*_{i,\uparrow,k})$$

$$-\psi_{QH,\uparrow,-k,L}\psi^\dagger_{QH,\uparrow,-k,R}(v_{i,\uparrow,-k}v^*_{i,\uparrow,-k}) + \psi_{QH,\uparrow,-k,L}\psi_{QH,\uparrow,k,R}(v_{i,\uparrow,-k}u^*_{i,\uparrow,k}) +$$

$$\psi^\dagger_{QH,\uparrow,k,R}\psi^\dagger_{QH,\uparrow,-k,L}(u_{i,\uparrow,k}v^*_{i,\uparrow,-k}) - \psi^\dagger_{QH,\uparrow,k,R}\psi_{QH,\uparrow,k,L}(u_{i,\uparrow,k}u^*_{i,\uparrow,k}) +$$

$$\psi^\dagger_{QH,\uparrow,k,R}\psi^\dagger_{QH,\uparrow,-k,R}(u_{i,\uparrow,k}v^*_{i,\uparrow,-k}) - \psi^\dagger_{QH,\uparrow,k,R}\psi_{QH,\uparrow,k,R}(u_{i,\uparrow,k}u^*_{i,\uparrow,k})$$

$$-\psi_{QH,\uparrow,-k,R}\psi^\dagger_{QH,\uparrow,-k,L}(v_{i,\uparrow,-k}v^*_{i,\uparrow,-k}) + \psi_{QH,\uparrow,-k,R}\psi_{QH,\uparrow,k,L}(v_{i,\uparrow,-k}u^*_{i,\uparrow,k})$$

$$-\psi_{QH,\uparrow,-k,R}\psi^\dagger_{QH,\uparrow,-k,R}(v_{i,\uparrow,-k}v^*_{i,\uparrow,-k}) + \psi_{QH,\uparrow,-k,R}\psi_{QH,\uparrow,k,R}(v_{i,\uparrow,-k}u^*_{i,\uparrow,k})\Big) \tag{A.9}$$

where we have used the fact that $H_{BCS}\,|i,k\rangle = (E_{GS}+E_i)\,|i,k\rangle$ and from the particle-hole symmetry $E_i(k) = E_i(-k)$. The E_{GS} is considered to be the energy where every energy band is filled.

A.3 Supplementary for the Feynman Path Integral Formalism

In this Appendix, we present the derivation in the various calculations we performed during the Feynman Path Integral formalism. First we begin by manipulating a little bit the action in eq. (2.62). That way, the path integral over superconducting fields is a Gaussian integral with exponent:

$$
\begin{aligned}
&S_{SC}[\overline{\Psi},\Psi]+S_{QH}[\overline{\Phi},\Phi]+S_t[\overline{\Psi},\Psi,\overline{\Phi},\Phi]= \\
&\int\frac{d\omega}{2\pi}\int dk\left[\overline{\Psi}\tilde{H}_{SC}\Psi+\overline{\Psi}T\Phi+\overline{\Phi}T^{\dagger}\Psi+\overline{\Phi}\tilde{H}_{QH}\Phi\right]= \\
&\int\frac{d\omega}{2\pi}\int dk\left[\left(\overline{\Psi}\tilde{H}_{SC}^{1/2}+\overline{\Phi}T^{\dagger}\tilde{H}_{SC}^{-1/2}\right)\left(\tilde{H}_{SC}^{1/2}\Psi+\tilde{H}_{SC}^{-1/2}T\Phi\right)+\overline{\Phi}\tilde{H}_{QH}\Phi-\overline{\Phi}T^{\dagger}\tilde{H}_{SC}^{-1}T\Phi\right]= \\
&\int\frac{d\omega}{2\pi}\int dk\left[\left(\overline{\Psi}+\overline{\Phi}T^{\dagger}\tilde{H}_{SC}^{-1}\right)\tilde{H}_{SC}^{1/2}\left(\tilde{H}_{SC}^{1/2}\Psi+\tilde{H}_{SC}^{-1/2}T\Phi\right)+\overline{\Phi}\tilde{H}_{QH}\Phi-\overline{\Phi}T^{\dagger}\tilde{H}_{SC}^{-1}T\Phi\right]= \\
&\int\frac{d\omega}{2\pi}\int dk\left[\left(\overline{\Psi}+\overline{\Phi}T^{\dagger}\tilde{H}_{SC}^{-1}\right)\tilde{H}_{SC}\left(\Psi+\tilde{H}_{SC}^{-1}T\Phi\right)+\overline{\Phi}\tilde{H}_{QH}\Phi-\overline{\Phi}T^{\dagger}\tilde{H}_{SC}^{-1}T\Phi\right]
\end{aligned}
\tag{A.10}
$$

where the $\tilde{H}_{SC}^{-1}$ can be calculated analytically as follows:

$$
\begin{aligned}
&\tilde{H}_{SC}^{-1}=\frac{1}{i\omega-H_{SC}}=\frac{1}{i\omega-\xi_k\tau_z-\alpha k\sigma_y\tau_z-\tilde{B}\sigma_z+\Delta\tau_x}= \\
&\frac{i\omega+\xi_k\tau_z+\alpha k\sigma_y\tau_z-\tilde{B}\sigma_z-\Delta\tau_x}{(i\omega-\xi_k\tau_z-\alpha k\sigma_y\tau_z-\tilde{B}\sigma_z+\Delta\tau_x)(i\omega+\xi_k\tau_z+\alpha k\sigma_y\tau_z-\tilde{B}\sigma_z-\Delta\tau_x)}= \\
&\frac{(i\omega-\tilde{B}\sigma_z)+(\xi_k+\alpha k\sigma_y)\tau_z-\Delta\tau_x}{((i\omega-\tilde{B}\sigma_z)-(\xi_k+\alpha k\sigma_y)\tau_z+\Delta\tau_x)((i\omega-\tilde{B}\sigma_z)+(\xi_k+\alpha k\sigma_y)\tau_z-\Delta\tau_x)}= \\
&\frac{(i\omega-\tilde{B}\sigma_z)+(\xi_k+\alpha k\sigma_y)\tau_z-\Delta\tau_x}{(i\omega-\tilde{B}\sigma_z)^2-(\xi_k+\alpha k\sigma_y)^2-\Delta^2}= \\
&\frac{(i\omega-\tilde{B}\sigma_z)+(\xi_k+\alpha k\sigma_y)\tau_z-\Delta\tau_x}{-\omega^2+\tilde{B}^2-2i\omega\tilde{B}\sigma_z-\xi_k^2-(\alpha k)^2-2\xi_k\alpha k\sigma_y-\Delta^2}= \\
&\frac{((i\omega-\tilde{B}\sigma_z)+(\xi_k+\alpha k\sigma_y)\tau_z-\Delta\tau_x)((-\omega^2-\xi_k^2-(\alpha k)^2+\tilde{B}^2-\Delta^2)+2i\omega\tilde{B}\sigma_z+2\xi_k\alpha k\sigma_y)}{((-\omega^2-\xi_k^2-(\alpha k)^2+\tilde{B}^2-\Delta^2)-2i\omega\tilde{B}\sigma_z-2\xi_k\alpha k\sigma_y)((-\omega^2-\xi_k^2-(\alpha k)^2+\tilde{B}^2-\Delta^2)+2i\omega\tilde{B}\sigma_z+2\xi_k\alpha k\sigma_y)} \\
&=\frac{((i\omega-\tilde{B}\sigma_z)+(\xi_k+\alpha k\sigma_y)\tau_z-\Delta\tau_x)((-\omega^2-\xi_k^2-(\alpha k)^2+\tilde{B}^2-\Delta^2)+2i\omega\tilde{B}\sigma_z+2\xi_k\alpha k\sigma_y)}{(-\omega^2-\xi_k^2-(\alpha k)^2+\tilde{B}^2-\Delta^2)^2-(2i\omega\tilde{B})^2-(2\xi_k\alpha k)^2}
\end{aligned}
\tag{A.11}
$$

By performing the calculations on the numerator $\mathcal{N}$ and the denominator $\mathcal{D}$, we end up with the

expressions:

$$\mathcal{N} = \Big[i\omega\Big((-\omega^2 - \xi_k^2 - (\alpha k)^2 + \tilde{B}^2 - \Delta^2) - 2\tilde{B}^2\Big) - \tilde{B}(2\omega^2 + (-\omega^2 - \xi_k^2 - (\alpha k)^2 + \tilde{B}^2 - \Delta^2))\sigma_z + 2i\omega\xi_k\alpha k\sigma_y + 2i\xi_k\alpha k\tilde{B}\sigma_x\Big] + \Big[-\Delta(-\omega^2 - \xi_k^2 - (\alpha k)^2 + \tilde{B}^2 - \Delta^2) - 2\xi_k\alpha k\Delta\sigma_y - 2i\omega\tilde{B}\Delta\sigma_z\Big]\tau_x + \Big(\xi_k(-\omega^2 - \xi_k^2 - (\alpha k)^2 + \tilde{B}^2 - \Delta^2) + (2i\xi_k(\alpha k)^2 - 2\omega\alpha\tilde{B})\sigma_x + \big(\alpha k(-\omega^2 - \xi_k^2 - (\alpha k)^2 + \tilde{B}^2 - \Delta^2) + 2\xi_k^2\alpha k\big)\sigma_y + 2i\omega\xi_k\tilde{B}\sigma_z\Big)\tau_z \tag{A.12}$$

and

$$\mathcal{D} = \omega^4 + \xi_k^4 + (\alpha k)^4 + \tilde{B}^4 + \Delta^4 + 2\omega^2(\xi_k^2 + (\alpha k)^2 + \tilde{B}^2 + \Delta^2) + 2\tilde{B}^2(-\xi_k^2 + (\alpha k)^2 - \Delta^2) + 2(\alpha k)^2(-\xi_k^2 + \Delta^2) + 2\xi_k^2\Delta^2 \tag{A.13}$$

It is worth noting (for reasons that will be obvious later), that the denominator $\mathcal{D}$ can be written as:

$$\tilde{\mathcal{D}} = (i\omega - E_1)(i\omega - E_2)(i\omega - E_3)(i\omega - E_4) = (\omega^2 + E_1^2)(\omega^2 + E_2^2) = \mathcal{D} \tag{A.14}$$

By performing the above calculations we end up to the same result.

Next, we present the results of the analytical methods trying to estimate the result of eq. (2.84). We start by finding the poles of eq. (A.14), where it is easily to see that the poles are:

$$\omega_1 = +iE_1, \quad \omega_2 = -iE_1, \quad \omega_3 = +iE_2, \quad \omega_4 = -iE_2 \tag{A.15}$$

The residues for each pole are:

- For $\omega_1 = +iE_1$, we have:

$$res\left(\frac{1}{\mathcal{D}(\omega)}, \omega_1\right) = \lim_{\omega\to\omega_1}\frac{(\omega - \omega_1)}{\mathcal{D}(\omega)} = \lim_{\omega\to\omega_1}\frac{(\omega - iE_1)}{(\omega + iE_1)(\omega - iE_1)(\omega^2 + E_2^2)} = \lim_{\omega\to\omega_1}\frac{1}{(\omega + iE_1)(\omega^2 + E_2^2)} = \frac{1}{(iE_1 + iE_1)(-E_1^2 + E_2^2)} = \frac{1}{2iE_1(E_2^2 - E_1^2)} = \frac{-i}{2E_1(E_2^2 - E_1^2)} \tag{A.16}$$

- For $\omega_2 = -iE_1$, we have:

$$res\left(\frac{1}{\mathcal{D}(\omega)}, \omega_2\right) = \lim_{\omega\to\omega_2} \frac{(\omega-\omega_2)}{\mathcal{D}(\omega)} = \lim_{\omega\to\omega_2} \frac{(\omega+iE_1)}{(\omega+iE_1)(\omega-iE_1)(\omega^2+E_2^2)} = \lim_{\omega\to\omega_2} \frac{1}{(\omega-iE_1)(\omega^2+E_2^2)} = \frac{1}{(-iE_1-iE_1)(-E_1^2+E_2^2)} = \frac{1}{-2iE_1(E_2^2-E_1^2)} = \frac{i}{2E_1(E_2^2-E_1^2)} \tag{A.17}$$

- For $\omega_3 = +iE_2$, we have:

$$res\left(\frac{1}{\mathcal{D}(\omega)}, \omega_3\right) = \lim_{\omega\to\omega_3} \frac{(\omega-\omega_3)}{\mathcal{D}(\omega)} = \lim_{\omega\to\omega_3} \frac{(\omega-iE_2)}{(\omega+iE_2)(\omega-iE_2)(\omega^2+E_1^2)} = \lim_{\omega\to\omega_3} \frac{1}{(\omega+iE_2)(\omega^2+E_1^2)} = \frac{1}{(iE_2+iE_2)(-E_2^2+E_1^2)} = \frac{1}{2iE_2(E_1^2-E_2^2)} = \frac{1}{-2iE_2(E_2^2-E_1^2)} = \frac{i}{2E_2(E_2^2-E_1^2)} \tag{A.18}$$

- For $\omega_4 = -iE_2$, we have:

$$res\left(\frac{1}{\mathcal{D}(\omega)}, \omega_4\right) = \lim_{\omega\to\omega_4} \frac{(\omega-\omega_4)}{\mathcal{D}(\omega)} = \lim_{\omega\to\omega_4} \frac{(\omega+iE_2)}{(\omega+iE_2)(\omega-iE_2)(\omega^2+E_1^2)} = \lim_{\omega\to\omega_4} \frac{1}{(\omega-iE_2)(\omega^2+E_1^2)} = \frac{1}{(-iE_2-iE_2)(-E_2^2+E_1^2)} = \frac{1}{-2iE_2(E_1^2-E_2^2)} = \frac{1}{2iE_2(E_2^2-E_1^2)} = \frac{-i}{2E_2(E_2^2-E_1^2)} \tag{A.19}$$

Putting now also the exponential term $e^{-i\omega(t_2-t_1)}$, we proceed by evaluating each term of the B matrix in a closed contour $\mathcal{C}$. For that purpose, we perform now the calculations in a closed contour $\mathcal{C}_1$ where it contains the singularities of the lower half-plane. The reason we choose this half for our integration is because we assume $t_2 > t_1$ and in order for our exponential term to be convergent we need to replace $\omega = -iE_n$ so that we will get $e^{-i\omega(t_2-t_1)} = e^{-E_n(t_2-t_1)}$ which will ensure that our integral is convergent. We also have to take into account if the terms $\frac{B_{ij}}{\mathcal{D}(\omega)}$ are also convergent. They will be convergent if and only if they depend on $\frac{B_{ij}}{\mathcal{D}(\omega)} \propto \frac{1}{|\omega|^a}$ with $a > 1$.This is easy to see, because $\int dx \frac{1}{x} = log(x)$, and the logarithm is a divergent function. Hence,going back to the residue theorem, we get:

- For the term B_{11}:

$$\oint_{\mathcal{C}_1} \frac{B_{11}e^{-i\omega(t_2-t_1)}}{\mathcal{D}(\omega)}d\omega = 2\pi i \sum_{n=2,4} res\left(\frac{B_{11}e^{-i\omega(t_2-t_1)}}{\mathcal{D}(\omega)}, \omega_n\right) =$$
$$2\pi i\left[res\left(\frac{B_{11}e^{-i\omega(t_2-t_1)}}{\mathcal{D}(\omega)}, \omega_2\right) + res\left(\frac{B_{11}e^{-i\omega(t_2-t_1)}}{\mathcal{D}(\omega)}, \omega_4\right)\right] =$$
$$2\pi i(-i)\left[-\frac{e^{E_1(t_2-t_1)}(E_1^3 - E_1^2C_1 + E_1C_2 + C_3)}{2E_1(E_2^2 - E_1^2)} + \frac{e^{E_2(t_2-t_1)}(E_2^3 - E_2^2C_1 + E_2C_2 + C_3)}{2E_2(E_2^2 - E_1^2)}\right] \tag{A.20}$$

- For the term B_{12}:

$$\oint_{\mathcal{C}_1} \frac{B_{12}e^{-i\omega(t_2-t_1)}}{\mathcal{D}(\omega)}d\omega = 2\pi i \sum_{n=2,4} res\left(\frac{B_{12}e^{-i\omega(t_2-t_1)}}{\mathcal{D}(\omega)}, \omega_n\right) =$$
$$2\pi i\left[res\left(\frac{B_{12}e^{-i\omega(t_2-t_1)}}{\mathcal{D}(\omega)}, \omega_2\right) + res\left(\frac{B_{12}e^{-i\omega(t_2-t_1)}}{\mathcal{D}(\omega)}, \omega_4\right)\right] =$$
$$2\pi i B_{12}\left[\frac{-ie^{-E_1(t_2-t_1)}}{2E_1(E_2^2 - E_1^2)} + \frac{ie^{-E_2(t_2-t_1)}}{2E_2(E_2^2 - E_1^2)} + \right] =$$
$$2\pi i B_{12}(-i)\left[-\frac{e^{-E_1(t_2-t_1)}}{2E_1(E_2^2 - E_1^2)} + \frac{e^{-E_2(t_2-t_1)}}{2E_2(E_2^2 - E_1^2)} =\right.$$
$$2\pi B_{12}\left[-\frac{e^{-E_1(t_2-t_1)}}{2E_1(E_2^2 - E_1^2)} + \frac{e^{-E_2(t_2-t_1)}}{2E_2(E_2^2 - E_1^2)}\right] \tag{A.21}$$

- Similar we get the terms B_{22} and B_{21}.

As we said before, we are interested in finding the local term in time. This means that we will take in the above relations the condition $t_2 = t_1$, which will effect the term $e^0 = 1$ Calculating again each term separately, we get:

- For the diagonal term B_{11} in $t_2 = t_1$:

$$\frac{2\pi}{2(E_2^2 - E_1^2)}\left[-\frac{E_1^3 - E_1^2C_1 + E_1C_2 + C_3}{E_1} + \frac{E_2^3 - E_2^2C_1 + E_2C_2 + C_3}{E_2}\right] =$$
$$\frac{2\pi}{2(E_2^2 - E_1^2)}\left[-E_1^2 + E_1C_1 - C_2 - \frac{C_3}{E_1} + E_2^2 - E_2C_1 + C_2 + \frac{C_3}{E_2}\right] =$$
$$\pi - \frac{\pi C_1}{E_2 + E_1} - \frac{C_3}{E_1E_2(E_2 + E_1)} \tag{A.22}$$

- For the off-diagonal term B_{12} in $t_2 = t_1$:

$$\frac{2\pi B_{12}}{2(E_2^2 - E_1^2)}\left[-\frac{1}{E_1} + \frac{1}{E_2}\right] = \frac{2\pi B_{12}}{2(E_2^2 - E_1^2)}\left[-\frac{E_2}{E_2 E_1} + \frac{E_1}{E_1 E_2}\right] = \frac{2\pi B_{12}}{2(E_2^2 - E_1^2)}\left[\frac{E_1 - E_2}{E_2 E_1}\right] = \frac{-\pi B_{12}}{E_2 E_1 (E_2 + E_1)} \tag{A.23}$$

Our next step is to apply again the Residue theorem but this time we want integrate out the dependence in momentum k. Before proceeding with the calculation on the integral, we need to make sure that these integrals are well defined, i.e that they converge. As before, we assume $r_2 > r_1$ and the exponential $e^{-ik(r_2 - r_1)}$ converges. The important part will be to check if the terms we calculated above are analytical. We know from mathematics that an analytical function f(x) is analytic in a region $\mathcal{R}$, if it has a derivative at each point of $\mathcal{R}$ and if f(x) is single valued. Furthermore, the summation and a product of 2 analytic functions remains analytic. Our eigenvalues E_1 and E_2 follow these rules. This means that the whole integral in real space converges. But is not hard to see that trying to perform these integrals even computationally one encounters some difficulties and can not get an analytical result. Luckily for us, we are physicists and not mathematicians which means that in order to overcome these difficulties we do not have to integrate all the momentum space. For our case, the frame of interest is a small window around the Fermi momentum $k_{f,QH}$. By changing the integration over k to a summation we are able to keep only the values of interested and "throw out" the rest of them. We are interested in the terms that give the induced superconductivity, i.e the off-diagonal terms in the previous calculations. The result for the off-diagonal term B_{12} (by taking also $x_2 = x_1$, local in space) is now:

$$\frac{-\pi B_{12}}{E_2 E_1 (E_2 + E_1)} \tag{A.24}$$

where in the above expression we replace the momentum k with $k_{f,QH}$. Next, we perform a Taylor expansion in the above expressions in terms of Δ, where we assume it weak, but still have in mind that we have weak tunneling $\Delta \gg t$.

As we can see from the result we have

$$\Delta_{ind} \propto \alpha^2 t^2 \Delta. \tag{A.25}$$

B Appendix

In this Appendix we will show some of the explicit calculations during the bosonization procedure.

B.1 Bosonized form of the terms

B.2 Bosonized form of magnetic pairing

First, we calculate the magnetic pairing terms and show that all of them are Fast-Oscillating terms. We have:

$$H_{\tilde{B}} = \tilde{B}(\psi_+^\dagger(x)\psi_-(x) \; + \; H.C) = \\ \tilde{B}\Big(\big(\psi_{L,1}^\dagger(x) + \psi_{R,1}^\dagger(x)\big)\big(\psi_{L,2}(x) + \psi_{R,2}(x)\big) \;\; + \;\; H.C\Big) \tag{B.1}$$

where we have:

- For the term $\psi_{L,1}^\dagger(x)\psi_{L,2}(x) + \psi_{L,2}^\dagger(x)\psi_{L,1}(x)$:

$$\psi_{L,1}^\dagger(x)\psi_{L,2}(x) + \psi_{L,2}^\dagger(x)\psi_{L,1}(x) \\ = \frac{1}{4\pi}e^{2i\alpha x}\Big(\mathcal{C}_{+,+1,-1}\mathcal{C}_{+,+1,+1}(1 - i\epsilon[\partial_x\phi_+(x) + \partial_x\theta_+(x)])e^{\frac{i\pi}{2}} + \mathcal{C}_{-,+1,-1}\mathcal{C}_{-,+1,+1} \\ -\mathrm{k}_+\mathrm{k}_-\mathcal{C}_{+,+1,-1}\mathcal{C}_{-,+1,+1}e^{-i\sqrt{2}(\phi_s(x)+\theta_s(x))} + \mathrm{k}_+\mathrm{k}_-\mathcal{C}_{-,+1,-1}\mathcal{C}_{+,+1,+1}e^{i\sqrt{2}(\phi_s(x)+\theta_s(x))}\Big) \\ +\frac{1}{4\pi}e^{-2i\alpha x}\Big(\mathcal{C}_{+,+1,-1}\mathcal{C}_{+,+1,+1}(1 - i\epsilon[\partial_x\phi_-(x) + \partial_x\theta_-(x)])e^{\frac{i\pi}{2}} + \mathcal{C}_{-,+1,-1}\mathcal{C}_{-,+1,+1} \\ +\mathrm{k}_+\mathrm{k}_-\mathcal{C}_{+,+1,-1}\mathcal{C}_{-,+1,+1}e^{i\sqrt{2}(\phi_s(x)+\theta_s(x))} - \mathrm{k}_+\mathrm{k}_-\mathcal{C}_{-,+1,-1}\mathcal{C}_{+,+1,+1}e^{-i\sqrt{2}(\phi_s(x)+\theta_s(x))}\Big) \tag{B.2}$$

- For the term $\psi^{\dagger}_{R,1}(x)\psi_{R,2}(x)+\psi^{\dagger}_{R,2}(x)\psi_{R,1}(x)$:

$$\begin{aligned}
&\psi^{\dagger}_{R,1}(x)\psi_{R,2}(x)+\psi^{\dagger}_{R,2}(x)\psi_{R,1}(x)\\
&=\frac{1}{4\pi}e^{-2i\alpha x}\Big(\mathcal{C}_{+,-1,-1}\mathcal{C}_{+,-1,+1}(1-i\epsilon[\partial_x\phi_+(x)-\partial_x\theta_+(x)])e^{-\frac{i\pi}{2}}+\mathcal{C}_{-,-1,-1}\mathcal{C}_{-,-1,+1}\\
&-\mathrm{k}_+\mathrm{k}_-\mathcal{C}_{+,-1,-1}\mathcal{C}_{-,-1,+1}e^{-i\sqrt{2}(\phi_s(x)-\theta_s(x))}+\mathrm{k}_+\mathrm{k}_-\mathcal{C}_{-,-1,-1}\mathcal{C}_{+,-1,+1}e^{i\sqrt{2}(\phi_s(x)-\theta_s(x))}\Big)+\\
&\frac{1}{4\pi}e^{2i\alpha x}\Big(\mathcal{C}_{+,-1,-1}\mathcal{C}_{+,-1,+1}(1-i\epsilon[\partial_x\phi_-(x)-\partial_x\theta_-(x)])e^{\frac{-i\pi}{2}}+\mathcal{C}_{-,-1,-1}\mathcal{C}_{-,-1,+1}\\
&+\mathrm{k}_+\mathrm{k}_-\mathcal{C}_{+,-1,-1}\mathcal{C}_{-,-1,+1}e^{i\sqrt{2}(\phi_s(x)-\theta_s(x))}-\mathrm{k}_+\mathrm{k}_-\mathcal{C}_{-,-1,-1}\mathcal{C}_{+,-1,+1}e^{-i\sqrt{2}(\phi_s(x)-\theta_s(x))}\Big)
\end{aligned}\tag{B.3}$$

where in the above calculations we used the fact that:

$$\begin{aligned}
&\psi^{\dagger}_{L,1,+}(x+\epsilon)\psi_{L,2,+}(x)\sim e^{2i\alpha x}e^{-i(\phi_+(x+\epsilon)+\theta_+(x+\epsilon))}e^{i(\phi_+(x)+\theta_+(x))}=\\
&e^{2i\alpha x}e^{-i(\phi_+(x+\epsilon)+\theta_+(x+\epsilon)-\phi_+(x)-\theta_+(x))+\frac{1}{2}[\theta_+(x+\epsilon),\phi_+(x)]}=\\
&e^{2i\alpha x}e^{-i(\phi_+(x)+\theta_+(x)+\epsilon[\partial_x\phi_+(x)+\partial_x\theta_+(x)]-\phi_+(x)-\theta_+(x))+\frac{i\pi}{2}}=e^{2i\alpha x}e^{+\frac{i\pi}{2}}(1-i\epsilon[\partial_x\phi_+(x)+\partial_x\theta_+(x)]
\end{aligned}\tag{B.4}$$

with $\epsilon>0$ and small. In the first equality we used the CBH formula, then we Taylor expand the bosonic fields and then we Taylor expand again the exponential. Similar for the rest of the terms where the ϕ,θ fields tend to vanish.

- For the term $\psi^{\dagger}_{L,1}(x)\psi_{R,2}(x)+\psi^{\dagger}_{R,2}(x)\psi_{L,1}(x)$:

$$\begin{aligned}
&\psi^{\dagger}_{L,1}(x)\psi_{R,2}(x)+\psi^{\dagger}_{R,2}(x)\psi_{L,1}(x)\\
&=\frac{1}{4\pi}e^{2i(k_{SC,F}+\alpha)x}\Big(\mathcal{C}^2_{+,-1,+1}e^{-2i\theta_+(x)}+\mathcal{C}^2_{-,-1,+1}e^{-2i\theta_-(x)}\\
&+2\mathrm{k}_+\mathrm{k}_-\mathcal{C}_{+,-1,+1}\mathcal{C}_{-,-1,+1}\cos\left(\sqrt{2}(\phi_s(x)-\theta_c(x))\right)\Big)\\
&+\frac{1}{4\pi}e^{-2i(k_{SC,F}+\alpha)x}\Big(-\mathcal{C}^2_{+,-1,+1}e^{2i\theta_+(x)}+\mathcal{C}^2_{-,-1,+1}e^{2i\theta_-(x)}\\
&-2\mathrm{k}_+\mathrm{k}_-\mathcal{C}_{+,-1,+1}\mathcal{C}_{-,-1,+1}\cos\left(\sqrt{2}(\phi_s(x)-\theta_c(x))\right)\Big)
\end{aligned}\tag{B.5}$$

- For the term $\psi^{\dagger}_{R,1}(x)\psi_{L,2}(x)+\psi^{\dagger}_{L,2}(x)\psi_{R,1}(x)$:

$$\begin{aligned}
&\psi^{\dagger}_{R,1}(x)\psi_{L,2}(x)+\psi^{\dagger}_{L,2}(x)\psi_{R,1}(x)\\
&=\frac{1}{4\pi}e^{-2i(k_{SC,F}-\alpha)x}\Big(-\mathcal{C}^2_{+,-1,-1}e^{2i\theta_+(x)}+\mathcal{C}^2_{-,-1,-1}e^{2i\theta_-(x)}\\
&\quad -2\mathrm{k}_+\mathrm{k}_-\mathcal{C}_{+,-1,-1}\mathcal{C}_{,-1,-1}\cos\left(\sqrt{2}(\phi_s(x)-\theta_c(x))\right)\Big)\\
&+\frac{1}{4\pi}e^{2i(k_{SC,F}+\alpha)x}\Big(-\mathcal{C}^2_{+,-1,-1}e^{-2i\theta_+(x)}+\mathcal{C}^2_{-,-1,-1}e^{-2i\theta_-(x)}\\
&\quad +2\mathrm{k}_+\mathrm{k}_-\mathcal{C}_{+,-1,-1}\mathcal{C}_{-,-1,-1}\cos\left(\sqrt{2}(\phi_s(x)-\theta_c(x))\right)\Big)
\end{aligned}\tag{B.6}$$

It is easy to see that all the above terms are Fast Oscillating (for $k_{SC,F}\neq\pm\alpha$), thus we can neglect them.

B.3 Bosonized form of superconducting pairing

Our next step is to calculate the Δ pairing term which couples terms with different spin between the modes:

$$H_{\Delta}=-\Delta(\psi^{\dagger}_{L,1}(x)\psi^{\dagger}_{R,2}(x)+\psi^{\dagger}_{R,1}(x)\psi^{\dagger}_{L,2}(x)\ +\ H.C)\tag{B.7}$$

where we have:

- For the term $\psi^{\dagger}_{L,1}(x)\psi^{\dagger}_{R,2}(x)$:

$$\begin{aligned}
&\psi^{\dagger}_{L,1}(x)\psi^{\dagger}_{R,2}(x)=\\
&\frac{1}{\sqrt{4\pi}}e^{i(k_{SC,F}+\alpha)x}\left[\mathrm{k}_+\mathcal{C}_{+,+1,-1}e^{-i(\phi_+(x)+\theta_+(x))}-\mathrm{k}_-\mathcal{C}_{-,+1,-1}e^{-i(\phi_-(x)+\theta_-(x))}\right]\\
&\frac{1}{\sqrt{4\pi}}e^{-i(k_{SC,F}+\alpha)x}\left[\mathrm{k}_+\mathcal{C}_{+,-1,+1}e^{-i(\phi_+(x)-\theta_+(x))}-\mathrm{k}_-\mathcal{C}_{,-1,+1}+e^{-i(\phi_-(x)-\theta_-(x))}\right]=\\
&\frac{1}{4\pi}\Big[-\mathrm{k}_+\mathrm{k}_-\mathcal{C}_{+,+1,-1}\mathcal{C}_{-,-1,+1}e^{-i(\phi_+(x)+\theta_+(x))}e^{-i(\phi_-(x)-\theta_-(x))}\\
&-\mathrm{k}_-\mathrm{k}_+\mathcal{C}_{+,-1,+1}\mathcal{C}_{-,+1,-1}e^{-i(\phi_-(x)+\theta_-(x))}e^{-i(\phi_+(x)-\theta_+(x))}=\\
&\frac{1}{4\pi}\Big[+\mathrm{k}_+\mathrm{k}_-\mathcal{C}_{+,-1,+1}\mathcal{C}_{-,-1,+1}e^{-i\sqrt{2}(\phi_c(x)+\theta_s(x))}\\
&+\mathrm{k}_+\mathrm{k}_-\mathcal{C}_{+,-1,+1}\mathcal{C}_{-,-1,+1}e^{-i\sqrt{2}(\phi_c(x)-\theta_s(x))}\Big]
\end{aligned}\tag{B.8}$$

- For the term $\psi_{R,2}(x)\psi_{L,1}(x)$:

$$\psi^{\dagger}_{L,1}(x)\psi^{\dagger}_{R,2}(x) =$$
$$\frac{1}{\sqrt{4\pi}}e^{i(k_{SC,F}+\alpha)x}\Big[\mathrm{k}_{+}\mathcal{C}_{+,-1,+1}e^{i(\phi_{+}(x)-\theta_{+}(x))} - \mathrm{k}_{-}\mathcal{C}_{-,-1,+1} + e^{i(\phi_{-}(x)-\theta_{-}(x))}\Big]$$
$$\frac{1}{\sqrt{4\pi}}e^{-i(k_{SC,F}+\alpha)x}\Big[\mathrm{k}_{+}\mathcal{C}_{+,+1,-1}e^{i(\phi_{+}(x)+\theta_{+}(x))} - \mathrm{k}_{-}\mathcal{C}_{-,+1,-1}e^{i(\phi_{-}(x)+\theta_{-}(x))}\Big] =$$
$$\frac{1}{4\pi}\Big[- \mathrm{k}_{+}\mathrm{k}_{-}\mathcal{C}_{+,-1,+1}\mathcal{C}_{-,+1,-1}e^{i(\phi_{-}(x)-\theta_{-}(x))}e^{i(\phi_{+}(x)+\theta_{+}(x))}$$
$$-\mathrm{k}_{-}\mathrm{k}_{+}\mathcal{C}_{-,-1,+1}\mathcal{C}_{+,+1,-1}e^{i(\phi_{+}(x)-\theta_{+}(x))}e^{i(\phi_{-}(x)+\theta_{-}(x))} =$$
$$\frac{1}{4\pi}\Big[- \mathrm{k}_{+}\mathrm{k}_{-}\mathcal{C}_{+,-1,+1}\mathcal{C}_{-,-1,+1}e^{i\sqrt{2}(\phi_{c}(x)+\theta_{s}(x))}$$
$$-\mathrm{k}_{+}\mathrm{k}_{-}\mathcal{C}_{+,-1,+1}\mathcal{C}_{-,-1,+1}e^{i\sqrt{2}(\phi_{c}(x)-\theta_{s}(x))}\Big] \tag{B.9}$$

- Similar for the terms $\psi^{\dagger}_{R,1}(x)\psi^{\dagger}_{L,2}(x) \; + \; H.c.$

Putting everything back together, will result to:

$$H_{\Delta} = -\Delta(\psi^{\dagger}_{L,1}(x)\psi^{\dagger}_{R,2}(x) + \psi^{\dagger}_{R,1}(x)\psi^{\dagger}_{L,2}(x) \; + \; H.C) =$$
$$i\mathrm{k}_{+}\mathrm{k}_{-}\frac{\Delta}{\pi\tilde{\alpha}}\Big(\mathcal{C}_{+,L,-1}\mathcal{C}_{-,L,-1} + \mathcal{C}_{+,R,+1}\mathcal{C}_{-,R,+1}\Big)\Big[\sin\big(\sqrt{2}(\phi_{c}(x)+\theta_{s}(x))\big) + \sin\big(\sqrt{2}(\phi_{c}(x)-\theta_{s}(x))\big)\Big] \tag{B.10}$$

To derive the above calculations we use some trigonometric identities, the commutation relations between the dual fields and the anti-commutation relations between the klein factors as defined in the main text. Furthermore, use made use of the the Baker Campbell Hausdorff formula (BCH) for 2 operators A and B:

$$e^{A}e^{B} = e^{A+B+\frac{1}{2}[A,B]} \tag{B.11}$$

to calculate our vortex operators.

B.4 Bosonized form of tunneling pairing

Here, we will calculate the bosonized description of our tunneling Hamiltonian:

$$H_{t}(x) = -t\sum_{j=L,R}[\psi^{\dagger}_{FQH,\uparrow,j}(x)\psi_{SC,\uparrow}(x) + H.C] \approx$$
$$\frac{-t}{\sqrt{2\pi}}\int dx\Big[\sum_{\eta'=L,R}\psi_{\eta'}(x)\sum_{\eta=L,R}\sum_{j=1,2}\psi^{-}_{\eta,j}(x) + H.C\Big] \tag{B.12}$$

where as we noted in the main text, we replace the terms $\mathcal{C}_{\sigma,\eta,j} = \mathcal{C}_{\sigma,\eta,-\sigma}$, because the spin the Rashba coefficient is locked with the spin now and the terms with $\mathcal{C}_{\sigma,\eta,\sigma}$ are consider small corrections when $\tilde{B} \neq 0$. Furthermore, we are gonna make use of the property $\mathcal{C}_{+,\eta,-sigma}(-k) = \mathcal{C}_{-,\eta,-sigma}(-k)$ (which is easy to check that it is true). By calculating each term explicitly and by starting from the term $\sum_{j=L,R} \psi^{\dagger}_{FQH,\uparrow,j}(x)\psi_{SC,\uparrow}(x)$, we get

- For the L,1 mode, we have:

$$\sum_{j=L,R} \psi^{\dagger}_{FQH,\uparrow,j}(x)\psi_{L1,\uparrow}(x) = \mathrm{k}_{FQH,\uparrow}\Big(e^{ik_{FQH,F}x}e^{-i(\phi'(x)+\theta'(x))} + e^{-ik_{FQH,F}x}e^{-i(\phi'(x)-\theta'(x))}\Big)$$
$$\frac{1}{\sqrt{4\pi}}e^{i(-k_{SC,F}-\alpha)x}\Big[\mathrm{k}_{Sc,+}\mathcal{C}_{+,+1,-1}e^{i(\phi^{SC}_{+}(x)+\theta^{SC}_{+}(x))} - \mathrm{k}_{Sc,-}\mathcal{C}_{-,+1,-1}e^{i(\phi^{SC}_{-}(x)+\theta^{SC}_{-}(x))}\Big]$$
$$= \frac{\mathrm{k}_{FQH,\uparrow}\mathrm{k}_{Sc,+}}{\sqrt{4\pi}}\mathcal{C}_{+,+1,-1}\big[e^{i(k_{FQH,F}-k_{SC,F}-\alpha)x}e^{-i(3\phi(x)+\theta(x)-\phi^{SC}_{+}(x)-\theta^{SC}_{+}(x))}$$
$$+e^{-i(k_{FQH,F}+k_{SC,F}+\alpha)x}e^{-i(3\phi(x)-\theta(x)-\phi^{SC}_{+}(x)-\theta^{SC}_{+}(x))}\big]$$
$$-\frac{\mathrm{k}_{FQH,\uparrow}\mathrm{k}_{Sc,-}}{\sqrt{4\pi}}\mathcal{C}_{-,+1,-1}\big[e^{i(k_{FQH,F}-k_{SC,F}-\alpha)x}e^{-i(3\phi(x)+\theta(x)-\phi^{SC}_{-}(x)-\theta^{SC}_{-}(x))}+$$
$$e^{-i(k_{FQH,F}+k_{SC,F}+\alpha)x}e^{-i(3\phi(x)-\theta(x)-\phi^{SC}_{-}(x)-\theta^{SC}_{-}(x))}\big] =$$
$$\frac{\mathrm{k}_{FQH,\uparrow}\mathrm{k}_{Sc,+}}{\sqrt{4\pi}}\mathcal{C}_{+,+1,-1}\big[e^{i(k_{FQH,F}-k_{SC,F}-\alpha)x}e^{-i(3\phi(x)+\theta(x)-\frac{\phi_c+\phi_s}{\sqrt{2}}-\frac{\theta_c+\theta_s}{\sqrt{2}})}+$$
$$e^{-i(k_{FQH,F}+k_{SC,F}+\alpha)x}e^{-i(3\phi(x)-\theta(x)-\frac{\phi_s+\phi_c}{\sqrt{2}}-\frac{\theta_s+\theta_c}{\sqrt{2}})}\big]$$
$$-\frac{\mathrm{k}_{FQH,\uparrow}\mathrm{k}_{Sc,-}}{\sqrt{4\pi}}\mathcal{C}_{-,+1,-1}\big[e^{i(k_{FQH,F}-k_{SC,F}-\alpha)x}e^{-i(3\phi(x)+\theta(x)-\frac{\phi_c-\phi_s}{\sqrt{2}}-\frac{\theta_c-\theta_s}{\sqrt{2}})}$$
$$+e^{-i(k_{FQH,F}+k_{SC,F}+\alpha)x}e^{-i(3\phi(x)-\theta(x)-\frac{\phi_c-\phi_s}{\sqrt{2}}-\frac{\theta_c-\theta_s}{\sqrt{2}})}\big] =$$
$$\psi^{\dagger}_{FQH,\uparrow,L}(x)\psi_{L1}(x) + \psi^{\dagger}_{FQH,\uparrow,R}(x)\psi_{L1}(x) \tag{B.13}$$

and its H.C is:

$$\sum_{j=L,R} \psi^{\dagger}_{L,1}(x)\psi_{FQH,\uparrow,j}(x) =$$
$$-\frac{\mathrm{k}_{FQH,\uparrow}\mathrm{k}_{Sc,+}}{\sqrt{4\pi}}\mathcal{C}_{+,+1,-1}\big[e^{-i(k_{FQH,F}-k_{SC,F}-\alpha)x}e^{i(3\phi(x)+\theta(x)-\frac{\phi_c+\phi_s}{\sqrt{2}}-\frac{\theta_c+\theta_s}{\sqrt{2}})}+$$
$$e^{i(k_{FQH,F}+k_{SC,F}+\alpha)x}e^{i(3\phi(x)-\theta(x)-\frac{\phi_s+\phi_c}{\sqrt{2}}-\frac{\theta_s+\theta_c}{\sqrt{2}})}\big]$$
$$+\frac{\mathrm{k}_{FQH,\uparrow}\mathrm{k}_{Sc,-}}{\sqrt{4\pi}}\mathcal{C}_{-,+1,-1}\big[e^{-i(k_{FQH,F}-k_{SC,F}-\alpha)x}e^{i(3\phi(x)+\theta(x)-\frac{\phi_c-\phi_s}{\sqrt{2}}-\frac{\theta_c-\theta_s}{\sqrt{2}})}$$
$$+e^{i(k_{FQH,F}+k_{SC,F}+\alpha)x}e^{i(3\phi(x)-\theta(x)-\frac{\phi_c-\phi_s}{\sqrt{2}}-\frac{\theta_c-\theta_s}{\sqrt{2}})}\big] =$$
$$\psi^{\dagger}_{L,1,\uparrow}(x)\psi_{FQH,\uparrow,L}(x) + \psi^{\dagger}_{L,1,\uparrow}(x)\psi_{FQH,\uparrow,R}(x) \tag{B.14}$$

- For R,1 mode, we have:

$$\sum_{j=L,R}\psi^{\dagger}_{FQH,\uparrow,j}(x)\psi_{R,1}(x)=\mathrm{k}_{FQH,\uparrow}\Big(e^{ik_{FQH,F}x}e^{-i(\phi'(x)+\theta'(x))}+e^{-ik_{FQH,F}x}e^{-i(\phi'(x)-\theta'(x))}\Big)$$
$$\frac{1}{\sqrt{4\pi}}e^{i(k_{SC,F}-\alpha)x}\Big[\mathrm{k}_{Sc,+}\mathcal{C}_{+,-1,-1}e^{i(\phi^{SC}_{+}(x)-\theta^{SC}_{+}(x))}-\mathrm{k}_{Sc,-}\mathcal{C}_{-,-1,-1}e^{i(\phi^{SC}_{-}(x)-\theta^{SC}_{-}(x))}\Big]$$
$$=\frac{\mathrm{k}_{FQH,\uparrow}\mathrm{k}_{Sc,+}}{\sqrt{4\pi}}\mathcal{C}_{+,-1,-1}\big[e^{i(k_{FQH,F}+k_{SC,F}-\alpha)x}e^{-i(3\phi(x)+\theta(x)-\phi^{SC}_{+}(x)+\theta^{SC}_{+}(x))}$$
$$+e^{-i(k_{FQH,F}-k_{SC,F}+\alpha)x}e^{-i(3\phi(x)-\theta(x)-\phi^{SC}_{+}(x)+\theta^{SC}_{+}(x))}\big]$$
$$-\frac{\mathrm{k}_{FQH,\uparrow}\mathrm{k}_{Sc,-}}{\sqrt{4\pi}}\mathcal{C}_{-,-1,-1}\big[e^{i(k_{FQH,F}+k_{SC,F}-\alpha)x}e^{-i(3\phi(x)+\theta(x)-\phi^{SC}_{-}(x)+\theta^{SC}_{-}(x))}+$$
$$e^{-i(k_{FQH,F}-k_{SC,F}+\alpha)x}e^{-i(3\phi(x)-\theta(x)-\phi^{SC}_{-}(x)+\theta^{SC}_{-}(x))}\big]=$$
$$\frac{\mathrm{k}_{FQH,\uparrow}\mathrm{k}_{Sc,+}}{\sqrt{4\pi}}\mathcal{C}_{+,-1,-1}\big[e^{i(k_{FQH,F}+k_{SC,F}-\alpha)x}e^{-i(3\phi(x)+\theta(x)-\frac{\phi_c+\phi_s}{\sqrt{2}}+\frac{\theta_c+\theta_s}{\sqrt{2}})}+$$
$$e^{-i(k_{FQH,F}-k_{SC,F}+\alpha)x}e^{-i(3\phi(x)-\theta(x)-\frac{\phi_s+\phi_c}{\sqrt{2}}+\frac{\theta_s+\theta_c}{\sqrt{2}})}\big]$$
$$-\frac{\mathrm{k}_{FQH,\uparrow}\mathrm{k}_{Sc,-}}{\sqrt{4\pi}}\mathcal{C}_{-,-1,-1}\big[e^{i(k_{FQH,F}+k_{SC,F}-\alpha)x}e^{-i(3\phi(x)+\theta(x)-\frac{\phi_c-\phi_s}{\sqrt{2}}+\frac{\theta_c-\theta_s}{\sqrt{2}})}$$
$$+e^{-i(k_{FQH,F}-k_{SC,F}+\alpha)x}e^{-i(3\phi(x)-\theta(x)-\frac{\phi_c-\phi_s}{\sqrt{2}}+\frac{\theta_c-\theta_s}{\sqrt{2}})}\big]=$$
$$\psi^{\dagger}_{R,1,\uparrow}(x)\psi_{FQH,\uparrow,L}(x)+\psi^{\dagger}_{R,1,\uparrow}(x)\psi_{FQH,\uparrow,R}(x) \tag{B.15}$$

and its H.C is:

$$\sum_{j=L,R}\psi^{\dagger}_{R,1}(x)\psi_{FQH,\uparrow,j}(x)=$$
$$-\frac{\mathrm{k}_{FQH,\uparrow}\mathrm{k}_{Sc,+}}{\sqrt{4\pi}}\mathcal{C}_{+,-1,-1}\big[e^{-i(k_{FQH,F}+k_{SC,F}-\alpha)x}e^{i(3\phi(x)+\theta(x)-\frac{\phi_c+\phi_s}{\sqrt{2}}+\frac{\theta_c+\theta_s}{\sqrt{2}})}+$$
$$e^{i(k_{FQH,F}-k_{SC,F}+\alpha)x}e^{i(3\phi(x)-\theta(x)-\frac{\phi_s+\phi_c}{\sqrt{2}}+\frac{\theta_s+\theta_c}{\sqrt{2}})}\big]$$
$$+\frac{\mathrm{k}_{FQH,\uparrow}\mathrm{k}_{Sc,-}}{\sqrt{4\pi}}\mathcal{C}_{-,-1,-1}\big[e^{-i(k_{FQH,F}+k_{SC,F}-\alpha)x}e^{i(3\phi(x)+\theta(x)-\frac{\phi_c-\phi_s}{\sqrt{2}}+\frac{\theta_c-\theta_s}{\sqrt{2}})}$$
$$+e^{i(k_{FQH,F}-k_{SC,F}+\alpha)x}e^{i(3\phi(x)-\theta(x)-\frac{\phi_c-\phi_s}{\sqrt{2}}+\frac{\theta_c-\theta_s}{\sqrt{2}})}\big]=$$
$$\psi^{\dagger}_{R,1,\uparrow}(x)\psi_{FQH,\uparrow,L}(x)+\psi^{\dagger}_{R,1,\uparrow}(x)\psi_{FQH,\uparrow,R}(x) \tag{B.16}$$

- For L,2 mode, we have:

$$\sum_{j=L,R}\psi^{\dagger}_{FQH,\uparrow,j}(x)\psi_{L,2}(x)=\mathrm{k}_{FQH,\uparrow}\Big(e^{ik_{FQH,F}x}e^{-i(\phi'(x)+\theta'(x))}+e^{-ik_{FQH,F}x}e^{-i(\phi'(x)-\theta'(x))}\Big)$$
$$\frac{1}{\sqrt{4\pi}}e^{i(-k_{SC,F}+\alpha)x}\Big[\mathrm{k}_{Sc,+}\mathcal{C}_{+,+1,+1}e^{i(\phi^{SC}_{+}(x)+\theta^{SC}_{+}(x))}-\mathrm{k}_{Sc,-}\mathcal{C}_{-,+1,+1}e^{i(\phi^{SC}_{-}(x)+\theta^{SC}_{-}(x))}\Big]$$
$$=\frac{\mathrm{k}_{FQH,\uparrow}\mathrm{k}_{Sc,+}}{\sqrt{4\pi}}\mathcal{C}_{+,+1,+1}\big[e^{i(k_{FQH,F}-k_{SC,F}+\alpha)x}e^{-i(3\phi(x)+\theta(x)-\frac{\phi_c+\phi_s}{\sqrt{2}}-\frac{\theta_c+\theta_s}{\sqrt{2}})}+$$
$$e^{-i(k_{FQH,F}+k_{SC,F}-\alpha)x}e^{-i(3\phi(x)-\theta(x)-\frac{\phi_s+\phi_c}{\sqrt{2}}-\frac{\theta_s+\theta_c}{\sqrt{2}})}\big]$$
$$-\frac{\mathrm{k}_{FQH,\uparrow}\mathrm{k}_{Sc,-}}{\sqrt{4\pi}}\mathcal{C}_{-,+1,+1}\big[e^{i(k_{FQH,F}-k_{SC,F}+\alpha)x}e^{-i(3\phi(x)+\theta(x)-\frac{\phi_c-\phi_s}{\sqrt{2}}-\frac{\theta_c-\theta_s}{\sqrt{2}})}$$
$$+e^{-i(k_{FQH,F}+k_{SC,F}-\alpha)x}e^{-i(3\phi(x)-\theta(x)-\frac{\phi_c-\phi_s}{\sqrt{2}}-\frac{\theta_c-\theta_s}{\sqrt{2}})}\big]=$$
$$\psi^{\dagger}_{FQH,\uparrow,L}(x)\psi_{L,2,\uparrow}(x)+\psi^{\dagger}_{FQH,\uparrow,R}(x)\psi_{L,2,\uparrow}(x) \tag{B.17}$$

and its H.C is:

$$\sum_{j=L,R}\psi^{\dagger}_{L,2}(x)\psi_{FQH,\uparrow,j}(x)=$$
$$-\frac{\mathrm{k}_{FQH,\uparrow}\mathrm{k}_{Sc,+}}{\sqrt{4\pi}}\mathcal{C}_{+,+1,+1}\big[e^{-i(k_{FQH,F}-k_{SC,F}+\alpha)x}e^{i(3\phi(x)+\theta(x)-\frac{\phi_c+\phi_s}{\sqrt{2}}-\frac{\theta_c+\theta_s}{\sqrt{2}})}+$$
$$e^{i(k_{FQH,F}+k_{SC,F}-\alpha)x}e^{i(3\phi(x)-\theta(x)-\frac{\phi_s+\phi_c}{\sqrt{2}}-\frac{\theta_s+\theta_c}{\sqrt{2}})}\big]$$
$$+\frac{\mathrm{k}_{FQH,\uparrow}\mathrm{k}_{Sc,-}}{\sqrt{4\pi}}\mathcal{C}_{-,+1,+1}\big[e^{-i(k_{FQH,F}-k_{SC,F}+\alpha)x}e^{i(3\phi(x)+\theta(x)-\frac{\phi_c-\phi_s}{\sqrt{2}}-\frac{\theta_c-\theta_s}{\sqrt{2}})}$$
$$+e^{i(k_{FQH,F}+k_{SC,F}-\alpha)x}e^{i(3\phi(x)-\theta(x)-\frac{\phi_c-\phi_s}{\sqrt{2}}-\frac{\theta_c-\theta_s}{\sqrt{2}})}\big]=$$
$$\psi^{\dagger}_{L,2,\uparrow}(x)\psi_{FQH,\uparrow,L}(x)+\psi^{\dagger}_{L,2,\uparrow}(x)\psi_{FQH,\uparrow,R}(x) \tag{B.18}$$

- For R,2 mode, we have:

$$\sum_{j=L,R}\psi^{\dagger}_{FQH,\uparrow,j}(x)\psi_{R,2}(x)=\mathrm{k}_{FQH,\uparrow}\Big(e^{ik_{FQH,F}x}e^{-i(\phi'(x)+\theta'(x))}+e^{-ik_{FQH,F}x}e^{-i(\phi'(x)-\theta'(x))}\Big)$$
$$\frac{1}{\sqrt{4\pi}}e^{i(k_{SC,F}+\alpha)x}\Big[\mathrm{k}_{Sc,+}\mathcal{C}_{+,-1,+1}e^{i(\phi^{SC}_{+}(x)-\theta^{SC}_{+}(x))}-\mathrm{k}_{Sc,-}\mathrm{k}_{Sc,+}\mathcal{C}_{-,-1,+1}e^{i(\phi^{SC}_{-}(x)-\theta^{SC}_{-}(x))}\Big]$$
$$=\frac{\mathrm{k}_{FQH,\uparrow}\mathrm{k}_{Sc,+}}{\sqrt{4\pi}}\mathrm{k}_{Sc,+}\mathcal{C}_{+,-1,+1}\big[e^{i(k_{FQH,F}+k_{SC,F}+\alpha)x}e^{-i(3\phi(x)+\theta(x)-\frac{\phi_c+\phi_s}{\sqrt{2}}+\frac{\theta_c+\theta_s}{\sqrt{2}})}+$$
$$e^{-i(k_{FQH,F}-k_{SC,F}-\alpha)x}e^{-i(3\phi(x)-\theta(x)-\frac{\phi_s+\phi_c}{\sqrt{2}}+\frac{\theta_s+\theta_c}{\sqrt{2}})}\big]$$
$$-\frac{\mathrm{k}_{FQH,\uparrow}\mathrm{k}_{Sc,-}}{\sqrt{4\pi}}\mathrm{k}_{Sc,+}\mathcal{C}_{-,-1,+1}\big[e^{i(k_{FQH,F}+k_{SC,F}+\alpha)x}e^{-i(3\phi(x)+\theta(x)-\frac{\phi_c-\phi_s}{\sqrt{2}}+\frac{\theta_c-\theta_s}{\sqrt{2}})}$$
$$+e^{-i(k_{FQH,F}-k_{SC,F}-\alpha)x}e^{-i(3\phi(x)-\theta(x)-\frac{\phi_c-\phi_s}{\sqrt{2}}+\frac{\theta_c-\theta_s}{\sqrt{2}})}\big]=$$
$$\psi^{\dagger}_{FQH,\uparrow,L}(x)\psi_{R,2,\uparrow}(x)+\psi^{\dagger}_{FQH,\uparrow,R}(x)\psi_{R,2,\uparrow}(x) \tag{B.19}$$

and its H.C is:

$$\sum_{j=L,R}\psi^{\dagger}_{R,2}(x)\psi_{FQH,\uparrow,j}(x)=$$
$$-\frac{\mathrm{k}_{FQH,\uparrow}\mathrm{k}_{Sc,+}}{\sqrt{4\pi}}\mathrm{k}_{Sc,+}\mathcal{C}_{+,-1,+1}\big[e^{-i(k_{FQH,F}+k_{SC,F}+\alpha)x}e^{i(3\phi(x)+\theta(x)-\frac{\phi_c+\phi_s}{\sqrt{2}}+\frac{\theta_c+\theta_s}{\sqrt{2}})}+$$
$$e^{i(k_{FQH,F}-k_{SC,F}-\alpha)x}e^{i(3\phi(x)-\theta(x)-\frac{\phi_s+\phi_c}{\sqrt{2}}+\frac{\theta_s+\theta_c}{\sqrt{2}})}\big]$$
$$+\frac{\mathrm{k}_{FQH,\uparrow}\mathrm{k}_{Sc,-}}{\sqrt{4\pi}}\mathrm{k}_{Sc,+}\mathcal{C}_{-,-1,+1}\big[e^{-i(k_{FQH,F}+k_{SC,F}+\alpha)x}e^{i(3\phi(x)+\theta(x)-\frac{\phi_c-\phi_s}{\sqrt{2}}+\frac{\theta_c-\theta_s}{\sqrt{2}})}$$
$$+e^{i(k_{FQH,F}-k_{SC,F}-\alpha)x}e^{i(3\phi(x)-\theta(x)-\frac{\phi_c-\phi_s}{\sqrt{2}}+\frac{\theta_c-\theta_s}{\sqrt{2}})}\big]=$$
$$\psi^{\dagger}_{R,2,\uparrow}(x)\psi_{FQH,\uparrow,L}(x)+\psi^{\dagger}_{R,2,\uparrow}(x)\psi_{FQH,\uparrow,R}(x) \tag{B.20}$$

Putting together each term and its H.C, we get:

- For L,1 mode and its H.C, we have:

$$\sum_{j=L,R}\left(\psi^{\dagger}_{FQH,\uparrow,j}(x)\psi_{L,1}(x)+\psi^{\dagger}_{L,1}(x)\psi_{FQH,\uparrow,j}(x)\right)=$$
$$-2i\frac{\mathrm{k}_{FQH,\uparrow}\mathrm{k}_{Sc,+}}{\sqrt{4\pi}}\mathcal{C}_{+,+1,-1}\Bigg(\sin\left(3\phi(x)+\theta(x)-\frac{\phi_s+\phi_c}{\sqrt{2}}-\frac{\theta_s+\theta_c}{\sqrt{2}}-(k_{FQH,F}-k_{SC,F}-\alpha)x\right)$$
$$+\sin\left(3\phi(x)-\theta(x)-\frac{\phi_s+\phi_c}{\sqrt{2}}-\frac{\theta_s+\theta_c}{\sqrt{2}}+(k_{FQH,F}+k_{SC,F}+\alpha)x\right)\Bigg)+$$
$$+2i\frac{\mathrm{k}_{FQH,\uparrow}\mathrm{k}_{Sc,-}}{\sqrt{4\pi}}\mathcal{C}_{-,+1,+1}\Bigg(\sin\left(3\phi(x)+\theta(x)-\frac{\phi_c-\phi_s}{\sqrt{2}}-\frac{\theta_c-\theta_s}{\sqrt{2}}-(k_{FQH,F}-k_{SC,F}-\alpha)x\right)$$
$$+\sin\left(3\phi(x)-\theta(x)-\frac{\phi_c-\phi_s}{\sqrt{2}}-\frac{\theta_c-\theta_s}{\sqrt{2}}+(k_{FQH,F}+k_{SC,F}+\alpha)x\right)\Bigg) \tag{B.21}$$

- For R,1 mode and its H.C, we have:

$$\sum_{j=L,R}\left(\psi^{\dagger}_{FQH,\uparrow,j}(x)\psi_{R,1}(x)+\psi^{\dagger}_{R,1}(x)\psi_{FQH,\uparrow,j}(x)\right)=$$
$$-2i\frac{\mathrm{k}_{FQH,\uparrow}\mathrm{k}_{Sc,+}}{\sqrt{4\pi}}\mathcal{C}_{+,-1,-1}\Bigg(\sin\left(3\phi(x)+\theta(x)-\frac{\phi_c+\phi_s}{\sqrt{2}}+\frac{\theta_c+\theta_s}{\sqrt{2}}-(k_{FQH,F}+k_{SC,F}-\alpha)x\right)$$
$$+\sin\left(3\phi(x)-\theta(x)-\frac{\phi_c+\phi_c}{\sqrt{2}}+\frac{\theta_s+\theta_c}{\sqrt{2}}+(k_{FQH,F}-k_{SC,F}+\alpha)x\right)\Bigg)$$
$$+2i\frac{\mathrm{k}_{FQH,\uparrow}\mathrm{k}_{Sc,-}}{\sqrt{4\pi}}\mathcal{C}_{-,-1,-1}\Bigg(\sin\left(3\phi(x)+\theta(x)-\frac{\phi_c-\phi_s}{\sqrt{2}}+\frac{\theta_c-\theta_s}{\sqrt{2}}-(k_{FQH,F}+k_{SC,F}-\alpha)x\right)$$
$$+\sin\left(3\phi(x)-\theta(x)-\frac{\phi_c-\phi_s}{\sqrt{2}}+\frac{\theta_c-\theta_s}{\sqrt{2}}+(k_{FQH,F}-k_{SC,F}+\alpha)x\right)\Bigg) \tag{B.22}$$

- For L,2 mode and its H.C, we have:

$$\sum_{j=L,R}\left(\psi^{\dagger}_{FQH,\uparrow,j}(x)\psi_{L,2}(x)+\psi^{\dagger}_{L,2}(x)\psi_{FQH,\uparrow,j}(x)\right)=$$
$$-2i\frac{\mathrm{k}_{FQH,\uparrow}\mathrm{k}_{Sc,+}}{\sqrt{4\pi}}\mathcal{C}_{+,+1,+1}\Bigg(\sin\Big(3\phi(x)+\theta(x)-\frac{\phi_c+\phi_s}{\sqrt{2}}-\frac{\theta_c+\theta_s}{\sqrt{2}}-(k_{FQH,F}-k_{SC,F}+\alpha)x\Big)$$
$$+\sin\Big((3\phi(x)-\theta(x)-\frac{\phi_c+\phi_s}{\sqrt{2}}-\frac{\theta_c+\theta_s}{\sqrt{2}}+(k_{FQH,F}+k_{SC,F}-\alpha)x\Big)\Bigg)$$
$$+2i\frac{\mathrm{k}_{FQH,\uparrow}\mathrm{k}_{Sc,-}}{\sqrt{4\pi}}\mathcal{C}_{-,+1,+1}\Bigg(\sin\Big(3\phi(x)+\theta(x)-\frac{\phi_c-\phi_s}{\sqrt{2}}-\frac{\theta_c-\theta_s}{\sqrt{2}}-(k_{FQH,F}-k_{SC,F}+\alpha)x\Big)$$
$$+\sin\Big((3\phi(x)-\theta(x)-\frac{\phi_c-\phi_s}{\sqrt{2}}-\frac{\theta_c-\theta_s}{\sqrt{2}}+(k_{FQH,F}+k_{SC,F}-\alpha)x\Big)\Bigg) \tag{B.23}$$

- For R,2 mode and its H.C, we have:

$$\sum_{j=L,R}\left(\psi^{\dagger}_{FQH,\uparrow,j}(x)\psi_{R,2}(x)+\psi^{\dagger}_{R,2}(x)\psi_{FQH,\uparrow,j}(x)\right)=$$
$$-2i\frac{\mathrm{k}_{FQH,\uparrow}\mathrm{k}_{Sc,+}}{\sqrt{4\pi}}\mathcal{C}_{+,-1,+1}\Bigg(\sin\Big(3\phi(x)+\theta(x)-\frac{\phi_c+\phi_s}{\sqrt{2}}+\frac{\theta_c+\theta_s}{\sqrt{2}}-(k_{FQH,F}+k_{SC,F}+\alpha)x\Big)$$
$$+\sin\Big((3\phi(x)-\theta(x)-\frac{\phi_c+\phi_s}{\sqrt{2}}+\frac{\theta_c+\theta_s}{\sqrt{2}}+(k_{FQH,F}-k_{SC,F}-\alpha)x\Big)\Bigg)$$
$$+2i\frac{\mathrm{k}_{FQH,\uparrow}\mathrm{k}_{Sc,-}}{\sqrt{4\pi}}\mathcal{C}_{-,-1,+1}\Bigg(\sin\Big(3\phi(x)+\theta(x)-\frac{\phi_c-\phi_s}{\sqrt{2}}+\frac{\theta_c-\theta_s}{\sqrt{2}}-(k_{FQH,F}+k_{SC,F}+\alpha)x\Big)$$
$$+\sin\Big((3\phi(x)-\theta(x)-\frac{\phi_c-\phi_s}{\sqrt{2}}+\frac{\theta_c-\theta_s}{\sqrt{2}}+(k_{FQH,F}-k_{SC,F}-\alpha)x\Big)\Bigg) \tag{B.24}$$

The above results can be written in a composite form as:

$$H_t(x)=\frac{-t2i}{\sqrt{2\pi\tilde{\alpha}}}\int dx\sum_{\eta=L/R=\pm1}\sum_{\eta'=L/R=\pm1}\sum_{\sigma=\pm1}$$
$$\Bigg(\mathrm{k}_{FQH,\uparrow}\mathrm{k}_{Sc,+}\mathcal{C}_{+,\eta}\sin\Big(3\phi(x)-\eta'\theta(x)-\frac{\phi_c+\phi_s}{\sqrt{2}}-\eta\frac{\theta_c+\theta_s}{\sqrt{2}}-\eta'(k_{FQH,F}-\eta\eta' k_{SC,F}-\sigma\alpha)x\Big)$$
$$-\mathrm{k}_{FQH,\uparrow}\mathrm{k}_{Sc,-}\mathcal{C}_{-,\eta}\sin\Big(3\phi(x)-\eta'\theta(x)-\frac{\phi_c-\phi_s}{\sqrt{2}}-\eta\frac{\theta_c-\theta_s}{\sqrt{2}}-\eta'(k_{FQH,F}-\eta\eta' k_{SC,F}-\sigma\alpha)x\Big)\Bigg) \tag{B.25}$$

B.5 2nd-order of RG

In this sector, we present the main results one should expect to get by performing the 2nd-order of RG in the tunneling Hamiltonian. We must note here also, that we are not interested to see the scalling dimension of the second order, but rather we are interested in the combination that will give us the S.O terms. By keeping that in mind, we present the main results by combining Left and Right movers with different energy modes. The results are:

- For the combination of $\sum_{j=L,R}\left(\psi^{\dagger}_{FQH,\uparrow,j}(x)\psi_{L,1}(x)+\psi^{\dagger}_{L,1}(x)\psi_{FQH,\uparrow,j}(x)\right)\left(\psi^{\dagger}_{FQH,\uparrow,j}(x)\psi_{R,2}(x)+\psi^{\dagger}_{R,2}(x)\psi_{FQH,\uparrow,j}(x)\right)$ we get the terms:
  1. $\frac{2}{\pi}\mathcal{C}^2_{+,-1,+1}\cos\left(6\phi-\sqrt{2}(\phi_c+\phi_s)\right)$
  2. $-i\mathrm{k}_{Sc,+}\mathrm{k}_{Sc,-}\frac{2}{\pi}\mathcal{C}_{+,-1,+1}\mathcal{C}_{-,-1,+1}\cos\left(6\phi-\sqrt{2}(\phi_c+\theta_s)\right)$
  3. $-i\mathrm{k}_{Sc,+}\mathrm{k}_{Sc,-}\frac{2}{\pi}\mathcal{C}_{+,-1,+1}\mathcal{C}_{-,-1,+1}\cos\left(6\phi-\sqrt{2}(\phi_c-\theta_s)\right)$
  4. $-\frac{2}{\pi}\mathcal{C}^2_{-,-1,+1}\cos\left(6\phi-\sqrt{2}(\phi_c-\phi_s)\right)$
- and from the combination of $\sum_{j=L,R}\left(\psi^{\dagger}_{FQH,\uparrow,j}(x)\psi_{R,1}(x)+\psi^{\dagger}_{R,1}(x)\psi_{FQH,\uparrow,j}(x)\right)\left(\psi^{\dagger}_{FQH,\uparrow,j}(x)\psi_{L,2}(x)+\psi^{\dagger}_{L,2}(x)\psi_{FQH,\uparrow,j}(x)\right)$ we get the terms:
  5. $\frac{2}{\pi}\mathcal{C}^2_{+,-1,-1}\cos\left(6\phi-\sqrt{2}(\phi_c+\phi_s)\right)$
  6. $i\mathrm{k}_{Sc,+}\mathrm{k}_{Sc,-}\frac{2}{\pi}\mathcal{C}_{+,-1,-1}\mathcal{C}_{-,-1,-1}\cos\left(6\phi-\sqrt{2}(\phi_c+\theta_s)\right)$
  7. $i\mathrm{k}_{Sc,+}\mathrm{k}_{Sc,-}\frac{2}{\pi}\mathcal{C}_{+,-1,-1}\mathcal{C}_{-,-1,-1}\cos\left(6\phi-\sqrt{2}(\phi_c-\theta_s)\right)$
  8. $-\frac{2}{\pi}\mathcal{C}^2_{-,-1,-1}\cos\left(6\phi-\sqrt{2}(\phi_c-\phi_s)\right)$

We can combine them now to get the S.O terms:

$$\begin{aligned}\langle\mathcal{S}^2_{S.O,t}(x)\rangle = t^2\frac{2}{\pi}\Bigg[&\left(\mathcal{C}^2_{+,-1,+1}+\mathcal{C}^2_{+,-1,-1}\right)\cos\left(6\phi-\sqrt{2}(\phi_c+\phi_s)\right)\\&-\left(\mathcal{C}^2_{-,-1,+1}+\mathcal{C}^2_{-,-1,-1}\right)\cos\left(6\phi-\sqrt{2}(\phi_c-\phi_s)\right)\\&+i\mathrm{k}_{Sc,+}\mathrm{k}_{Sc,-}\left(\mathcal{C}_{+,-1,-1}\mathcal{C}_{-,-1,-1}-\mathcal{C}_{+,-1,+1}\mathcal{C}_{-,-1,+1}\right)\\&\left(\cos\left(6\phi-\sqrt{2}(\phi_c+\theta_s)\right)+\cos\left(6\phi-\sqrt{2}(\phi_c-\theta_s)\right)\right)\Bigg]\end{aligned}\tag{B.26}$$

We can rewrite these results in a composite form as:

$$\mathcal{H}^2_{S.O,t}(x) = t^2 \frac{4}{\pi \tilde{a}} \sum_{\mu=\pm 1} \left(i \mathrm{k}_{Sc,+} \mathrm{k}_{Sc,-} \mathcal{H}_\mu \cos\left(6\phi - \sqrt{2}(\phi_c + \mu\theta_s)\right)\right) + \mu \mathcal{H}'_\mu \cos\left(6\phi - \sqrt{2}(\phi_c + \mu\phi_s)\right)\Bigg) \tag{B.27}$$

where we denote as $\mathcal{H}_\mu = \mathcal{H} = \mathcal{C}_{+,-1,-1}\mathcal{C}_{-,-1,-1} - \mathcal{C}_{+,-1,+1}\mathcal{C}_{-,-1,+1}$, $\mathcal{H}'_+ = \mathcal{C}^2_{+,-1,+1} + \mathcal{C}^2_{+,-1,-1}$ and $\mathcal{H}'_- = \mathcal{C}^2_{-,-1,+1} + \mathcal{C}^2_{-,-1,-1}$. These are the terms that we need to introduce the $\mathcal{S}_h$ in the new effective Interacting action for the $\mathcal{II}$-step of RG. For completeness here we include also the Klein factors and the coefficients for each term. To derive eq. (B.27) we made use of the anti-commutation relation of the Klein factors and the trigonometric properties for the $\mathcal{C}$ terms.

We are now in place to introduce the extra action that we will consider in the 2-step RG analysis. This action has the form:

$$\mathcal{S}_h = \int d^2z \sum_{\mu=\pm 1} \left(i \mathrm{k}_{Sc,+} \mathrm{k}_{Sc,-} h_\mu \cos\left(6\phi - \sqrt{2}(\phi_c + \mu\theta_s)\right)\right) + \mu h'_\mu \cos\left(6\phi - \sqrt{2}(\phi_c + \mu\phi_s)\right)\Bigg) \tag{B.28}$$

where h_μ and h'_μ is used to distinguish the two different kind of S.O terms that appear.

In the main text, we present a more elegant way on how to treat this action. Here we will present another way which gives the same results.

We define the operators:

$$\mathcal{O}^\nu_{h,\mu}(z) = e^{i\nu(6\phi(z) - \sqrt{2}(\phi_c + \mu\theta_s))} \tag{B.29}$$

where again $\nu = \pm 1$ and $\mu = \pm 1$. In this way we can write the $\mathcal{S}_h$ as:

$$\mathcal{S}_h = \frac{h}{2i} \mathrm{k}_{Sc,+} \mathrm{k}_{Sc,-} \int d^2z \sum_{\nu=\pm 1} \sum_{\mu=\pm 1} \mathcal{O}^\nu_{h,\mu}(z) \tag{B.30}$$

We will begin our analysis by focusing on the non-trivial terms $\mathcal{B}$ of eq. (3.3.1) by using the effective Interacting action of eq. (3.81) that we introduced in $\mathcal{II}$-step of RG. This means that now the most important terms will be the ones we introduced in the $\mathcal{II}$-step of RG:

$$\Big\langle \mathcal{S}_h(z_1)\mathcal{S}_h(z_2) \Big\rangle_{\mathbf{f}} \tag{B.31}$$

In particular, we see that we have terms like:

$$\Big\langle \mathcal{S}_h(z_1)\mathcal{S}_h(z_2) \Big\rangle_{\mathbf{f}} = \frac{h^2}{(2i)^2} \int d^2z \sum_{\nu=\pm 1} \sum_{\mu=\pm 1} \sum_{\nu'=\pm 1} \sum_{\mu'=\pm 1} \Big\langle \mathcal{O}^\nu_{h,\mu}(z) \mathcal{O}^{\nu'}_{h,\mu'}(z) \Big\rangle \tag{B.32}$$

where these terms can be written as:

$$\Big\langle \mathcal{O}^{\nu}_{h,\mu}(z_1)\mathcal{O}^{\nu'}_{h,\mu'}(z_2)\Big\rangle_{\mathbf{f}} = \Big\langle e^{i\nu(6\phi(z_1)-\sqrt{2}(\phi_c+\mu\theta_s))}e^{i\nu'(6\phi(z_2)-\sqrt{2}(\phi_c+\mu'\theta_s))}\Big\rangle_{\mathbf{f}} =$$
$$e^{i(6(\nu\phi(z_1)+\nu'\phi(z_2))-\sqrt{2}(\nu(\phi_c+\mu\theta_s)+\nu'(\phi_c+\mu'\theta_s)))}e^{-36\nu\nu'\langle\phi(z_1)\phi(z_2)\rangle_{\mathbf{f}}-\frac{1}{2}(36\langle\phi^2(z_1)\rangle_{\mathbf{f}})-\frac{1}{2}(36\langle\phi^2(z_1)\rangle_{\mathbf{f}})} =$$
$$e^{i(6(\nu\phi(z_1)+\nu'\phi(z_2))-\sqrt{2}((\nu+\nu')\phi_c+(\nu\mu+\nu'\mu')\theta_s)))}e^{\left(-36\nu\nu'\frac{\mathcal{C}(z_1-z_2)}{6}-\frac{2}{2}\frac{36}{6}\right)\ln\left(\frac{\Lambda}{\tilde{\Lambda}}\right)\Big)} =$$
$$e^{i(6(\nu\phi(z_1)+\nu'\phi(z_2))-\sqrt{2}((\nu+\nu')\phi_c+(\nu\mu+\nu'\mu')\theta_s)))}\Big(\frac{\tilde{\Lambda}}{\Lambda}\Big)^{6\nu\nu'\mathcal{C}(z_1-z_2)-6} =$$
$$e^{i(6(\nu\phi(z_1)+\nu'\phi(z_2))-\sqrt{2}((\nu+\nu')\phi_c+(\nu\mu+\nu'\mu')\theta_s)))}\Big(1-\big(6\nu\nu'\mathcal{C}(z_1-z_2)+6\big)dl\Big) \tag{B.33}$$

In total we will get in second-order for the non-trivial term $\mathcal{B}$ for $\mathcal{S}_h$ that:

$$\Big\langle \mathcal{S}_h(z_1)\mathcal{S}_h(z_2)\Big\rangle_{\mathbf{f}} = \frac{h^2}{(2i)^2}\int d^2z \sum_{\nu=\pm1}\sum_{\mu=\pm1}\sum_{\nu'=\pm1}\sum_{\mu'=\pm1}\Big\langle \mathcal{O}^{\nu}_{h,\mu}(z)\mathcal{O}^{\nu'}_{h,\mu'}(z)\Big\rangle =$$
$$-\frac{h^2}{4}\int d^2z_1' d^2z_2' \sum_{\nu=\pm1}\sum_{\nu'=\pm1}\sum_{\mu=\pm1}\sum_{\mu'=\pm1}$$
$$\Bigg(\underbrace{\Big\langle \mathcal{O}^{+}_{h,\mu}(z)\mathcal{O}^{+}_{h,\mu'}(z)\Big\rangle}_{\nu=\nu'=+1}+\underbrace{\Big\langle \mathcal{O}^{-}_{h,\mu}(z)\mathcal{O}^{-}_{h,\mu'}(z)\Big\rangle}_{\nu=\nu'=-1}+\underbrace{\Big\langle \mathcal{O}^{-}_{h,\mu}(z)\mathcal{O}^{+}_{h,\mu'}(z)\Big\rangle}_{\nu=-1,\nu'=+1}+\underbrace{\Big\langle \mathcal{O}^{+}_{h,\mu}(z)\mathcal{O}^{-}_{h,\mu'}(z)\Big\rangle}_{\nu=+1,\nu'=-1}\Bigg) =$$
$$-\frac{h^2}{2}\int d^2z_1' d^2z_2' \sum_{\mu=\pm1}\sum_{\mu'=\pm1}\Big(1+\Big(4-\big(6\mathcal{C}(z_1'-z_2')+6\big)\Big)dl\Big)\cos\big(6(\phi_1+\phi_2)-\sqrt{2}(2\phi_c+(\mu+\mu')\theta_s)\big)$$
$$+\Big(1+\Big(4-\big(-6\mathcal{C}(z_1'-z_2')+6\big)\Big)dl\Big)\cos\big(6(\phi_1-\phi_2)-\sqrt{2}(\mu-\mu')\theta_s\big) \tag{B.34}$$

where we wrote the fields as $\phi(z_1') = \phi_1$ and $\phi(z_2') = \phi_2$. By taking the square of the first-order result

we get in second order the terms $\mathcal{A}^2$:

$$\Big\langle \mathcal{S}_h(z)\Big\rangle_{\mathbf{f}}^2 = \Big\langle \mathcal{S}_h(z_1)\Big\rangle_{\mathbf{f}}\Big\langle \mathcal{S}_h(z_2)\Big\rangle_{\mathbf{f}} =$$
$$\frac{h^2}{(2i)^2}\int d^2z_1' d^2z_2' \sum_{\nu=\pm1}\sum_{\nu'=\pm1}\sum_{\mu=\pm1}\sum_{\mu'=\pm1}\Big\langle \mathcal{O}^{\nu}_{h,\mu}(z_1)\Big\rangle_{\mathbf{f}}\Big\langle \mathcal{O}^{\nu'}_{h,\mu'}(z_2)\Big\rangle_{\mathbf{f}} =$$
$$-\frac{h^2}{4}\int d^2z_1' d^2z_2' \sum_{\mu=\pm}\sum_{\mu'=\pm}\Bigg(\underbrace{\Big\langle \mathcal{O}^{+}_{h,\mu}(z_1)\Big\rangle_{\mathbf{f}}\Big\langle \mathcal{O}^{+}_{h,\mu'}(z_2)\Big\rangle_{\mathbf{f}}}_{\nu=\nu'=+1} + \underbrace{\Big\langle \mathcal{O}^{-}_{h,\mu}(z_1)\Big\rangle_{\mathbf{f}}\Big\langle \mathcal{O}^{-}_{h,\mu'}(z_2)\Big\rangle_{\mathbf{f}}}_{\nu=\nu'=-1}$$
$$+\underbrace{\Big\langle \mathcal{O}^{-}_{h,\mu}(z_1)\Big\rangle_{\mathbf{f}}\Big\langle \mathcal{O}^{+}_{h,\mu'}(z_2)\Big\rangle_{\mathbf{f}}}_{\nu=-1,\nu'=+1} + \underbrace{\Big\langle \mathcal{O}^{+}_{h,\mu}(z_1)\Big\rangle_{\mathbf{f}}\Big\langle \mathcal{O}^{-}_{h,\mu'}(z_2)\Big\rangle_{\mathbf{f}}}_{\nu=+1,\nu'=-1}\Bigg) =$$
$$-\frac{h^2}{2}\big(1+(4-6)dl\big)\int d^2z_1' d^2z_2' \sum_{\mu=\pm1}\sum_{\mu'=\pm1}\Big(\cos\big(6(\phi_1+\phi_2)-\sqrt{2}(2\phi_c+(\mu+\mu')\theta_s)\big)$$
$$+\cos\big(6(\phi_1-\phi_2)-\sqrt{2}(\mu-\mu')\theta_s\big)\Big) \tag{B.35}$$

Now it is very easy to see that by combining these terms we left with:

$$\mathcal{B}-\mathcal{A}^2 = -\frac{h^2}{2}\int d^2z_1' d^2z_2' \sum_{\mu=\pm1}\sum_{\mu'=\pm1}\Bigg(\Big(1-6\mathcal{C}(z_1'-z_2')dl\Big)\cos\big(6(\phi_1+\phi_2)-\sqrt{2}(2\phi_c+(\mu+\mu')\theta_s)\big)$$
$$-\Big(1+6\mathcal{C}(z_1'-z_2')dl\Big)\cos\big(6(\phi_1-\phi_2)-\sqrt{2}(\mu-\mu')\theta_s\big)\Bigg) \tag{B.36}$$

Note that in the above calculations we treat the ϕ_c and θ_s fields as constants and they do not contribute in the scaling dimensions of the system.